

5-2016

Cell-based therapies for ischemic cardiomyopathy : investigations of intramyocardial retention and safety of high dose intracoronary delivery of c-kit positive cardiac progenitor cells, and therapeutic utility of a novel population of cardiac mesenchymal stem cells expressing stage-specific embryonic antigen-3 (SSEA-3).

Matthew C. L. Keith
University of Louisville

Follow this and additional works at: <https://ir.library.louisville.edu/etd>

Part of the [Medical Cell Biology Commons](#)

Recommended Citation

Keith, Matthew C. L., "Cell-based therapies for ischemic cardiomyopathy : investigations of intramyocardial retention and safety of high dose intracoronary delivery of c-kit positive cardiac progenitor cells, and therapeutic utility of a novel population of cardiac mesenchymal stem cells expressing stage-specific embryonic antigen-3 (SSEA-3)." (2016). *Electronic Theses and Dissertations*. Paper 2390.

<https://doi.org/10.18297/etd/2390>

This Doctoral Dissertation is brought to you for free and open access by ThinkIR: The University of Louisville's Institutional Repository. It has been accepted for inclusion in Electronic Theses and Dissertations by an authorized administrator of ThinkIR: The University of Louisville's Institutional Repository. This title appears here courtesy of the author, who has retained all other copyrights. For more information, please contact thinkir@louisville.edu.

CELL-BASED THERAPIES FOR ISCHEMIC CARDIOMYOPATHY–
INVESTIGATIONS OF INTRAMYOCARDIAL RETENTION AND SAFETY OF
HIGH DOSE INTRACORONARY DELIVERY OF C-KIT POSITIVE CARDIAC
PROGENITOR CELLS, AND THERAPEUTIC UTILITY OF A NOVEL
POPULATION OF CARDIAC MESENCHYMAL STEM CELLS EXPRESSING
STAGE-SPECIFIC EMBRYONIC ANTIGEN– 3 (SSEA-3)

By

Matthew C. L. Keith, MD
B.S., Oklahoma State University, 2005
M.D., Louisiana State University-Shreveport, School of Medicine, 2009

A Dissertation
Submitted to the Faculty of the
School of Medicine, University of Louisville
in Partial Fulfillment of the Requirements
for the Degree of

Doctor of Philosophy in Physiology and Biophysics

Department of Physiology and Biophysics
School of Medicine, University of Louisville
Louisville, Kentucky

May 2016

Copyright 2016 by Matthew C. L. Keith, MD

All rights reserved

CELL-BASED THERAPIES FOR ISCHEMIC CARDIOMYOPATHY–
INVESTIGATIONS OF INTRAMYOCARDIAL RETENTION AND SAFETY OF
HIGH DOSE INTRACORONARY DELIVERY OF C-KIT POSITIVE CARDIAC
PROGENITOR CELLS, AND THERAPEUTIC UTILITY OF A NOVEL
POPULATION OF CARDIAC MESENCHYMAL STEM CELLS EXPRESSING
STAGE-SPECIFIC EMBRYONIC ANTIGEN– 3 (SSEA-3)

By

Matthew C. L. Keith, MD
B.S., Oklahoma State University, 2005
M.D., Louisiana State University-Shreveport, School of Medicine, 2009

A Dissertation Approved on

March 18, 2016

by the following Dissertation Committee:

Primary mentor and dissertation director:
Dr. Roberto Bolli

Dr. Irving Joshua

Dr. Dale Schuschke

Dr. Claudio Maldonado

Dr. Daniel J. Conklin

DEDICATION

This dissertation is dedicated to my wife, Morgan Keith, and parents, Ronnie & Pat Keith, who provided me with the opportunities, courage, determination, and support to follow my dreams, overcome obstacles before me, maintain clear perspectives, and become a better physician, husband, and son daily. *Sine labore nihil.*

ACKNOWLEDGEMENTS

First, I would like to thank my mentor and friend, Dr. Roberto Bolli, for his unwavering support and guidance throughout my medical career. His unparalleled work ethic and scholarly approach to exploring novel therapies that may improve not only the function of damaged hearts but also a patient's quality of life, will forever have a guiding and positive influence on me as a physician, scientific investigator, future mentor, and person. I cannot overstate the respect I have for Dr. Bolli and how appreciative I am for the time I have been allowed to work so closely with him. He has praised me when I succeeded, but importantly also allowed me to fail at times, learning valuable lessons along the way. I will always take with me his approach to controversial data and topics, whether scientific or social. I will also use the word "salubrious" in every manuscript I prepare. I would also like to thank my committee members, Dr. Irving Joshua, Dr. Dale Schuschke, Dr. Claudio Maldonado, and Dr. Daniel Conklin for their guidance and support throughout my research fellowship and unconventional dissertation project.

I extend a special thanks to Dr. Joseph Moore, IV and Dr. Marcin Wysoczynski for their friendship, encouragement, direction, colorful discussions, and professional scientific advices over the past three years. I look forward to continued collaborative efforts. Additionally, I express thanks to Dr. Michael Flaherty for his friendship, and advice. Dr. Flaherty's ambition and desire to "Fix broken hearts" both clinically and through scientific endeavors, has further affirmed my aspiration to overlap and integrate science and clinical excellence. Further, I express gratitude to my friends, colleagues,

parents, and family for their support, especially my wife, Morgan, whose unfaltering care, love, and encouragement throughout the years continues to have a profound, daily influence on my life.

Last but not least, I would like to thank the Physiology and Biophysics Department, for affording me the opportunity to pursue this degree in such an unconventional fashion first during my internal medicine residency and then into my cardiology fellowship, especially after the loss of my initial mentor. Specifically, I would like to thank Dr. William Wead and Ms. Denise Hughes who have exhibited such support of my progress throughout the completion of this degree. Without their help, I doubt I would have stayed on track and met any deadlines necessary to graduate. This can essentially be conveyed to all the faculty members as well, as each contributed in some way to my growth and development. Thank you all!

ABSTRACT

CELL-BASED THERAPIES FOR ISCHEMIC CARDIOMYOPATHY– INVESTIGATIONS OF INTRAMYOCARDIAL RETENTION AND SAFETY OF HIGH DOSE INTRACORONARY DELIVERY OF C-KIT POSITIVE CARDIAC PROGENITOR CELLS, AND THERAPEUTIC UTILITY OF A NOVEL POPULATION OF CARDIAC MESENCHYMAL STEM CELLS EXPRESSING STAGE-SPECIFIC EMBRYONIC ANTIGEN– 3 (SSEA-3)

Matthew C. L. Keith, MD

March 18, 2016

Over the last decade attempts at reducing morbidity and mortality of patients with chronic heart failure have been made via the development and implementation of novel cell based therapies. Substantial advances in cell based therapies with indications of efficacy have been shown along with a robust safety profile. Despite these advances, there is a substantial unmet need for novel therapies, specifically addressing repair and regeneration of the damaged or lost myocardium and its vasculature. Accordingly, cardiac cell-based therapies have gained attention. Various cell-types have been utilized, including bone marrow-derived mononuclear cells, bone marrow-derived mesenchymal stem cells, mobilized CD34⁺ cells, and more recently, cardiosphere-derived cells and cardiac-derived c-kit positive progenitor cells. Early studies have suggested a potential of cell-based therapies to reduce cardiac scar size and to improve cardiac function in patients with ischemic cardiomyopathy. However, variability of results has been observed necessitating improvement of current methodologies related to

optimizing the cell type(s), infusion techniques, timing, dosage, acuity related to ischemic injury, and perhaps repeat dosing over time among others, all the while ensuring complete and total patient safety. Accordingly, present efforts and goals of my research are aimed at i.) Optimizing methodologies utilized within the recent phase I clinical trial (SCIPIO) that showed intracoronary infusion of 1 million c-kit positive cardiac progenitor cells was safe with indications of efficacy in cardiac repair, as well as, ii.) Development of a novel cell based approach with a newly discovered cardiac cell type.

Within the present dissertation, I explored the impact of coronary stop-flow on cardiac retention of intracoronarily infused c-kit positive cardiac progenitor cells given that balloon inflation in a non-stented coronary artery is inherently dangerous, especially in already damaged hearts. I demonstrate that intracardiac retention with or without stop-flow is equivalent and balloon inflation confers an undue risk to patients. Furthermore, I investigated the safety of intracoronary infusion of 20 million c-kit positive cardiac progenitor cells in pigs, an equivalent dose 40 times larger than was used in the SCIPIO trial. High dose of cells delivered intracoronarily is safe and does not result in myocardial injury or functional deficit. Therefore, larger doses may reasonably be utilized in future clinical trials. Finally, I describe a novel adult cardiac cell type that maintains expression of an embryonic stem cell associated marker, stage-specific embryonic antigen (SSEA)-3, resides within the native adult heart, and can be isolated and utilized for cardiac repair as a cell based therapy.

TABLE OF CONTENTS

	PAGE
DEDICATION.....	iii
ACKNOWLEDGEMENTS.....	iv
ABSTRACT.....	vi
LIST OF FIGURES.....	x
LIST OF TABLES.....	xii
CHAPTER	
I: CELL BASED THERAPIES FOR CARDIAC REPAIR	1
Introduction.....	1
Review of approaches in cell therapy for myocardial repair.....	3
Non-cardiac cells utilized for cell therapy.....	3
Intrinsic cardiac cell types utilized for cardiac repair	17
C-kit positive cardiac progenitor cells.....	24
Dissertation Overview.....	28
Hypothesis and Research Aims.....	29
II: EFFECT OF THE STOP-FLOW TECHNIQUE ON CARDIAC RETENTION OF C-KIT POSITIVE HUMAN CARDIAC PROGENITOR CELLS AFTER INTRACORONARY INFUSION IN A PORCINE MODEL OF CHRONIC ISCHEMIC CARDIOMYOPATHY	
Introduction.....	32

	Design and Methods.....	34
	Results.....	41
	Discussion.....	49
III:	SAFETY OF INTRACORONARY INFUSION OF 20 MILLION C-KIT POSITIVE HUMAN CARDIAC PROGENITOR CELLS IN PIGS	
	Introduction.....	54
	Design and Methods.....	56
	Results.....	71
	Discussion.....	84
IV:	A NOVEL POPULATION OF HUMAN CARDIAC PROGENITOR CELLS EXPRESSING STAGE-SPECIFIC EMBRYONIC ANTIGEN-3: PHENOTYPE AND THERAPEUTIC UTILITY IN A MURINE MODEL OF ISCHEMIC CARDIOMYOPATHY	
	Introduction.....	89
	Design and Methods.....	91
	Results.....	109
	Discussion.....	136
	REFERENCES.....	139
	CURRICULUM VITAE.....	170

LIST OF FIGURES

FIGURE	PAGE
1. Stop-flow study experimental protocol and timeline	35
2. C-kit positivity, cell product radioactivity, radiolabeling efficiency, cell product viability, cell number, and diffusive loss of indium-111 oxine.	42
3. LV ejection fraction	44
4. Nuclear imaging of hCSC retention.	46
5. Myocardial hCSC retention at 24 h.	48
6. Safety Study protocol and timeline.	58
7. Isolation and expansion of c-kit ^{POS} hCPCs	60
8. Flow cytometric validation and immunocytochemistry of c-kit ^{POS} hCPCs.	63
9. Cumulative c-kit positivity by flow cytometry and Trypan blue cell product viability.	64
10. Intracoronary infusion of 20 million human c-kit ^{POS} CPCs does not impair left ventricular (LV) function or morphology.	72
11. Intracoronary infusion of 20 million human c-kit ^{POS} CPCs does not cause myocardial damage as assessed by cardiac troponin I (cTnI) release.	75

12. Intracoronary infusion of 20 million human c-kit ^{pos} CPCs does not cause myocardial damage as assessed by cardiac CK-MB release.	76
13. Intracoronary infusion of 20 million human c c-kit ^{pos} CPCs does not impair renal function.	78
14. Intracoronary infusion of 20 million human c-kit ^{pos} CPCs does not impair liver function.....	81
15. Detection of human CPCs in control versus hCPC-treated pig hearts.....	83
16. Cells expressing the embryonic stem cell-associate antigen SSEA-3 are present in the human heart and lack hematopoietic lineage markers (lin ^{neg}).....	110
17. SSEA-3 ^{pos} cardiac cells are located within the subepicardium and myocardial interstitium predominantly as solitary cells, and a subpopulation of SSEA-3 positive cells express c-kit, likely representing an intermediate phenotype of cardiac progenitors.....	112
18. SSEA-3 immunoselection: Enrichment of pluripotency associated markers, cardiac mesodermal markers, isolation and expansion.....	116
19. Characterization of <i>in vitro</i> expanded SSEA-3 ^{pos} lin ^{neg}	120
20. Immunophenotype of <i>in vitro</i> expanded SSEA-3 ^{pos} lin ^{neg} CPCs.....	123
21. Validation of PCR products.....	125
22. SSEA-3 ^{pos} lin ^{neg} cells display clonogenic and multipotent differentiation capacities expressing mature cardiac markers of myocytes, smooth muscle, and endothelial cells under directed <i>in vitro</i> differentiation conditions.....	128
23. Left ventricular morphometric analyses.....	131
24. Left ventricular volumetric comparison.....	132
25. Ejection Fraction.....	133
26. Stroke work and cardiac output.....	135

LIST OF TABLES

TABLE	PAGE
1. Antibodies for flow cytometric analyses.....	95
2. Antibodies for immunocytochemistry and immunohistochemistry.....	98
3. PCR genomic target sequences.....	101
4. Antibodies utilized in analyses of terminal <i>in vitro</i> differentiation.....	104

CHAPTER I
CELL BASED THERAPIES FOR CARDIAC REPAIR

Introduction

Cardiovascular disease accounts for more than 30 % of global mortality making it the largest contributor to death worldwide. In the U.S., coronary heart disease accounts for approximately 17 million cases annually^{1, 2}, and there are approximately 5-6 million patients who currently have a diagnosis of heart failure. The most prevalent cause of heart failure is the loss of viable, functioning myocytes which are replaced by noncontractile scar after myocardial infarction, although heart failure from nonischemic causes is quickly becoming more prevalent.³ Nevertheless, the majority of treatment options (medical therapy, catheter-based or surgical revascularization for earlier stages, and mechanical support for later stages) employ strategies to limit further scar formation and curtail deleterious adverse cardiac remodeling while enhancing or supplementing the function of residual myocardium.^{4, 5} While some therapies have improved mortality and work to provide what is essentially a palliative relief of heart failure symptoms, the issue of replacing, reducing, or transforming non-viable scar tissue to functional, contractile and supporting cells remains the ultimate goal. To this end, recent efforts within regenerative medicine have been aimed at adoptive transfer of various stem cell populations in an attempt to accomplish this “holy grail”.

Stem cells are undifferentiated, clonal, self-renewing cells that possess a multi-lineage differentiation potential toward terminal mature phenotypes.⁶ Multiple classifications of stem cells exist that describe the degree of lineages to which one cell may commit. Cells that can differentiate to all of the body's cell types are termed pluripotent or totipotent (such as embryonic stem cells), and others with differentiation limited to one or more lineages of a particular organ are termed unipotent or multipotent progenitors respectively.⁶ Within this framework various types of stem cells, both pluripotent and multipotent, have been evaluated for their utilities in the treatment of heart failure with the goal to curatively replace damaged cardiac tissue and not simply to delay progression of disease.^{7, 8}

The recent explosion of regenerative medicine has led to the exploration of a wide variety of cell types and their respective cardiac differentiation potentials, both *in vitro* and *in vivo*. Knowledge of developmental biology and identification of cellular markers associated with known stem/progenitor phenotypes have enabled identification of candidate cell types that may have cardiomyogenic potential and repair damaged hearts. These include pluripotent embryonic stem cells and induced pluripotent stem cells (and their derivatives) as well as postnatal stem cells that persist into adulthood. Among postnatal cells, populations both intrinsic to the heart (c-kit⁺ cardiac progenitor cells and cardiosphere derived cells), and extrinsic to the heart (bone marrow and adipose derived cells) are under investigation. Importantly, how, when, and the dosage of these progenitor cells that are administered to damaged hearts have been found to drastically impact safety and efficacy of cell based therapy affecting engraftment, longevity, and therapeutic response, which further adds tremendous complexity independent of the intricate cellular

biologic processes. Intuitively, cells of cardiac origin have demonstrated superior ability to adopt more mature cardiac phenotypes⁹, likely secondary to genetic predisposition related to chromatin structure and arrangement, than that of progenitors not of cardiac origin. Moreover, cardiac progenitor cells have demonstrated more robust myocardial reparative effects via a variety of mechanisms independent of their direct differentiation capacity.⁹ Of these, c-kit⁺ cardiac progenitor cells have been the most widely investigated.¹⁰ These cardiac progenitor cells have largely been the focus of our investigations here within the Institute of Molecular Cardiology at the University of Louisville. A brief overarching review of past and present cell based modalities that have been evaluated for cardiac repair and regeneration is provided below with expanded focus on c-kit⁺ cardiac progenitor cells as they are specifically relevant to the present work. The limitations and gaps in knowledge associated with individual modalities and methodologies are highlighted to lay out the rationale for the newly conducted studies described within the present dissertation.

Cell based therapies for heart failure: Extracardiac cell populations

Skeletal Myoblasts

Skeletal myoblasts are cells derived from satellite cells, a skeletal muscle progenitor cell population located beneath the basal membrane of myofibers. Satellite cells undergo proliferation in response to injury and promote repair and regeneration of skeletal muscle via differentiation into new myotubes and muscle fibers.^{11, 12} They are easily obtained from muscle biopsies, rapidly expandable in vitro, and have shown

resistance to hypoxic and ischemic conditions.^{13, 14} Accordingly, skeletal myoblasts were the first cells to be tested in preclinical¹⁵ and clinical¹⁶ studies of HF.

The ability of skeletal myoblasts to promote cardiac repair and recovery has been evaluated in both preclinical and clinical models of HF.¹⁷⁻¹⁹ Studies using both intramyocardial and intracoronary administration of myoblasts demonstrated formation of myotubes and viable skeletal muscle-like grafts within damaged cardiac tissue. Myoblast administration was associated with attenuation of adverse ventricular remodeling, decreased interstitial fibrosis, and improvement of cardiac performance after ischemic injury. Beneficial effects of myoblasts, other than direct supplementation contractility, are mediated by the correction of the imbalance between matrix metalloproteinases (MMPs) and tissue inhibitors of matrix metalloproteinases (TIMPs) involved in extracellular matrix (ECM) remodeling as well as activation of intrinsic cardiac stem cells via the secretion of growth factors.²⁰

The first human transplantation of myoblasts was performed by Menasche et al. in patients with HF secondary to ischemic injury.^{16, 21} Injection of myoblasts into a scarred left ventricular (LV) region at the time of coronary artery bypass grafting (CABG) was associated with a significant improvement in LV function and NYHA classification. However, some treated patients experienced dangerous arrhythmias, specifically, ventricular tachycardia, necessitating implantation of internal cardioverter-defibrillators (ICDs). The electrical instability of treated hearts is due to the lack of electromechanical coupling, and failure of differentiated myotubes to express key gap junction proteins involved in cardiac excitation-contraction coupling, namely connexin.²² This phenomenon is likely due to the fact that myoblasts transplanted in injured hearts form

skeletal (striated) muscle fibers rather than cardiac muscle.^{16, 22} Myoblasts have proven to be unipotent lacking multipotent plasticity to adopt alternate muscle phenotypes. Menasche et al. conducted MAGIC, a phase II randomized, placebo-controlled, double-blind trial that examined the effects of intramyocardial injection of skeletal myoblasts (at two doses: 400 or 800 millions) plus CABG vs. CABG alone (controls) in 97 patients with severe LV dysfunction (LV ejection fraction [EF] between 15-35%). No significant difference in cardiac function or occurrence of malignant arrhythmias between patients receiving myoblasts and controls at the end of 6 months was observed.²¹ Other investigators have used catheter-based intramyocardial injection of skeletal myoblasts in ischemic HF. However, no tangible benefits to LV function or patient quality of life were able to be reproducibly obtained that mirrored those in preclinical models. Presently, attempts at improving cardiac function and ameliorating HF through the use of myoblasts have been all but completely abandoned.²⁰

Bone marrow cells

Unfractionated bone marrow mononuclear cells (BMMNCs) are a heterogeneous population composed of mesenchymal stem cells (MSCs), hematopoietic stem cells (HSCs) such as CD34⁺ cells, and endothelial progenitor cells expressing CD133 (EPCs), as well as more committed cell lineages. BMMNCs, and thereby all the cellular subtypes, can be easily obtained in large numbers by standard technique using density gradient centrifugation and do not require extensive culture or in vitro expansion.²³ They have the advantage of being able to be utilized shortly after isolation thus maximizing therapeutic utility and maximal preservation of intrinsic differentiation potential that may be diminished by prolonged culture in vitro.²³⁻²⁵ Nevertheless, conflicting results have been

obtained with preclinical models of acute MI and chronic HF.²⁵ In sheep and pig models of ischemic heart failure, BMMNCs (injected directly into the scar tissue) produced no improvement in LV function (although one study reported increased angiogenesis and reduction in infarct size).²³ In contrast, studies in dogs and rats have reported improvement in myocardial function and increased angiogenesis.²³

Clinical trials utilizing BMMNCs to treat ischemic heart failure have yielded less than exciting results of efficacy although overwhelming safety has been observed without any teratogenicity.²³ Perin et al. were the first to evaluate the safety and efficacy of autologous BMMNCs, injected transendocardially in patients with ischemic HF demonstrating statistically significant improvement in LVEF and a reduction in end-systolic volume in cell-treated patients.²⁶⁻²⁸ Observations by other investigators using BMMNCs seemed to support these findings.^{29, 30} However, other trials have failed to show any tangible benefit of BMMNCs in the setting of acute or chronic ischemic cardiac injury.^{31, 32} The reasons for discrepant results are not apparent. Additional studies using intracoronary infusion of BMMNCs in patients with HF have also been conducted. Similarly, mixed results have been obtained related to efficacy. Without exhaustively comparing the numerous clinical trials, it may best serve to hypothesize that variations in dosages of cells, cellular consistency of specific phenotypes such as CD34⁺ stem cells or MSCs, route of administration such as intramyocardial vs intracoronary, site of injection such as peri-infarct border zone or direct cell injection into the scar, and timing of cell administration after injury, i.e. chronicity of myocardial dysfunction, may all impact the efficacy of BMMNC therapy.

As is easily seen, these aforementioned factors apply much more broadly to cell based therapies in general and contribute to the totality of lacking knowledge related to not only the optimal cell type to administer to sick hearts to induce functional recovery, but also the how, when, and where to infuse these cells.

In efforts to determine if specific cellular subsets within the bone marrow may offer superior beneficial effects related to cardiac functional improvement, studies have utilized purified mesenchymal stem cells (MSCs)³³ as well as CD34⁺ bone marrow cells. MSCs, also known as bone marrow stromal cells, are a subset of non-hematopoietic bone marrow cells that are multipotent and plastic-adherent under in vitro expansion culture conditions. MSCs have demonstrated chondrogenic, adipogenic, and osteogenic differentiation potential.³³⁻³⁵ MSCs have also been reported to differentiate into cardiomyocytes^{36, 37} and endothelial cells³⁸, although this cardiogenic potential remains controversial^{39, 40} as no mature cardiomyocytes with complete functional sarcomeric apparatus has been observed to arise from MSCs in vitro. In vivo, mature cardiomyocytes observed to possibly arise from implanted MSCs have largely been attributed to fusion events in which MSCs and native cardiomyocytes merge to form one cell.⁴⁰ MSCs typically express the cell surface markers CD105, CD73, CD90, CD29, CD44, and CD166 but lack hematopoietic markers (CD45, CD34 and CD14/CD11b).^{34, 35, 41}

The results of MSC administration in animal models of chronic heart failure have demonstrated salubrious effects of MSC therapy using various intramyocardial and intracoronary injection techniques. Studies utilizing autologous MSCs injected directly into myocardial scar, reduced infarct size and attenuated further deleterious LV remodeling in a porcine model of ischemic cardiomyopathy (ICM).⁴² Intramyocardial

injection of MSCs in rodent models of both ischemic and nonischemic cardiomyopathy have shown improvement in indices of cardiac function and angiogenesis along with reduced myocardial fibrosis.⁴²⁻⁴⁶ These and other preclinical studies provided the groundwork for randomized, double-blind, placebo-controlled studies using autologous and allogeneic MSCs in patients with chronic ischemic LV dysfunction undergoing CABG (PROMETHEUS; NCT00587990)⁴⁷ as well as the POSEIDON trial conducted by Hare et al.⁴² The latter additionally compared three doses of autologous or allogeneic MSCs (20, 100, and 200 ×10⁶ cells) in patients with ischemic cardiomyopathy and demonstrated that all doses favorably impacted patient functional capacity, quality of life, and ventricular remodeling. Further trials using intramyocardial injection of autologous and allogeneic MSCs in ischemic and nonischemic CM are currently underway, specifically, the CONCERT and SENECA phase I/II clinical trials which were conceived and designed here at the University of Louisville within the Department of Cardiovascular Medicine in conjunction with the National Heart, Lung, and Blood Institute (NHLBI) sponsored Cardiovascular Cell Therapy Research Network (CCTRN). I was fortunate to have made substantial contributions to these endeavors under the guidance of my mentor, who is the primary investigator of these studies, Dr. Roberto Bolli.

Hematopoietic stem cells reside in the bone marrow and differentiate into cells of both myeloid and lymphoid lineages centrally within the bone marrow. EPCs, on the other hand, are mobilized into peripheral blood, often in response to ischemic injury, and differentiate into endothelial cells peripherally promoting neovascularization (re-endothelialization).^{48, 49} CD34 is a typical surface marker of both HSCs and EPCs.⁵⁰

Thusly, CD34⁺ cells have the capacity to give rise to all blood cell types as well as endothelial cells (<1% of nucleated cells in the blood are CD34⁺). Autologous CD34⁺ cell transplantation has been performed in patients with ischemic⁵¹ and nonischemic^{52, 53} cardiomyopathy. Injection of CD34⁺ cells into the peri-infarct regions of the left ventricle during coronary bypass surgery produced greater improvement in left ventricular ejection fraction than did coronary bypass alone.⁵¹ Additionally, a study by Vrtovec et al. concluded that intracoronary infusion of CD34⁺ cells led to a modest increase in functional endpoints of ejection fraction and 6-min walk distance and a decrease in levels of the cardiac stress marker NT-proBNP.^{52, 53} Importantly, these beneficial effects were sustained over time. Additional studies by the same group have shown reproducibility of these results related to cardiac function as well as provided data on the effective intracardiac doses responsible for patient response to CD34⁺ bone marrow cell therapy.

Adipose-derived MSCs

Similar to bone marrow, adipose tissue contains a pool of multipotent stem cells, designated as adipose-derived MSCs that are able to differentiate into not only mature adipocytes but also aforementioned cell types of the mesenchymal lineage.⁵⁴ Adipose-derived MSCs have also demonstrated the capacity to upregulate cardiac proteins although this differentiation is incomplete as no organized, functional sarcomeric structure has thus far been able to be obtained, similar to other studies using bone marrow derived MSCs. Nevertheless, adipose derived MSCs administered in animal models of heart failure have shown beneficial effects, mirroring bone marrow MSC preclinical studies.⁵⁴ For example, using a cell sheet technology, Miyahara et al. reported that transplantation of monolayer MSCs into infarcted myocardium reversed wall thinning

and resulted in improved ejection fraction.⁵⁵ In another study, the effects of transplanting undifferentiated or cardiac pre-differentiated adipose-derived MSCs were compared with those of unfractionated BMMNCs in a rat model of chronic ICM.⁵⁶ One month after transplantation into infarcted hearts, undifferentiated adipose-derived MSCs improved EF, augmented angiogenesis, and decreased fibrosis to a greater degree than that observed with adipose-derived cardiomyogenic cells or BMMNCs injection. Additionally, intramyocardial injection of adipose derived MSCs just 1 week after coronary occlusion abrogated the decline in myocardial contractile function and enhanced post infarction angiogenesis in rodents.⁵⁷ Clinical trials utilizing adipose derived MSCs are currently underway.⁵⁸

Embryonic stem cells (ESCs) and ESC-derived cells

Embryonic stem cells (ESCs) are pluripotent cells harvested from the inner cell mass of pre-implantation-stage blastocysts.^{59, 60} When cultured in suspension, allowing sphere formation during in vitro proliferation leading to formation of embryoid bodies, both mouse (m) and human (h) ESCs have demonstrated the capacity to differentiate into cells of all three germ layers, namely, ectoderm, endoderm, and mesoderm (including cardiac myocytes, endothelium, and smooth muscle cells).⁵⁹⁻⁶¹ Particularly, hESC-derived cardiomyocytes exhibit the morphology of adult cardiomyocytes with expression of mature sarcomeric proteins and mature structural arrangement of the contractile apparatus.^{23, 62-64} They also express cardiac-specific transcription factors such as Nkx2.5, GATA-4, and MEF2C and display spontaneous beating activity with characteristic atrial, ventricular, and nodal action potentials.⁶²⁻⁶⁴ The strong cardiogenic potential of ESCs and the availability of hESC-derived cardiomyocytes have motivated research into their

effects in the treatment of heart failure in preclinical models via replacement of lost contractile cells.

Menard et al. first reported that cardiac-committed mouse ESCs, transplanted into infarcted sheep myocardium, engrafted and differentiated into cardiomyocytes and improved LV function.⁶⁵ Similarly, using hESC-derived cardiomyocytes, Caspi et al.⁶⁶ and Cai et al.⁶⁷ reported formation of stable cardiomyocyte grafts, attenuated LV remodeling, and improvement in LV systolic function in rat models with old myocardial infarction (MI) (although in the latter study they caused formation of teratomas). More recently, studies reporting the use of hESC-derived cardiomyocytes (hESC-CMs) in chronic animal models of ischemic cardiomyopathy in other large animals, including non-human primates (specifically macaques)⁶⁸, focused specifically on aspects of engraftment, functional integration, and electrophysiological behavior of transplanted ESC-derived cardiomyocytes in injured myocardium. In guinea pig models, Shiba and colleagues observed re-muscularization with human myocardium which occupied approximately 8% of the scar area. While vehicle and non-cardiac control cell groups demonstrated progressive LV dilatation and fractional shortening deterioration, ESC-CM recipients demonstrated sustained fractional shortening and displayed overall superior fractional shortening relative to controls.⁶⁹ In addition to improved cardiac function, animals transplanted with ESC-CMs also exhibited reduced occurrences of both spontaneous and induced ventricular tachycardic events. Utilizing a genetically encoded calcium sensor (GCaMP3), the activity of hESC-CM grafted cells was tracked *in vivo* suggesting successful electromechanical integration of grafted cells with host myocardium; however, graft-host coupling in injured hearts was notably heterogeneous.⁶⁹

Similar results were observed in a later study employing hESC-CMs in a chronic non-human primate model of ischemic cardiomyopathy.⁶⁸ Here, an unprecedented number of hESC-CMs (1 billion) were delivered intramyocardially to macaques 2 weeks following ischemia-reperfusion injury. According to the authors, hearts of hESC-CM recipient monkeys demonstrated significant re-muscularization of infarct regions which ranged from 0.7 to 5.3% (an average of 3% at 4 weeks and 1% at 12 weeks), comprising approximately 40% of the infarct volume.⁶⁸ Despite the fact that hESC-CMs assumed only an immature phenotype, electromechanical junctions were evident among hESC-CMs and host myocytes shortly after engraftment (2 weeks). The authors showed evidence of electromechanical coupling whereby hESC-CMs exhibited regular calcium transients that synchronized with host electrocardiograms. However, contrary to the guinea pig model where hESC-CMs afforded protection against arrhythmias⁶⁹, increased incidence of ventricular arrhythmias was noted in primate that was given hESC-CMs.⁶⁸

Strong objections to the validity and applicability of the study by Chong et al.⁶⁸ were recently published. In a commentary, Anderson and colleagues highlight notable issues of i.) small number of animals studied; ii.) small size of infarcts; iii.) a lack of infarct size reduction compared to controls in the setting of claims of hESC-CM induced remuscularization; iv.) possible off target effects of the zinc finger nuclease methodology used for gene targeting of the Ca²⁺ indicator GCaMP3 that was utilized to assess electrical coupling; v.) a lack of assessment of cardiac functional parameters or electrical properties; vi.) increased prevalence of cardiac arrhythmias resulting from hESC-CM administration; vii.) a lack of long term follow-up to assess true myocyte regeneration which is characterized by permanent survival and terminal differentiation of engrafted

electrically coupled cells; viii.) a lack of sufficient assessment of teratogenicity of hESC-CMs given that hESC-derived cells are intrinsically heterogeneous, and one cannot guarantee that no cells remain in an undifferentiated, pluripotent state and may therefore give rise to malignancies.⁷⁰ Given the plethora of concerns^{70, 71}, the use of such hESC-CMs in humans and the conclusions of Chong et al regarding the utility of hESC-CMs in treating ischemic cardiomyopathy are untenable. Clear objections to the use of ESCs and ESC-derived cells have been made.⁷¹

Despite the well-documented capacity of ESCs for cardiac differentiation, both ethical and biological concerns have prevented their use as a treatment modality in human patients. Specifically, because of their pluripotency and allogeneic nature, adoptive transfer of ESCs is plagued by teratoma formation^{72, 73} and graft rejection⁷², which essentially preclude the clinical use of these cells. In human clinical research, tolerance for even the possibility of tumor formation is zero. Despite efforts to reduce the probability of this occurrence by various ESC manipulations, it cannot be completely eliminated. Therefore, no clinical trial of ESCs in cardiovascular disease has been conducted, as one neoplastic occurrence within a human trial subject would be sufficient to all but halt clinical investigation of ESCs for the foreseeable future. However, the recent emergence of induced pluripotent stem cells (*vide infra*), has provided an alternative that obviates one of the two major problems inherent in ESC-based therapies – graft rejection secondary to allogenicity.

Induced pluripotent stem cells (iPSCs)

Takahashi and Yamanaka were the first to produce a population of induced pluripotent stem cells (iPSCs) by transducing mouse adult fibroblasts with defined

transcription factors (OCT3/4, Sox2, c-Myc, and Klf4) (the “Yamanaka factors”).^{74, 75} These iPSCs express ESC surface markers and exhibit morphology and growth properties similar to those of ESCs, essentially being reversely reprogrammed from a differentiated cell type with finite phenotype toward an undifferentiated ESC-like cell with clonal expansion, self-renewal, and multilineage differentiation capacities.^{74, 75} This discovery ultimately resulted in a Nobel prize in 2012. Research evaluating the differentiation capacities of iPSCs demonstrated that the cardiogenic potential of iPSCs is very similar to that of ESCs, and that iPSC-derived cardiomyocytes possess functional properties typical of cardiac cells, such as spontaneous beating, contractility, and ion channel expression.⁷⁶ Additionally, iPSCs have shown capacity to form endothelial and smooth muscle cells. Thus, iPSC-derived cell lines have quickly gained momentum for cardiac regenerative applications and multiple strategies have been employed using iPSCs and iPSC-derived cells to treat heart failure in preclinical models.

In 2012, Gu and colleagues demonstrated the intramyocardial delivery of porcine iPSC-derived endothelial cells (piPSC-ECs) in murine infarct models yielded significant improvements in cardiac function via paracrine-mediated promotion of neovascularization and cardiomyocyte survival.⁷⁷ Congruent with these studies, the administration of human iPS-derived mesenchymal stem cells (iMSCs) in a murine infarct model was shown to mitigate ventricular remodeling and preserve myocardial strain via paracrine-mediated promotion of neovascularization and parenchymal/stromal cell integration in infarcted regions.⁷⁸ Thus, while iPS are heralded for their developmental potential, studies such as these suggest their salubrious effects on cardiac function are largely mediated through paracrine signaling mechanisms and not direct

functional integration with preexisting cardiac cell types. Such principles have been mirrored in swine models of ischemia-reperfusion injury.^{79, 80} In said studies, human ESC-derived vascular cells (hESC-VCs) were epicardially delivered via a fibrin patch. Patch-enhanced delivery of hESC-VCs ameliorated contractile dysfunction and LV wall stress, as well improved myocardial perfusion in border zone regions. Concomitantly, hESC-VC delivery promoted the recruitment of endogenous c-kit⁺ cells to infarct zones. Further, cardiac improvements were correlated with enhanced myocardial energetics assessed via *in vivo* ³¹P magnetic resonance spectroscopy-2-dimensional chemical shift imaging.⁷⁹ Shortly thereafter, a similar study was performed by the same group utilizing vascular cells derived from human iPSCs (hiPSC-VCs).⁸⁰ Patch-enhanced delivery of hiPSC-VCs in a swine model of ischemia-reperfusion injury ameliorated ventricular structural and functional abnormalities, reduced infarct size, enhanced vascular density and border zone perfusion, as well as promoted the mobilization of endogenous c-kit⁺ cells to the injury site. These combined effects had pronounced consequences on border zone physiology resulting in enhanced ATP turnover rates and improved contractility.

The ability of ESC/iPSC-derived vascular cells alone to enhance myocardial bioenergetics, border zone contractility, and ventricular function in the face of acute injury was startling and left investigators wondering whether the introduction of additional cardiac cell types sourced from totipotent precursors would have an even greater impact on infarct dynamics and myocardial physiology following injury. This was addressed in the most recent iPSC related study from the Zhang laboratory.⁸¹ Here, human iPSC-derived cardiomyocytes (CM), endothelial cells (EC), and smooth muscle cells (SMC) (totaling 6 million; 2 million per cell type) were simultaneously administered

intramyocardially in a swine ischemia-reperfusion injury model. Cells were delivered in combination with a 3D fibrin patch infused with insulin growth factor (IGF)-encapsulated microspheres. The results of this study showed improvements in ventricular function, infarct size, ventricular wall stress, vasculogenesis, and myocardial metabolism. Further tri-lineage cell transplantation revealed integration of cells into host myocardial tissues, arterioles, and capillaries; the quantity of surviving transplanted cells was substantially greater when used in conjunction with the IGF-infused fibrin patch. Just like what was suggested in previous studies utilizing ESC/iPSC-derived cell types, the molecular basis of the observed improvements in cardiac function and arteriole density, following their transplantation in infarct models, was credited to multiple paracrine mechanisms which could promote cardiomyocyte survival, neoangiogenesis, and cardiac repair.⁸¹

Although iPSCs hold great promise for cardiac regeneration, the transcription factors used to generate these cells (c-Myc, Oct4, and Klf4) are known oncogenes that may induce neoplastic transformation and tumor formation. Newer methods that involve only transient expression of the reprogramming factors rather than permanent over expression may circumvent this problem.⁸² Still, other problems with iPSCs include the extremely low efficiency of iPSC generation and the variability from one cell line to another due to issues such as viral transfection efficiency.⁸³ Technical aspects of these phenomena remain outside the scope of the present report. However, given the rapidity in which the technology in this field is evolving, it is possible that these hurdles will soon be overcome and iPSC-based approaches will become applicable for therapeutic use in the treatment of heart failure; at present, however, iPSCs have not proven ready for clinical application. Accordingly, alternative approaches to ESC-(*vide supra*) and iPSC-

based therapies continue to be explored using autologous and allogeneic postnatal multipotent progenitors.

Cell based therapies for heart failure: Cardiac cell populations

Brief synopsis of fetal cardiomyogenesis and known cardiac progenitors

The heart is the first functional organ formed during embryonic development, with cardiac progenitors specified in early gastrulation. Three spatially and temporally distinct cardiac precursors have been identified by lineage tracing experiments in embryonic development: cardiac mesodermal cells, proepicardial cells, and cardiac neural crest cells. These individual lineages have been established to give rise not only to specific cell types but also to regions of the mature heart.⁸⁴⁻⁸⁶ Understanding the specification of these lineages in forming the mature heart is crucial if insights into the residual progenitors' capacity to contribute to the contractile, vascular, and interstitial compartments, as well as response to injury, are to be gained. A brief synopsis of embryonic cardiac development is provided below.

Within the primitive streak, time-dependent differential co-expression of vascular endothelial growth factor receptor 2 (VEGR2, KDR, Flk-1) allows the divergence of hematopoietic and peripheral vasculature progenitors from the cardiovascular progenitors that give rise to the heart and central portions of the great vessels^{84, 85, 87-89}. The latter are designated by up-regulation of the T-box transcription factors Eomesodermin (Eomes) and mesoderm posterior 1 (Mesp1). These Mesp1⁺/Eomes⁺/KDR⁺ progenitors give rise to cardiac mesodermal cells that create the first and second heart fields (FHF, SHF) with thin endocardium and the proepicardium (PE)^{84, 85, 87-92}. Cooperatively, these mesodermal

progenitors and their progeny form the near entirety of the adult heart. The ectodermal originating cardiac neural crest cells also contribute to fetal cardiomyogenesis, but their contributions to the contractile compartment are thought to be minimal and, therefore, are not covered in this review.⁹³⁻⁹⁵

FHF progenitors in the cardiac crescent are exposed to local cytokines and growth factors, which induce differentiation and up-regulation of essential cardiac regulators such as Nkx2.5, Tbx5, and GATA4, among others. These transcription factors induce commitment to myocyte lineage and sarcomeric protein expression.^{84, 85, 91, 92} Progenitor tracking and lineage tracing studies have shown that the progeny of the FHF eventually gives rise to the myocytes and some smooth muscle cells that predominantly make up the left ventricle and the two atria. The endocardium may also arise from FHF progenitors as early simultaneous development is observed to form the primitive heart tube, although efforts are ongoing to further delineate early divergence of these two fields from one or more upstream progenitors.^{84, 85, 87, 93, 94, 96, 97} Subsequent to FHF commitment and formation of the primitive heart tube, the SHF progenitors, identified by the expression of Isl-1, Nkx2.5, and KDR, begin to proliferate and migrate, undergoing commitment and differentiation under the influence of local FGF, BMP, and Wnt signaling. SHF progenitors have been shown to generate myocytes, some smooth muscle, and some endothelial constituents of the right ventricle and ventricular outflow tract.^{84, 85, 90, 98} Importantly, these Isl-1⁺ progenitors have been found to lack c-kit and Sca-1^{96, 99, 100}, thus likely excluding this compartment as a source of residual myogenic progenitors having a c-kit⁺ phenotype.

At this stage of cardiac development, the myocardium of the first and second heart fields, possessing only a thin endocardial lining within the contorting primitive heart tube is essentially naked, lacking adventitia, perforating vasculature, or surrounding epicardium.^{84, 85, 101} These constituents have been traced to arise from distinct proepicardial progenitor populations that express the transcription factors Wilms' tumor protein (Wt1) and Tbx-18^{84-86, 93, 94, 102}, largely giving rise to adventitial and smooth muscle lineages, as well as Scleraxis (Scx) and Semaphorin3D (Sema3D), giving rise to adventitia and some vascular endothelium not of endocardial origin.¹⁰³ Some of these proepicardial progenitors have been found within endocardial cushions, areas well known to be formed by early endocardial progenitors. This co-localization indicates that these two fields undergo intermigration, essentially cooperating to form the mature structures of the atrioventricular (AV) valves and cardiac septa through epithelial to mesenchymal transition (EMT).^{61, 104, 105} It is currently unclear whether these proepicardial populations stem from Isl-1⁺/Nkx2.5⁺ precursors of the SHF or are separately derived lineages. Tracing studies show that these progenitors migrate over the surface of the exposed myocardium, derived from the first and second heart fields, and form the epicardium and epicardium-derived cells (EPDCs).^{84, 106-109} Once formation of the epicardium is complete, epicardial cells proliferate in a direction parallel to the basement membrane (BM), resulting in thickening of the epicardial lining, or perpendicular to the BM, undergoing epithelial to mesenchymal transition beginning around E12.5-13.5. Ultimately, penetrating mesenchymally-transitioned EPDCs, which populate the subepicardial region, migrate inward to form the coronary plexus (which later becomes the coronary vasculature, with contributions of endocardium-derived endothelial cells and

cardiac adventitial fibroblasts.^{84-86, 98, 104} Additionally, the epicardium and EPDCs are involved in septation and function to stimulate myocardial growth and myocyte division, specifically to aid formation of compact myocardium. Endocardium-derived adventitia aids in forming the inner trabecular myocardium.⁶⁰

It has recently been suggested that EPDCs may generate cardiomyocytes in fetal development, but this is currently unresolved. Questions have been raised regarding the specificity of the initial model that used Tbx-18 for in vivo tracing of EPDCs.^{110, 111} However, similar subsequent evaluation of EPDCs by Zhou et al using WT1 also suggested that EPDCs can in fact contribute to mature cardiomyocytes during fetal cardiogenesis although this was rare.¹⁰⁹ The same group also performed tracing studies of WT1⁺ epicardial cells in adult mice but did not find that these cells contribute to cardiomyocytes or endothelium after infarction; lineage commitment after ischemic injury-induced epicardial activation was primarily limited to smooth muscle and adventitial cells.¹⁰⁹ Importantly, the study did observe that epicardial activation did occur as a result of ischemic injury, leading to proliferation and migration of EPDCs into the damaged myocardium in a reparative role. However, the aforementioned findings would support the concept that the differentiation capacity of WT1⁺ epicardial cells that persists into adulthood is less than that present in fetal development, because a more limited lineage commitment, restricted almost entirely to non-myocytes, was seen in adult mice.¹⁰⁹ Scx/Sema3D⁺ cells were found to be a distinct population of proepicardial cells having only 33% overlapping co-expression of either WT1 or Tbx-18. Scx/Sema3D⁺ cells were found to give rise predominantly to coronary endothelial cells and adventitial cells with some additional contributions to smooth muscle, and rarely cardiomyocytes in

the embryonic heart.¹⁰³ This disproportionately low magnitude of cardiomyogenic potential mirrors that observed by the Zhou et al tracing study of WT1⁺ cells.^{109, 112} Although initial studies in zebrafish suggested that activation of epicardial progenitors was responsible for cardiomyocyte replacement after injury, more recent work has shown that they act by inducing division of existing cardiomyocytes; epicardial cells were traced to give rise only to non-myocyte lineages in that model.^{86, 103, 113-116} The current consensus is that the direct contribution of EPDCs to the myocardium is minimal and that cardiomyocyte differentiation is a rarity among EPDCs, at least in the postnatal heart.⁸⁶

Recent studies of the origin of the endocardium, its formation, and its eventual contribution to mature cardiac lineages have found that its proportional contributions to mature lineages is similar to that attributed to proepicardium-derived cells. The endocardium arises very early in cardiac embryogenesis, simultaneously with the FHF, likely stemming from a common progenitor. Endocardial cells have been shown to arise from Bry⁺/Flk-1⁺/Nkx2.5⁺ progenitors forming the primitive heart tube.¹⁰¹ These progenitors are distinct from hemangioblast precursors and are identified by a distinct expression profile (an E-cadherin^{low}, Flk1^{low}, NF-ATc1⁺ phenotype).¹¹⁷ NF-ATc1 was found to be expressed exclusively in endocardium, providing a lineage specific marker that enables differentiation of the endocardium from other endothelial cell types.¹¹⁸ Tracing and knockout studies performed by de la Pompa et al. demonstrated that endocardial cells not only contribute to a subset of cardiac endothelial cells, but also are integral to cardiac cushion formation, valvulogenesis, septation of the atria, ventricles, and aortopulmonary trunks, as well as to guiding myocardial trabeculation.^{101, 118} These processes are governed by EMT of endocardial cells (similar with respect to mechanism

and signaling pathways to that widely recognized to occur in EPDCs) that precipitates differential commitment to various mature cardiac lineages.¹⁰⁴ The complex regulatory pathways underlying EMT of endocardial cells (as well as that of EPDCs) involve Notch, TGF beta superfamilies, SMADs, Wnt/ β -catenin, and bone morphogenic proteins (BMPs) signaling among others. Comprehensive reviews of these signaling cascades have recently been published.¹⁰⁴ NF-ATc1 null mice, which lacked endocardium and therefore endocardial contributions to cardiac morphogenesis, showed marked abnormalities in trunkal, valvular and septal formation which were ultimately embryonically lethal. Interestingly, myocardial, adventitial, and most vascular endothelial compartments were found to be unaffected indicating that the endocardium does not contribute significantly to these compartments.¹⁰¹ Similarly, studies in Tie-1/TEK(Tie2) null mice showed early embryonic lethality with impairment not only of endocardium formation but also of valvular and septal derivatives, and a lack of myocardial trabeculation.¹¹⁹ Interestingly, there was no impairment of early cardiomyocyte formation.¹¹⁹ It remains unclear, however, whether there are subpopulations of endocardial cells not defined by NF-ATc1 or Tie1/TEK expression that may contribute to these lineages.

Cardiosphere-derived cells

Cardiospheres were first described by Messina et al. in 2004.¹²⁰ Using atrial or ventricular human biopsy samples and murine hearts, these authors identified a population of cells that grew as self-adherent clusters and showed ability to differentiate into cardiomyocytes, endothelial cells, and smooth muscle cells. Messina et al. termed these clusters “cardiospheres”. Cardiospheres were also able to be obtained from

percutaneous endomyocardial biopsy specimens. Cardiospheres were plated and expanded *in vitro* to yield cardiosphere-derived cells (CDCs)¹²¹. Cardiospheres and CDCs are a heterogeneous mixture of many different cell types, including cells that express endothelial (KDR [human]/ flk-1 [mouse], CD31), stem cell (CD34, c-kit, Sca-1), and mesenchymal (CD105, CD90) antigenic markers.¹²⁰ Importantly, the precursor cell(s) that gives rise to cells capable of cardiosphere generation and CDCs has yet to be identified. CDCs were reported to differentiate into electrically stable cardiomyocytes *in vitro* and, to promote cardiac regeneration and improved cardiac function when injected into a murine infarct model.¹²¹ Johnston et al. reported that intracoronary delivery of human CDCs in pigs with old MI resulted in cardiac regeneration, reduction in “relative” infarct size, abrogation of adverse LV remodeling, and improvement in ejection fraction.¹²²

One clinical trial has been conducted to date using CDCs in patients with ICM. The safety and efficacy of direct intramyocardial injection of CDCs and cardiospheres were compared in a porcine model of ICM. Although CDCs and cardiospheres had equivalent effects on ejection fraction, the latter proved superior in improving hemodynamics, regional cardiac function, and reducing ventricular remodeling. This preclinical work was translated by Makkar et al. in a phase I, randomized trial (CADUCEUS) in patients with a recent myocardial infarction and LVEF \leq 45% but \geq 25%.¹²³ Patients received an intracoronary infusion of escalating doses of autologous CDCs (12.5, 17.3, or 25 x 10⁶ cells) or vehicle control with standard medical therapy. CDC-treated patients exhibited a 42% reduction in scar size (from 24% to 12% of the left ventricle), associated with an increase in viable tissue and regional systolic wall

thickening in the infarcted region. CDC therapy failed to increase ejection fraction, reduce LV volumes, or improve heart failure functional class or quality of life as assessed by standard questionnaire.¹²³ Further studies utilizing CDCs/cardiospheres are currently underway.

C-kit positive cardiac progenitor cells

The observation of sex mismatched cardiomyocytes of recipient origin in donor hearts led to the conclusion that cells circulating in the peripheral blood, likely originating from the bone marrow, engraft and transdifferentiate into integrated, functional cardiomyocytes.¹²⁴ Several studies of unfractionated bone marrow and bone marrow-derived mesenchymal stem cells (MSCs) have shown beneficial effects, but differentiation of these cells into cardiomyocytes seems unlikely^{125, 126}; more likely mechanisms include paracrine actions and/or cell fusion of cardiomyocytes and bone marrow derived cells.¹²⁵⁻¹²⁷ Importantly, evidence of cardiomyocyte division, coupled with carbon-14 labeling studies, has led to the recognition that there is cardiomyocyte turnover in the adult heart, fueling the search for a cardiac stem cell compartment that is innately endowed with cardiomyogenic potential.^{128, 129}

In 2003, Beltrami et al. reported the discovery of resident c-kit⁺ cardiac cells (CSCs) that were able to give rise to all cardiac lineages including cardiomyocytes.¹³⁰ The initial discovery was based on the presence of the c-kit receptor on hematopoietic progenitors; it was postulated that the presence of c-kit may identify a cardiac population of myocardial progenitors similar to that of the hematopoietic compartment.¹³⁰ In fact, this is what Beltrami and colleagues found. They observed co-localization of c-kit with Nkx2.5, GATA-4 (transcription factors active in cardiomyogenesis), and Ki-67 (a nuclear

antigen associated with cell division) but not with mature sarcomeric proteins, suggesting a precursor cell, i.e., a proliferating cell that is apparently committed to cardiac lineage but lacks a mature phenotype. The absence of the hematopoietic markers CD34 and CD45 indicated that the cells were not immediately from the bone marrow, and were therefore intrinsic to the heart. Therefore, it was concluded that the c-kit⁺ cardiac cells were derived from the embryonic cardiac compartments that give rise to the adult myocardium.¹³⁰

Since the c-kit receptor plays an important role in prosurvival and pro-proliferative signaling, the c-kit⁺ phenotype may represent an intermediate progenitor, derived from an upstream c-kit⁻, more undifferentiated cardiac progenitor in which c-kit expression increases in conjunction with cell cycle entry and differentiation. This remains a conjecture, however, as direct observation of this is currently lacking, although it is extremely probable. Beltrami and colleagues also alluded to this possible hierarchy in their report of c-kit⁺ cardiac cells, which were found to largely coexpress Nkx2.5.¹³⁰ This postulated upstream resident progenitor in the heart has yet to be identified. Evidence of a similar phenotypic progression, now widely accepted, was observed in the bone marrow with the isolation in 2003 of c-kit⁻ hematopoietic stem cells, which were found to give rise to c-kit⁺ intermediate phenotypes that ultimately were able to reconstitute all mature hematopoietic lineages.¹³¹

Over the last decade, conflicting results have been obtained with respect to the cardiomyogenic ability of c-kit⁺ cardiac cells. In vitro, differentiation of cells from adult hearts into mature beating cardiomyocytes has not been reported although expression of some sarcomeric proteins has been found^{130, 132, 133}. In vivo, reports of adult

cardiomyocyte formation^{130, 132, 134-138} have not been reproduced by several other labs^{9, 10, 139-146}. Whether this discrepancy is caused by differences in source (fetal and/or neonatal cells vs. adult cells), or culture, isolation, or expansion conditions remains to be determined.

Nevertheless, the ability of human and rodent c-kit⁺ cardiac progenitor cells to ameliorate left ventricular dysfunction and pathologic remodeling and promote regeneration has been repeatedly demonstrated by several laboratories in various preclinical animal models of acute myocardial infarction.^{132, 141-143, 145-147} Intramyocardial injection of c-kit⁺ cardiac progenitor cells within the border zones of an infarct 20 days after a permanent coronary occlusion in rats resulted in attenuation of LV dilation and preservation of LV function.¹⁴⁷ Additionally, Tang et al.¹⁴⁵ demonstrated that administration of CPCs is effective in regenerating cardiac tissue and alleviating post-infarction LV remodeling and dysfunction when these cells are infused intracoronarily in the setting of chronic ICM produced by a temporary coronary occlusion followed by reperfusion. One month after coronary occlusion/reperfusion, rats received an intracoronary infusion of vehicle or EGFP-labeled cells. Notably, CPC-treated rats exhibited more viable myocardium in the risk region, less fibrosis in the noninfarcted region, and improved LV function. Interestingly, the number of EGFP⁺ cells expressing markers of cardiogenic commitment was too small to account for the augmentation of LV function (EGFP⁺ cells accounted for only 2.6±1.1% of the region at risk and 1.1±0.4% in the noninfarcted region). In short, CPCs did not survive, engraft, or differentiate into mature cardiac phenotypes within the myocardium.¹⁴⁵ These observations suggest that the important mechanism whereby CPCs generate their beneficial effects was likely a

paracrine action of donor cells on the endogenous myocardium with secretion of cytokines/growth factors locally. Also, induction of endogenous CPC proliferated and differentiated into adult cardiac cells was indicated by the finding that the pool of endogenous CPCs expanded to a greater degree in CPC-treated than in control rats.¹⁴⁵ Similar results were obtained with intracoronary infusion of autologous CPCs into a large, clinically-relevant porcine model of ICM in which pigs underwent a 90-min coronary occlusion followed by reperfusion.¹³⁹ Intracoronarily delivered stem cells to the infarct-related artery using the stop-flow technique produced an increase in ejection fraction and systolic thickening fraction in the infarcted left ventricular wall, as well as a decrease in left ventricular end-diastolic pressure (LVEDP) and an increase in left ventricular dP/dtmax in pigs with old infarcts.¹³⁹ The encouraging results of these studies of intracoronary CSC infusion in the setting of an old MI laid the groundwork for SCIPIO, the first clinical trial of c-kit⁺ CPCs.^{139, 148}

Because of encouraging results of both preclinical and clinical studies, c-kit⁺ cardiac progenitor cells have emerged as one of the most attractive cell types for therapeutic application. At the preclinical level, numerous studies conducted by many independent laboratories in a wide variety of animal models of ischemic cardiomyopathy have consistently documented salubrious effect of exogenous c-kit⁺ cardiac progenitor cells on left ventricular function and structure, including evidence of regeneration of dead myocardium. At the clinical level, a small phase I study (the SCIPIO trial) has documented the safety of autologous c-kit⁺ cardiac cell administration in patients with ischemic heart failure.¹⁴⁸ Although SCIPIO was not designed to assess efficacy, its results suggest that c-kit⁺ cells may impart beneficial effects on left ventricular function, quality

of life, functional class, and infarct size, providing a rationale for larger trials aimed at determining efficacy. Such trials will undoubtedly utilize larger dose(s) of cells than was administered to patients within the SCIPIO trial (just 1 million).¹⁴⁸ However, no studies have evaluated the safety of escalating doses of cells delivered intracoronarily, which could have adverse effects such as embolization and resultant myocardial ischemia. Such an event could be catastrophic to already structurally and functionally compromised hearts damaged from prior infarction.

Dissertation Research: Overview

With the work contained in this dissertation, in addition to providing the above broad review of clinically relevant past and present cell based therapeutic approaches, I sought to expand current modalities of cell based therapies in the treatment of ischemic heart failure through discovery and evaluation of novel cardiac cell types and expansion of applications of existing approaches using intracoronarily delivered c-kit⁺ cardiac progenitor cells. I evaluated the safety of larger doses of intracoronarily administered c-kit⁺ cardiac progenitor cells as well as their intracardiac retention post intracoronary delivery within a clinically relevant porcine model of chronic ischemic cardiomyopathy. Such data are immediately relevant and translatable to the design of human clinical trials utilizing c-kit⁺ cardiac progenitor cells (CPCs). Data demonstrating this fact are included in two recently published peer reviewed publications and were also presented at the 2015 Scientific Sessions of the American Heart Association annual meeting by Dr. Roberto Bolli. These data directly aided in the design of the phase I/II clinical trial CONCERT that has recently initiated enrollment. In addition, I provide data related to the discovery,

characterization, and therapeutic potential of a novel population of postnatal cardiac progenitors, possibly hierarchically related to c-kit⁺ cardiac progenitor cells, that residually express embryonic stem cell associated antigens and are not yet described within the literature. Accordingly, some of the data represented herein remain unpublished and highly confidential. These data will be prefaced in much more detail throughout the manuscript (*vide infra*).

Hypothesis and Research Aims

Hypothesis:

A. The present research seeks to empirically examine the safety of high dose intracoronary administration of cardiac stem cells within a porcine model to provide relevant information to the design of future clinical trials of cell-based therapy for myocardial repair. B. Additionally, the research seeks test the validity of and provide rational for or against the use of the Stop-flow technique during intracoronary infusion based on the dogma that Stop-flow is necessary for improved cardiac retention of cells post infusion by abrogation of downstream cellular washout. C. Finally, the research seeks to ascertain whether additional populations of cardiac progenitors that may express stage-specific embryonic stem cell associated antigens (SSEAs), previously alluded to exist within the rodent myocardium), may be found within the human heart. Could such cells be isolated from the human heart, expanded *in vitro*, and utilized for myocardial repair after ischemic injury thus providing an new target cell type to be utilized in future human clinical trials in patients with ischemic heart failure.

Aims:

1. Measure and compare intramyocardial retention of intracoronarily infused

CPCs with vs without utilization of coronary stop-flow conditions via radiolabel tracking of cell distribution.

2. Determine safety of high dose intracoronary CPC administration via assessment of myocardial damage/injury via measurement of temporal cardiac biomarker release as well as functional parameters measured by 2D echocardiography over 1 month following intracoronary infusion. Additionally, determine safety of high dose CPC administration related to clinical indices of systemic organ function, namely hepatic and renal function.

3. In clinically relevant human right atrial appendage samples obtained from open heart surgeries, determine if there are intramyocardial populations expressing Stage-specific Embryonic Antigens-3&4 that may indicate existence of a yet undescribed cardiac progenitor pool. Additionally, characterize this population and ascertain *in vitro* differentiation capacity to possibly relate it to one or more embryonic cardiomyogenic compartments. Finally, determine reparative potential of such cells in a model of ischemic cardiomyopathy.

Hypothesis and Aims Summary:

I hypothesized that higher doses of c-kit⁺ CPCs delivered intracoronarily in pigs with prior infarctions would be safe and not result in myocardial damage via embolic phenomena. Furthermore, I hypothesized that intracardiac retention of intracoronarily delivered c-kit⁺ CPCs would be very low, indicating that the salubrious effects observed in prior studies were imparted by only a small fraction of the administered dose. In aim 1, I utilized indium-111 radiolabeling and nuclear gamma camera imaging to localized

the anatomic site of cell deposition/retention and quantify the intracardiac retention of cells 24 h post administration to confirm that only a small fraction of cells are actually retained within the heart and are responsible for beneficial effects irrespective of any attempt to maximize cell retention by coronary stop-flow. In aim 2, , I demonstrated that there was no release of cardiac biomarkers or decline in cardiac function indicative of myocardial injury after intracoronary administration of 20 million c-kit⁺ CPCs thus confirming safety of doses higher than that previously using in clinical trials to date. A comprehensive review of the literature related to the possible origins of c-kit⁺ CPCs led me to hypothesize that there were yet unidentified upstream progenitors within the heart that may give rise to c-kit positive intermediate phenotypes during differentiation. I hypothesized that these primitive cells may retain characteristics typical of other undifferentiated primitive cells, specifically embryonic stem cell associated antigens that may aid in identification and isolation. In aim 3, I successfully identified cardiac cells expressing stage-specific embryonic antigen (SSEA) – 3, demonstrating a partial overlapping phenotype with c-kit expression *in vivo*, and that SSEA-3⁺ cells possess therapeutic utility in the treatment of ischemic cardiomyopathy after isolation and *in vitro* expansion.

CHAPTER II

EFFECT OF THE STOP-FLOW TECHNIQUE ON CARDIAC RETENTION OF C-KIT POSITIVE HUMAN CARDIAC PROGENITOR CELLS AFTER INTRACORONARY INFUSION IN A PORCINE MODEL OF CHRONIC ISCHEMIC CARDIOMYOPATHY

Introduction

Since their initial discovery and characterization¹³⁰, c-kit⁺ (c-kit^{POS}) cardiac progenitor cells (CPCs) have emerged as a promising modality in the treatment of ischemic cardiomyopathy. Preclinical studies conducted over the last decade have reproducibly demonstrated the capacity of *in vitro* expanded c-kit^{POS} cardiac cells to induce myocardial repair and functional recovery.⁸ These observations led to the Cardiac Stem Cell Infusion in Patients with Ischemic Cardiomyopathy (SCIPIO) phase I clinical trial, which demonstrated the safety and feasibility of intracoronary delivery of c-kit^{POS} CPCs in humans.¹⁴⁸ Recently, the safety of even larger doses (up to 20 million *in vitro* expanded c-kit^{POS} CPCs) has been demonstrated in a porcine model and will be discussed later (*vide infra*).

In SCIPIO¹⁴⁸, as well as in almost every trial of intracoronary cell infusion performed to date, the cells were delivered with the stop-flow technique¹⁴⁹⁻¹⁵¹; that is, an intracoronary balloon was inflated to stop flow within the coronary artery and prevent rapid wash out of the cells, thus, in theory, promoting greater cell retention by enhancing vascular adhesion and extravasation into the surrounding myocardium. This approach is

being used in most ongoing and planned clinical trials in which cells are infused intracoronarily. Although theoretically attractive, however, the stop-flow technique has not been shown to be superior to non-occlusive cell delivery in terms of cell product retention. The stop-flow technique is potentially hazardous^{152, 153}, and therefore constitutes an impediment to the widespread use of cell therapy in patients with cardiovascular disease, particularly when, as is often the case in chronic ischemic cardiomyopathy, the culprit coronary arteries targeted for cell delivery are not stented. Manipulation of a non-stented coronary artery with an intraluminal balloon under pressure carries a significant risk of vascular damage, coronary artery dissection, and even life-threatening arterial perforation and rupture.¹⁵² In addition, the interruption of coronary flow may elicit myocardial injury, either directly from epicardial coronary artery occlusion or by distal microembolization of dislodged atherosclerotic plaque material^{154, 155}, and may cause arrhythmias in already dysfunctional hearts. Again, this issue is particularly relevant to patients with ischemic cardiomyopathy, whose targeted coronary arteries or bypass grafts are often not protected by stents.

Given the seriousness of the aforementioned complications, objective evidence of improved cell retention is essential to justify subjecting patients to increased procedural risks in future clinical trials involving intracoronary administration of cell-based products. However, as mentioned above, despite the widespread assumption that the stop-flow technique promotes improved extravasation and cardiac retention of cells, no studies have evaluated the utility of the technique using c-kit^{pos} CPCs or any cardiac-derived cell. Accordingly, we addressed this issue in a clinically relevant porcine model of ischemic cardiomyopathy in which we measured the cardiac retention of 10 million indium-111

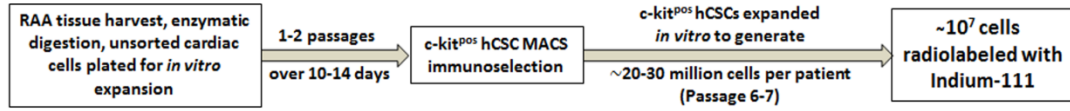
oxine radiolabeled c-kit^{pos} CPCs infused with or without the stop-flow technique. Additionally, this study allows determination of the effective intracardiac retention of CPCs that resulted in the salubrious effects of intracoronarily delivered CPCs observed in the SCIPIO trial.¹⁴⁸

Methods

Ethics Statement

This study was carried out in strict accordance with the Guide for the Care and Use of Laboratory Animals of the National Institutes of Health and the guidelines of the Animal Care and Use Committee of the University of Louisville (KY) School of Medicine following the guidelines set forth by the 1996 Guide for the Care and Use of Laboratory Animals.. The protocol was approved by the Institutional Animal Care and Use Committee (IACUC) of the University of Louisville (IACUC number: 12114). The experimental protocol is illustrated in Fig. 1.

A. Generation of indium-111 oxine-labeled c-kit^{POS} hCSCs



B. Administration of Indium-labeled hCSCs *in vivo* in Pigs

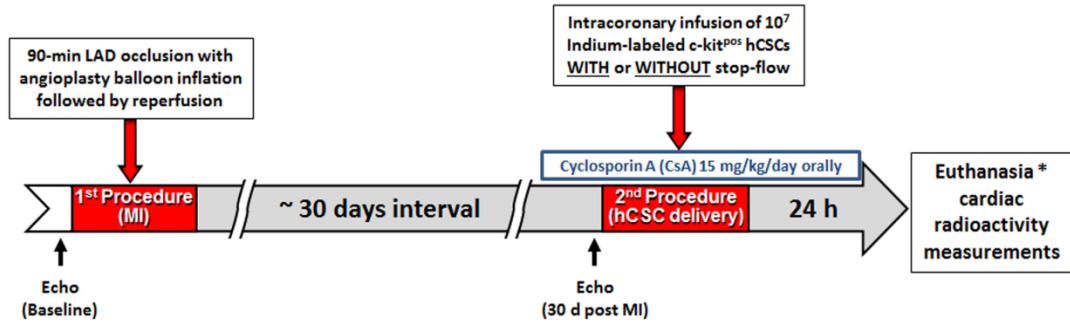


Figure 1. Stop-flow study experimental protocol and timeline.

Human c-kit^{pos} CSC isolation and flow cytometry

Isolation, immunomagnetic selection, and flow cytometric analysis of c-kit^{pos} hCPCs was performed as previously described.^{139, 156} Briefly, human right atrial appendage specimens (RAAs) were obtained with Jewish Hospital Institutional Review Board (IRB) approval (IRB number 07.0062) from patients undergoing open-heart, on pump, coronary artery bypass surgery at Jewish Hospital in Louisville, Kentucky. All patients were between 40 and 80 years of age, so as to approximate the ages of patients in the recently conducted SCIPIO trial.¹⁴⁸ RAAs were washed several times with PBS and were minced to obtain fragments < 1mm³. The tissue fragments were underwent multiple rounds of enzymatic digestion. Isolated cells were plated in a 6-well plate for passage 0 initial expansion. Passage 1 cells were sorted for c-kit with anti-CD117 Miltenyi microbeads and a Miltenyi magnetic sorting apparatus per manufacturer's specifications. Positively selected cells were expanded exponentially over 3-4 additional passages to obtain 2-3 x 10⁷ cells per patient. Multiple patients' cells were pooled to obtain a uniform cell product that was radiolabeled and infused intracoronarily into pigs. Cells were assessed for c-kit positivity by flow cytometric analysis at passage 3 after fixation and labeling with c-terminal specific Santa Cruz C19 rabbit polyclonal IgG anti-human c-kit antibody and secondary antibody, a FITC or APC conjugated Invitrogen donkey anti-rabbit IgG versus isotype control using a BD LSR flow cytometer. BD LSR DIVA software was used for final analysis of c-kit positivity.

Cell product generation and indium-111 oxine radiolabeling

In vitro expanded c-kit^{pos} CPCs were trypsinized and washed with sterile PBS and resuspended in Plasmalyte-A solution with ~750 µCi indium-111 oxine, purchased from

Cardinal Health, Nuclear Pharmacy Services in Louisville, Kentucky, for 20 min at 37°C with 5% CO₂. A Capintec CRC-15R Radioisotope Dose Calibrator was used to conduct all radioactivity measurements. After 20 min, the cells were washed twice in 10 mL of cold Plasmalyte-A to remove unbound radioisotope. The cells were resuspended in 1-2 mL of Plasmalyte-A for final cell count and viability by hemocytometer and Trypan blue. A final radioactivity measurement was made to assess percent radiolabeling efficiency.

After the intracoronary infusions were completed, tubes, catheters, plastic ware, and other materials that had come into contact with the radiolabeled cells were taken back to the dose calibrator for radioactivity measurement. The residual radioactivity was subtracted from that of the labeled cell product to obtain the radioactivity of the cell product that was administered intracoronarily. This number was recorded and utilized for all subsequent calculations of cardiac cellular retention.

Radiolabeling efficiency

Radiolabeling efficiency was defined as the ratio between the final radioactivity of the cell product prior to infusion and the initial dose of indium-111 to which the cells were exposed.

Adjustments for diffusive loss of Indium-111 oxine over the 24 h follow-up and calculation of cardiac radioactivity

Diffusion of unbound indium-111 oxine out of labeled cells continues over time, and this may lead to potential underestimation of cell retention. Similar observations have been made in prior studies.¹⁵⁷

Experiments were performed in triplicate. Ten million cells were radiolabeled with indium-111 oxine as described and placed in 5 mL serum-free Ham's F12 medium

for 24 h with periodic media changes. Media was completely changed every 4 h to maintain a high diffusive gradient similar to that which occurred in vivo after cell infusion. Extreme care was taken to avoid loss of cells. After 24 h, cells were centrifuged and the cell pellet assessed for radioactivity. Diffusive loss was quantified as percent of expected radioactivity after accounting for radioactive decay over the 24 h incubation period. A correction factor was generated by dividing 100 by this observed percent of theoretical maximum radioactivity, so as to account for all infused cells and avoid underestimation of intracardiac retention at 24 h.

The radioactivity measured in all cardiac segments was adjusted according to the correction factor (3.52) to obtain the corrected radioactivity for each cardiac tissue specimen. All radioactivities were then summed to obtain the total radioactivity of each heart. This total corrected cardiac radioactivity was divided by the expected maximum radioactivity of the infusate (adjusted for time dependent decay) to obtain the percent retention of the intracoronarily delivered indium-111 oxine labeled cell product.

Animal procedures

Female Yorkshire pigs (39.8 ± 5.2 kg, age 12-18 weeks) were sedated using a cocktail of ketamine (20 mg/kg, i.m.) and xylazine (2 mg/kg, i.m.), intubated, and mechanically ventilated with 100% oxygen. Anesthesia was maintained with 0.8-1.5% isoflurane. A femoral artery cut-down was performed and an 8F arterial sheath was placed; a 7F Hockey-stick guide catheter was advanced to the left coronary ostium. An angioplasty balloon catheter was positioned in the left anterior descending (LAD) coronary artery at a site distal to the first diagonal branch, after which the pigs were

subjected to a 90-min LAD coronary occlusion followed by reperfusion by inflation and deflation of the balloon, respectively (Fig.).

One to two months (45.3 ± 4.5 days) after MI, the pigs were reanesthetized. An angioplasty balloon catheter was placed in the LAD at the site of the previous occlusion. Indium-labeled hCSCs were administered with four infusions, each consisting of 3 ml over 30 s, with or without concurrent 3-min balloon inflation. In the pigs with balloon inflation, five cycles of 3-min balloon inflation/3-min deflation were performed. The aim of the first cycle, which was performed without infusing cells, was to increase microvascular permeability in the distal myocardium; during the following four cycles, hCPCs were infused into the coronary artery as described above. In the pigs without balloon inflation, hCPCs were infused four times; each infusion lasted 30 s and the four infusions were interspaced with intervals of 5 min and 30 s (Fig. 1).

Twenty-four hours after hCPC administration, the pigs were euthanized and various organs (heart, lung, liver, kidney and spleen) were harvested for analysis.

Immunosuppressive therapy

Pigs received 15 mg/kg/day of oral cyclosporine (Novartis) orally starting 3 days before cell infusion and continuing until euthanasia.

Echocardiography

Echocardiograms were obtained at baseline (before the induction of infarction) and again 30 d later (prior to radiolabeled hCPC intracoronary infusion) using an HP SONOS 7500 ultrasound system (Philips Medical Systems) equipped with a HP 21350A (S8) 3.0-8.0 MHz sector array ultrasound transducer. Briefly, pigs were anesthetized and placed in the left lateral decubitus position. Temperature was kept between 37.0°C and

37.5°C with a heating pad. The parasternal short-axis view was used to obtain 2D and M-mode images.¹⁴⁸ Systolic and diastolic anatomic parameters were obtained from M-mode tracings at the mid-papillary level. Digital images were analyzed off-line by a single blinded observer using the ComPACS Review Station (version 10.5) image analysis software (Medimatic, Las Cruces, NM 88004, USA) according to the American Society of Echocardiography standards.¹⁵⁸

Nuclear imaging and cardiac radioactivity measurements

Perfusion fixed porcine hearts were subjected to nuclear imaging and radioactivity measurements. After whole heart nuclear imaging with Picker Prism 2000 XP nuclear gamma camera, hearts were bread-loafed into five slices of equal thickness from the apex to the base; each slice above the apex was then subdivided into three regions: right ventricle, left ventricular free wall, and septum. The base was divided into right and left sections. The right and left atria were sectioned and placed into independent containers. The proximal portions of the great vessels were removed and placed together into another container. All specimens were measured with a Capintec CRC-15R Radioisotope Dose Calibrator and the anatomic regions were combined to create a regional distribution of radioactivity. The radioactivity in all regions was then combined to obtain the total radioactivity in each heart. The same dose calibrator was used throughout the study.

Statistics

Student's t-test, one-way ANOVA, or two-way repeated measures ANOVA, as appropriate, was employed for comparisons of echocardiographic parameters, radioactivities, and cell retention between groups. All data are reported as means \pm SEM.

Results

Flow cytometric analysis

Flow cytometric analysis for c-kit expression was performed for seven cell lines at early passage as described (c-kit positivity ranged from 72.6% to 90.8%). The mean c-kit positivity of the cells utilized for the study as assessed by standard protocol was $81.6 \pm 7.0\%$ compared with isotype control (Fig. 2A).

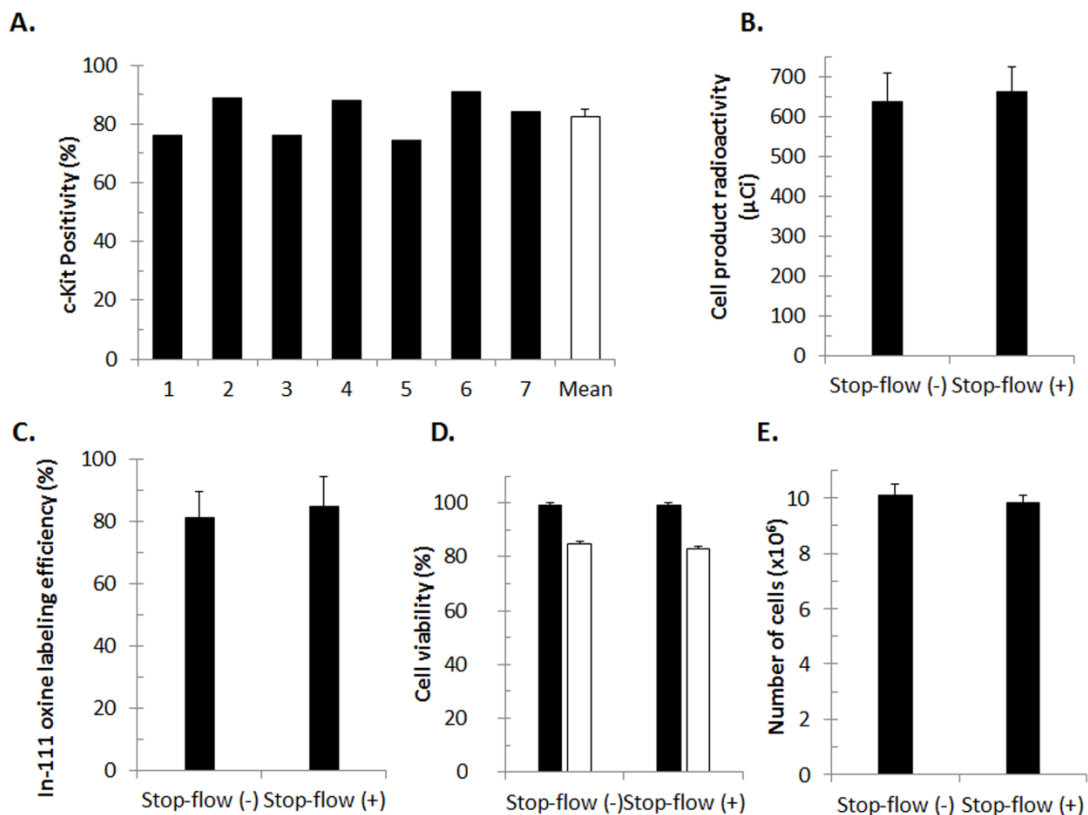


Figure 2. C-kit positivity, cell product radioactivity, radiolabeling efficiency, cell product viability, cell number, and diffusive loss of indium-111 oxine. A. C-kit positivity of individual cell lines is illustrated by black bars, with mean positivity shown in white. C-kit positivity ranged from 72.6% to 90.8% with mean c-kit positivity of $81.6 \pm 7.0\%$. Cell lines were combined to obtain a homogenous cell product. B. Mean final cell product radioactivity of cells infused with continuous flow [Stop-flow (-)] or stop-flow [Stop-flow(+)]. C. Indium labeling efficiency of cells administered with or without stop-flow. D. Mean cell viability, assessed by Trypan blue, before (black bars) and after (white bars) radiolabeling. E. Number of radiolabeled hCSCs in each group. All values are mean \pm SEM.

Final cell product radioactivity, labeling efficiency, cell viability, and cell number

Final radioactivity and radiolabeling efficiency were calculated for all cell products prior to intracoronary infusion. No significant difference between cell products was observed with regard to the final mean radioactivity (Fig. 2B) (635 ± 74.28 μ Ci in the continuous-flow group vs. 661 ± 63.28 μ Ci in the stop-flow group) or mean labeling efficiency (Fig. 2C) ($81.0 \pm 8.4\%$ in the continuous-flow group, $84.5 \pm 9.8\%$ in the stop-flow group).

Cell viability, measured by hemocytometer and Trypan blue, declined in both groups as a result of indium-111 oxine radiolabeling. However, no significant difference was observed in the viability of the cell products between the continuous-flow ($85.0 \pm 0.81\%$) and the stop-flow ($83.0 \pm 0.78\%$) groups (Fig. 2D). Similarly, there was no significant difference with respect to the final numbers of cells infused intracoronarily between the continuous-flow ($10.1 \pm 0.41 \times 10^6$ cells) and the stop-flow ($9.83 \pm 0.25 \times 10^6$ cells) groups (Fig. 2E).

Echocardiographic analyses

Baseline left ventricular (LV) ejection fraction (EF) was not significantly different between the continuous-flow group ($74.35 \pm 4.09\%$) and the stop-flow group ($71.16 \pm 4.11\%$) (Fig. 3). At 30 days after infarction, there was a significant decline in both the continuous-flow group ($44.57 \pm 6.75\%$) and the stop-flow group ($37.79 \pm 6.77\%$). The decline in ejection fraction did not differ significantly between the continuous-flow and stop-flow groups ($P=0.49$).

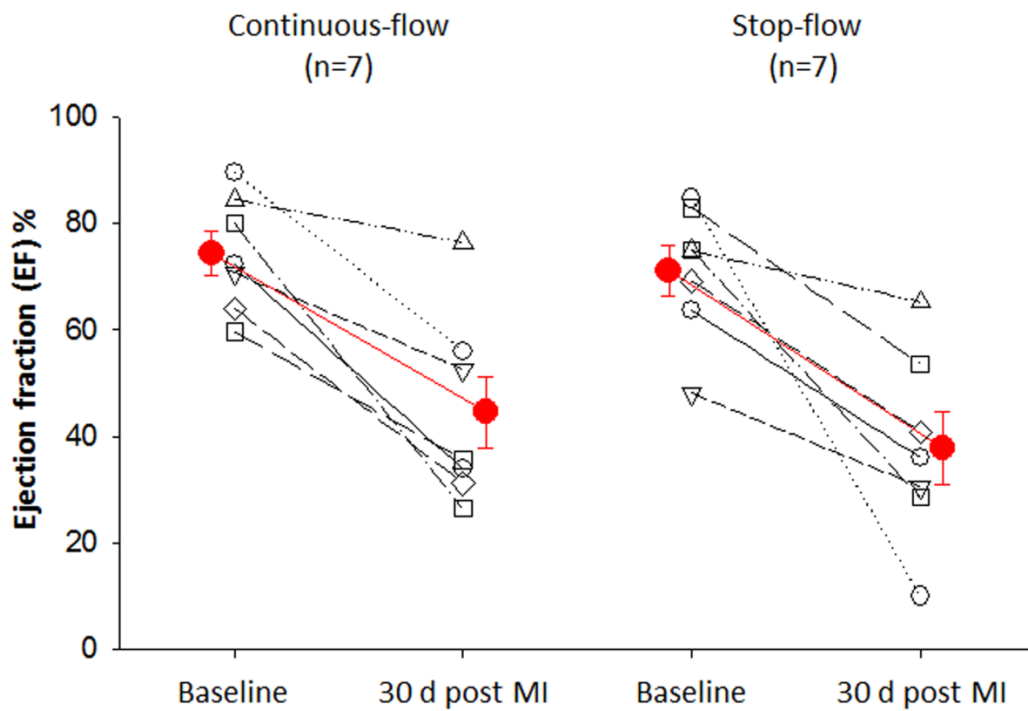


Figure 3. LV ejection fraction. Echocardiographic analyses were performed at baseline and again 30 d after infarction prior to intracoronary radiolabeled hCSC delivery to measure ejection fraction. Ejection fraction at 30 d after infarction was not significantly different between groups indicating similar degree of myocardial injury and functional decline ($P=0.49$).

Nuclear imaging

Myocardial nuclear imaging was performed to visualize the distribution of radioactivity and, indirectly, cell retention. As expected, cell (radioactivity) retention was observed in the distribution of the mid-distal LAD within the apical, anteroseptal, and anterolateral regions (Fig. 4).

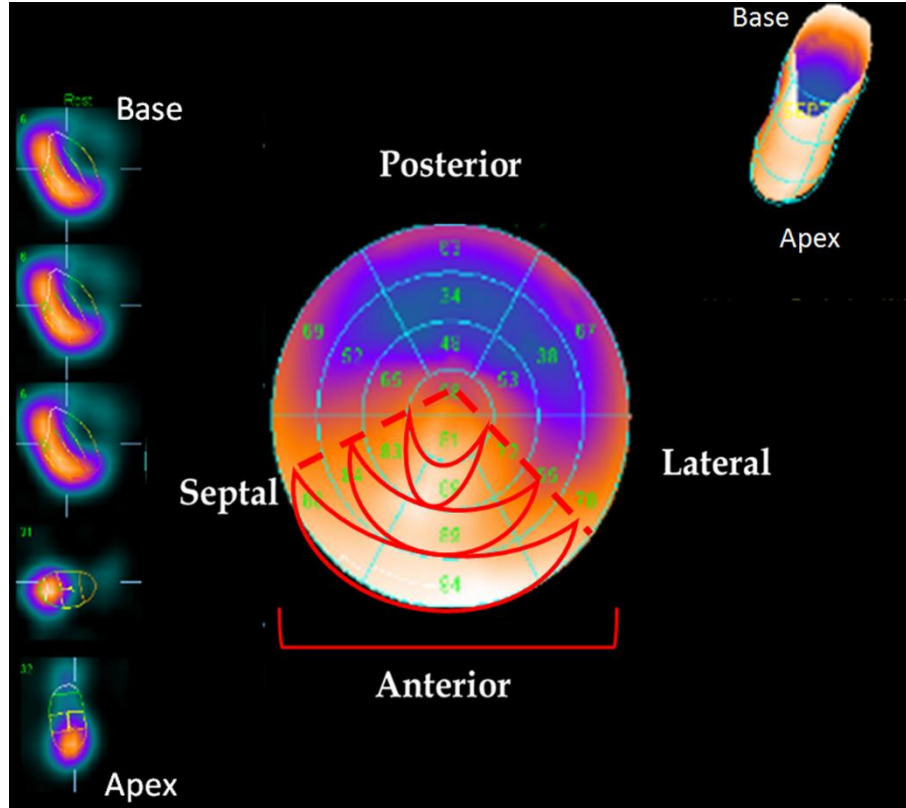


Figure 4. Nuclear imaging of hCSC retention. Cell retention was assessed by radioactivity and visualized by whole heart nuclear imaging. Radioactivity was observed in the distribution of the LAD, specifically, in the anteroseptal, anterior, and anterolateral walls of the left ventricle. Areas of high radioactivity and cell retention are identified by the bright orange coloration while areas with no or low radioactivity are identified by blue/purple coloration.

Cardiac retention of hCSCs

Measurements of total cardiac radioactivity demonstrated that the stop-flow technique did not result in significantly higher retention of hCPCs at 24 h compared with the continuous-flow technique ($5.41 \pm 0.80\%$ vs. $4.87 \pm 0.62\%$ of initial radioactivity, respectively, $P=0.61$) (Fig. 5). Regional retention was also not significantly different between stop-flow vs. continuous-flow (right ventricle: $1.60 \pm 0.30\%$ vs. $1.02 \pm 0.15\%$, respectively, $P=0.12$; LV septum: $1.88 \pm 0.43\%$ vs. $1.81 \pm 0.33\%$, $P=0.91$; LV anterolateral wall: $1.17 \pm 0.37\%$ vs. $1.10 \pm 0.17\%$, $P=0.87$; LV apex: $0.23 \pm 0.05\%$ vs. $0.31 \pm 0.11\%$, $P=0.56$; right atrium: $0.10 \pm 0.03\%$ vs. $0.11 \pm 0.02\%$, $P=0.81$; left atrium: $0.10 \pm 0.02\%$ vs. $0.12 \pm 0.03\%$, $P=0.61$; base: $0.33 \pm 0.38\%$ vs. $0.39 \pm 0.13\%$, $P=0.71$) (Fig. 5).

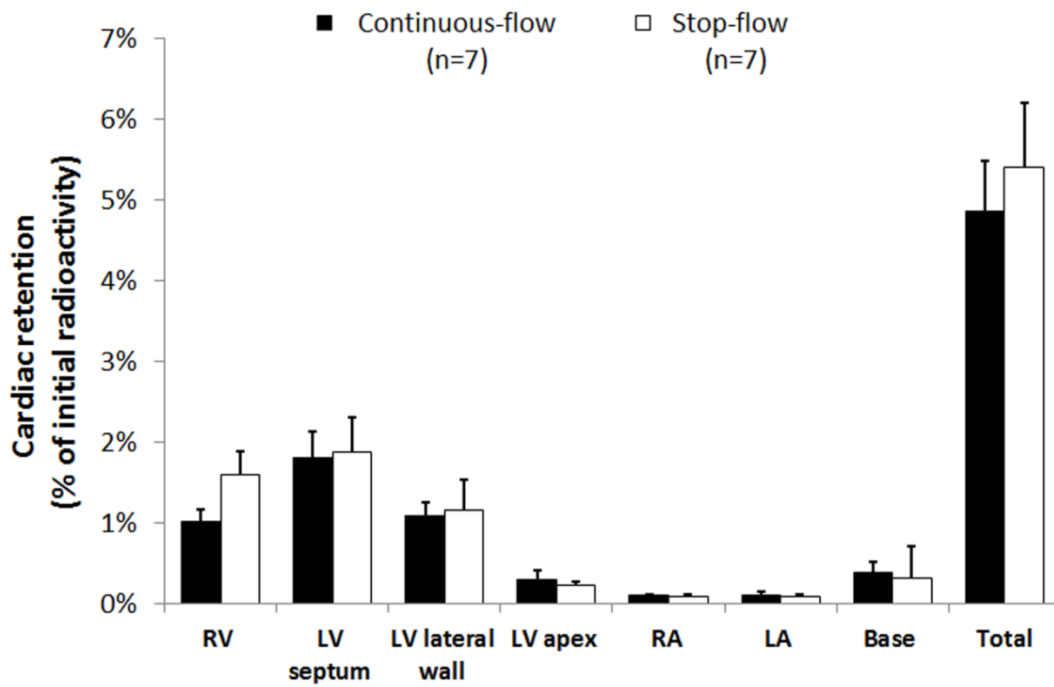


Figure 5. Myocardial hCSC retention at 24 h. Illustrated is the regional distribution of radioactivity in the continuous-flow (black) and stop-flow (white) groups. There was no significant difference in regional or total radioactivity (cell retention) between the continuous-flow ($4.87 \pm 0.62\%$) and the stop-flow ($5.41 \pm 0.80\%$) groups ($P=0.61$).

CSC distribution in noncardiac tissues

In all pigs, three small samples of lung, liver, kidney, and spleen were assessed for radioactivity. Radioactivity was highest in the lung ($17.48 \pm 0.11\%$ of initial dose), followed by the liver (9.52 ± 0.51 of initial dose), kidney ($3.08 \pm 0.43\%$), and lastly spleen ($0.26 \pm 0.06\%$). Radioactivity was highly variable in different regions of the same organ.

Discussion

This study simultaneously addressed three fundamental questions regarding intracoronary infusion of c-kit^{POS} hCPCs: i) what fraction of hCPCs is retained in the heart 24 h after intracoronary infusion?, ii) what may have been the effective dose of CPCs responsible for the indications of function benefits observed in the SCIPIO trial? and iii) is the stop-flow technique superior to continuous-flow in promoting cardiac retention of hCPCs? That is, is the increased risk of procedural complications associated with balloon inflation justified by increased hCPC retention? Our results indicate that, in pigs with an old myocardial infarction, intracoronary infusion of hCPCs without coronary occlusion is equivalent to intracoronary delivery utilizing the stop-flow technique in terms of cardiac hCPC retention at 24 h. It may also be reasonably inferred that ischemic preconditioning with intermittent balloon inflation/deflation, which has been shown to confer cardioprotective effects¹⁵⁵, does not affect cardiac retention of CPCs, thus eliminating this confounder in studies in which cell therapy has shown benefit when true stop-flow was utilized in the treatment group but was withheld in the vehicle control group to minimize risk of complication. With either method, we found that only ~4-5% of the infused hCPCs remained in the heart 24 h after intracoronary delivery. To our knowledge, this is the first head-to-head comparison of cardiac retention after

intracoronary delivery of hCPCs (or any cardiac-derived cell) using continuous flow vs. stop flow.

Previous studies have examined the retention of various stem/progenitor cell types using various routes of administration, such as intravenous, intracoronary, and transmucosal injections, in clinical and preclinical models.^{52, 141, 159-165} However, studies that specifically compared cell product retention under continuous-flow and stop-flow conditions have been limited to bone marrow cells, and most have infused cells after acute myocardial infarction.^{159, 162, 164} Doyle et al¹⁵⁹ infused ¹⁸F-FDG-labeled BMCs intracoronarily in pigs after acute myocardial infarction and observed that a single dose of cells given with continuous flow was superior to repeated infusions with stop-flow with respect to cardiac retention 1 hour later. Tussios et al¹⁶⁴ infused indium-111 oxine-labeled BMCs intracoronarily into pigs and found no difference in cardiac retention at both 1 h and 24 h after infusion comparing the two techniques. Perhaps of greater relevance, Musialek et al. infused ⁹⁹Tc-extameta-zime-labeled bone marrow CD34⁺ cells in patients 6-14 days after acute myocardial infarction under continuous and stop-flow conditions; they found equivalent cardiac retention (~ 5%) with both techniques at 36-48 h after infusion¹⁶², which is similar to the results of the present study. Our study differs from the aforementioned preclinical studies in that we evaluated cardiac-derived cells and used a model of old myocardial infarction (scar), which is more relevant to the clinical use of cardiac-derived cells.

Analysis of various cardiac regions showed that there were no significant differences in the distribution of indium-111 oxine-labeled hCPCs between the two infusion techniques (Fig. 5). The overall retention of cells observed at 24 h (~4-5%) was

comparable to that observed in previous preclinical and clinical investigations using a variety of cell types.^{26, 52, 141, 160, 162, 163, 165-167} Therefore, intracardiac retention may be more related to route of administration rather than cell type whether intrinsically native heart or from extra-cardiac organs. We found a relatively high level of radioactivity in the apical portions of the right ventricular wall (Fig. 5). This observation can be accounted for by the fact that, in the pig, an accessory arterial branch originating from the distal LAD supplies the apical portions of the right ventricle.^{168, 169} Radioactivity measurements of noncardiac organs indicated that the highest deposition of CPCs after intracoronary infusion is in the lungs followed by liver, kidneys, and spleen.

The specific protocol for the stop-flow technique (one 3-min occlusion without cell infusion followed by four 3-min occlusion/3-min reperfusion cycles) was chosen because it is the same protocol that was used in the SCIPIO trial. The infusion of radiolabeled cells made it impossible to perform histologic analysis of the myocardium, because of the prolonged decay period of indium-111 oxine and attendant safety concerns. We were unable to ascertain whether remaining CPCs were adherent to walls of the microvasculature or had extravasated into the myocardium. To verify that the magnitude of damage produced by coronary occlusion/reperfusion was comparable between the two groups of pigs, we assessed LV function before and 30 d after infarction using echocardiography. Our measurements show that, 30 d after infarction, LV function did not differ significantly between the two groups, indicating a similar severity of the ischemic damage (Fig. 3).

The choice of the animal model was dictated by considerations related to clinical relevance. Clinically, the question of whether the risk of balloon inflation is justified

arises most commonly in patients with chronic ischemic cardiomyopathy who have non-stented target coronary arteries. This issue is less relevant to patients with acute myocardial infarction, since in this setting the culprit vessel is usually stented during revascularization and the risk of dissection or injury associated with balloon inflation is therefore minimized. Accordingly, we decided to use a porcine model of old infarction and scarred myocardium, which mimics the clinical setting of chronic ischemic cardiomyopathy. Obviously, the effect of balloon inflation could not be studied in rodents. We could have used less complex and expensive porcine models (e.g., pigs without myocardial infarction or pigs with acute, rather than chronic, myocardial infarction); however, these models would not be relevant to the large cohort of patients with old stable myocardial infarcts (scars).

A variety of methods could have been used to assess cell retention at 24 h. The advantage of our methodology, based on quantification of residual radioactivity, is that it enabled us to assess the left ventricle as a whole. Alternative techniques such as PCR-based methods^{141, 170} have the advantage of high sensitivity and precision in small samples, such as in murine hearts; however, they are not applicable to large tissue samples because the large amount of native DNA in such samples would cause a dilution in the targeted sequences of human genomic DNA of the residual hCPCs. This would lead to an underestimation of cell numbers. Additionally, PCR-based methods, as well as other methods such as fluorescence in situ hybridization of sex-mismatched donor-recipient pairs¹⁷¹ and nuclear affinity labeling for cell tracking¹⁶⁰, enable quantification of cell numbers only in small myocardial samples assumed to be representative of the whole heart; these numbers must then be normalized to total myocardial weight to calculate

global cardiac retention. Because cells may be distributed heterogeneously within the heart, as observed in the present study (Figs. 4 and 5), these methodologies can potentially lead to inaccurate quantification due to sampling bias. We obviated these problems by measuring residual radioactivity in the entire heart.

In summary, using a clinically relevant porcine model of ischemic cardiomyopathy, we have demonstrated that the stop-flow technique does not result in superior hCPC retention 24 h after intracoronary infusion compared with non-occlusive hCPC infusion. Therefore, the increased procedural risks associated with balloon inflation do not appear to be warranted. These results have important practical implications for the design of future clinical trials in which hCPCs (or other stem/progenitor cells) are administered by the intracoronary route.

CHAPTER III

SAFETY OF INTRACORONARY INFUSION OF 20 MILLION C-KIT POSITIVE HUMAN CARDIAC PROGENITOR CELLS IN PIGS

Introduction

C-kit^{POS} cardiac progenitor cells (CPCs) are one of a number of stem/progenitor cells described in the mammalian heart and one of the two types ever used clinically for cardiac regeneration.^{130, 148} We recently reported the results of the first in-human clinical trial of autologous c-kit^{POS} CPCs in patients with ischemic cardiomyopathy.¹⁴⁸ In this phase I trial, designed to evaluate the safety and feasibility of intracoronary administration of c-kit^{POS} CPCs, 1 million cells were injected in the infarct-related artery using the stop-flow technique. The administration of c-kit^{POS} CPCs was shown to be safe and there were encouraging results related to efficacy, with a significant improvement in left ventricular (LV) ejection fraction in the hCPC treated group. These encouraging findings have sparked growing interest in utilizing c-kit^{POS} CPCs in additional trials with escalating doses >1 million cells, particularly in light of reports of dose-dependent responses with stem cells.¹⁷² However, the safety of higher doses of c-kit^{POS} CPCs has never been evaluated in any clinical or preclinical model.

Intracoronary administration has been utilized with many cell types. Mesenchymal stromal cells (MSCs) have been used in a large number of cardiac regeneration trials. Although these cells are usually administered via transendocardial injection, a number of clinical trials have used them intracoronarily.¹⁷³⁻¹⁷⁷ The cell dose

in these studies ranged from 1 million to > 100 million cells.^{173-175, 177, 178} A number of other studies are ongoing with intracoronary administration of MSCs (e.g., RELIEF-NCT01652209). Nevertheless, there still exist important safety concerns with intracoronary injection of MSCs.^{167, 179, 180} Grieve et al. demonstrated that although intracoronary infusion of 25 million MSCs was safe, 75 million cells caused biochemical and histological myocardial infarction in an ovine model.¹⁸⁰ Similarly, Vulliet et al. showed a dose-dependent rise in ST segments during intracoronary injection of MSCs in all 7 dogs studied.¹⁶⁷ The average size of MSCs and BMMNCs is $\sim 21.0 \pm 3.3 \mu\text{m}$ and $8.6 \pm 1.8 \mu\text{m}$, respectively.^{41, 181} At 7 to 10 μm , the typical capillary luminal diameter is smaller than the average sized MSCs, the likely explanation for the findings in the aforementioned studies.^{181, 182} In the CADUCEUS trial, 12.5 to 25 million cardiosphere-derived cells (CDCs) were injected intracoronarily with no significant safety concern.¹²³ However, administration of 50 million allogeneic CDCs resulted in large infarctions in pigs.¹⁸¹ Measuring $20.6 \pm 3.9 \mu\text{m}$ in diameter, CDCs are larger than the average capillary diameter, thereby causing microvascular obstruction in that model. Finally, bone marrow mononuclear cells (BMMNCs) have almost always been administered intracoronarily. Close to 100 phase I and II clinical trials using large numbers of BMMNCs have demonstrated that intracoronary administration is safe.¹⁸³ For instance, within the three phase II trials of BMMNCs led by the Cardiovascular Cell Therapy Research Network (CCTRN), 100-150 million cells were administered intracoronarily with no complications.^{184, 185}

C-kit^{pos} CPCs are similar in size to the unselected cell population from which they are sorted, ranging from ~ 12 to 20 μm in diameter in suspension. Therefore, it is

conceivable that they could bring about significant microvascular obstruction if administered in high enough doses. Therefore, we set out to investigate the safety of 20 million intracoronarily delivered c-kit^{POS} human CPCs, a dose ~40 times higher than that used in our previous porcine study¹³⁹, in a porcine model, as a preamble to future clinical trials.

Methods

A detailed timeline of the experimental protocol is illustrated (Fig. 6).

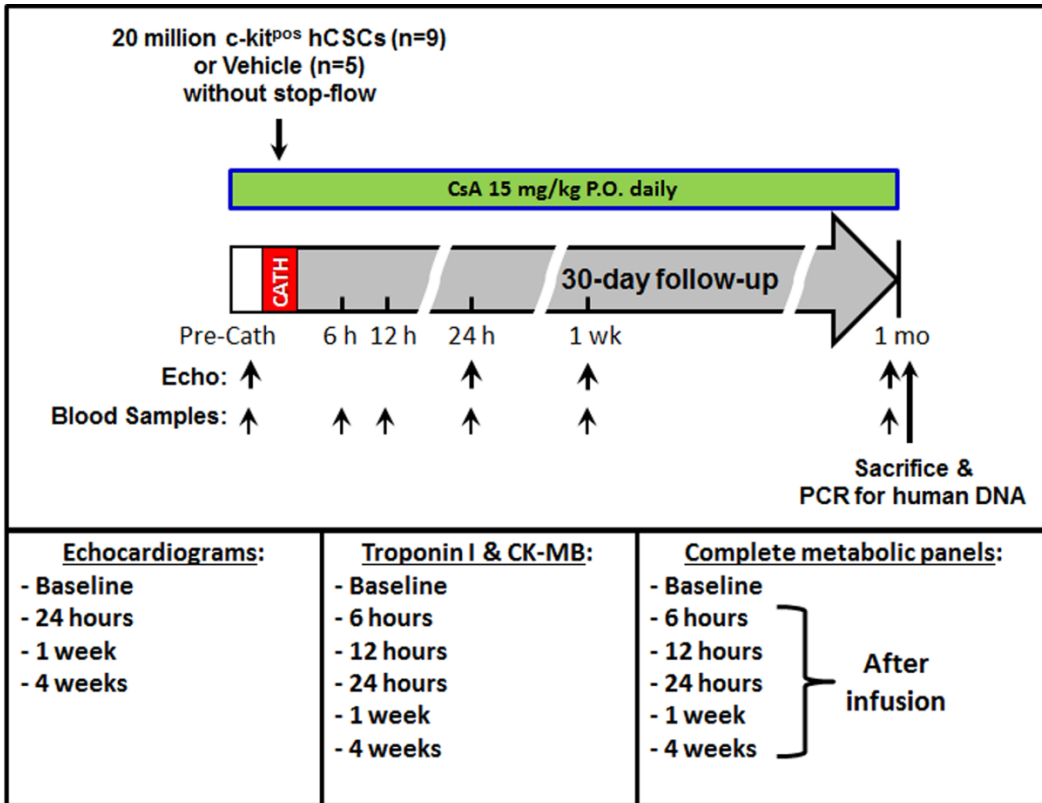


Fig. 6. Safety Study protocol and timeline.

Human c-kit^{pos} CPC isolation and expansion

Right atrial appendage specimens were obtained with IRB approval (IRB number 07.0062) from patients undergoing open-heart, on pump, coronary artery bypass surgery at Jewish Hospital in Louisville, Kentucky. All patients were between the ages of 50 and 75 years of age, so as to approximate the ages of patients that were included in the recently conducted SCIPIO phase I clinical trial.¹⁴⁸ Right atrial appendages were transported to the cell processing lab under sterile conditions on wet ice. The tissue was washed several times with ice cold PBS to remove gross blood. Adipose tissue was then resected manually from the external surface of the tissue with subsequent repeated washing in cold PBS. The tissue was then manually minced to obtain fragments < 1mm³ (Fig. 7). The tissue fragments were then incubated on a shaking incubator at 37°C in Worthington Collagenase type II/Hams F12 solution with multiple rounds enzymatic digestion. Once complete, the solution of released cells was centrifuged with discarding of the supernatant. The cells were washed in full growth media consisting of Ham's F12 (Gibco), 10% FBS (Thermo Scientific Hyclone), 10ng/ml Recombinant Human bFGF (PeproTech), 0.2mM L-Glutathion (Sigma), human Erythropoietin (Sigma), and 100U/ml penicillin/streptomycin (Gibco). The supernatant was discarded and the cells were resuspended in full growth media and plated in a 6-well plate for passage 0 initial expansion. Media was changed at 24 h completely. Additional media changes were performed every 3-4 days or if necessitated by visual examination of the culture. Cells were expanded until 70% confluence at which time they were passaged to T75 Flasks for additional subconfluent expansion prior to immunoselection for c-kit expression. Media was added or changed partially every 3-4 days for the remainder of the culture process.

Cells were passaged 1 time prior to immunomagnetic sorting for c-kit (CD117) using Miltenyi immunomagnetic beads according to manufacturer's recommendations.

Illustrations of the tissue processing and initial cell expansion are shown in Fig. 7.

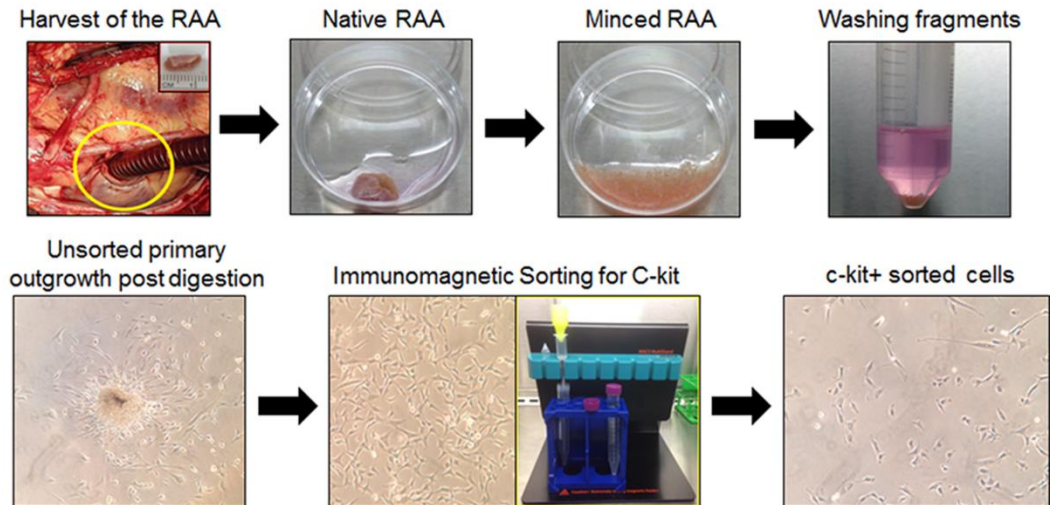


Fig. 7. Isolation and expansion of c-kit^{pos} hCPCs. Right atrial appendages (RAA) were harvested with subsequent mechanical and enzymatic digestion to obtain primary outgrowth of total adherent cardiac cells. Primary cells were immunomagnetically sorted for c-kit and the resultant cells expanded in vitro.

c-kit^{pos} hCPC immunomagnetic sorting (MACS)

Passage 1 cells at 70-75% confluence in T75 culture flasks were sorted for c-kit with anti-CD117 Miltenyi microbeads and Miltenyi magnetic sorting apparatus (Fig. 7). Cell sorting was performed through the direct technique. Cells were trypsinized and washed twice in ice cold MACS buffer made per manufacturer's specifications. All solutions were cooled on ice prior to beginning the sorting protocol. Cells were immunomagnetically sorted according to manufacturer's specifications using Miltenyi MS columns and pre-separation filters with magnetic stand. Positively selected cells were plated in 6-well plates at subconfluence for subsequent in vitro expansion of c-kit^{pos} cells (Fig. 7). Human c-kit^{pos} CPCs were expanded exponentially over 3-4 additional passages to ultimately obtain approximately 3×10^7 cells per patient. Multiple patients cells were pooled to obtain a uniform cell product that was ultimately infused intracoronarily into the treatment group of pigs (n = 9). Cells were assessed by flow cytometric analysis per standard protocol for c-kit positivity at passage 3-4. Only populations of cells showing greater than 70% c-kit positivity were used for the study.

Flow cytometric analysis and immunocytochemistry

Cells were trypsinized from dedicated flasks at passage 3-4 per standard protocol. Cells were washed 1x in ice cold buffer with 1% bovine serum albumin (BSA)/phosphate buffered saline (PBS) buffer followed by a second wash in cold PBS. Cells were then fixed with 15 minutes at room temperature in freshly prepared or commercially purchased 4% PFA buffered to pH 7. Fixed cells were washed twice in PBS. Cells were stained for c-kit directly after fixation. Cells were blocked for 10 minutes at RT in 1% BSA buffer and then stained for c-kit with c-terminal specific Santa Cruz C19 rabbit

polyclonal IgG anti-human c-kit antibody for 1 h at room temperature in the dark. Isotype rabbit polyclonal IgG in identical concentration was used in parallel as an isotype control. Cells were then washed twice with 1% BSA buffer. Secondary antibody, FITC or TRITC conjugated Invitrogen Donkey anti-rabbit IgG was then added for 1 h at room temperature in the dark for flow cytometry or confocal microscopic imaging after cells were spun onto glass slides. Confocal images were taken using Zeiss 510 inverted confocal microscope and image processing performed relative to isotype control labeling with integral instrument software only. Flow cytometric analysis was performed using BD Accuri C6 flow cytometer. All analysis gates were set for false positivity of <1% in respective isotype controls (Fig. 8). Accuri C6 software was used for final analysis of c-kit positivity. Illustrations of flow plots and immunocytochemistry images (Fig. 8) as well as data regarding c-kit positivity of all cell lines utilized for the study are shown (Fig. 9). Only cell lines with greater than 70% c-kit positivity measured by flow cytometric analysis were utilized for the study.

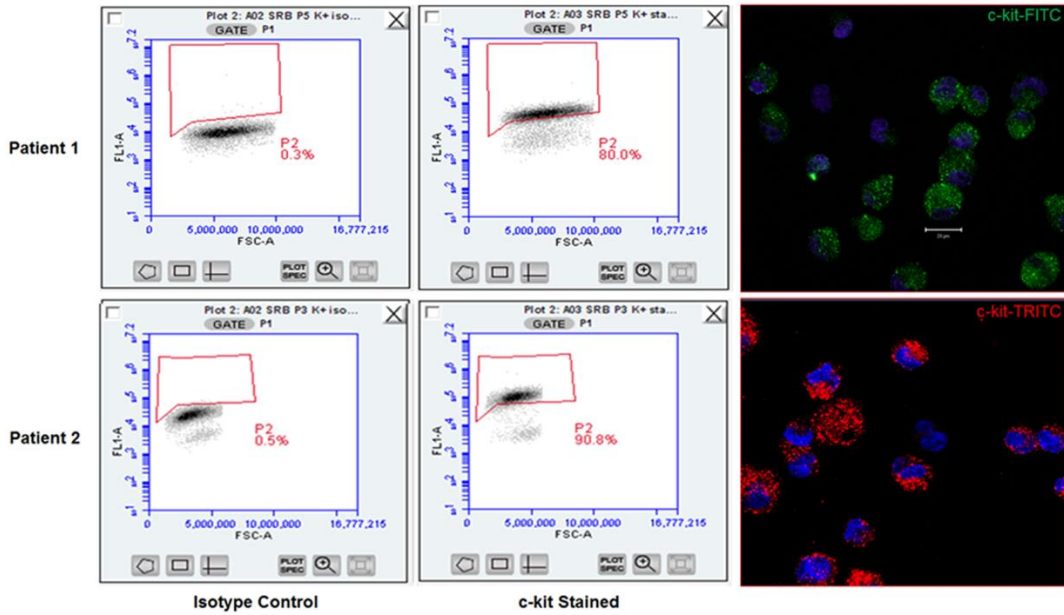


Fig. 8. Flow cytometric validation and immunocytochemistry of c-kit^{POS} hCPCs.

Representative flow cytometric analyses of isotype control (left) and c-kit-labeled cell flow plots (center) are shown. Suspension immunocytochemistry of c-kit^{POS} hCPCs showing positive anti-c-kit labeling is shown in the right panels, with DAPI labeled nuclei in blue.

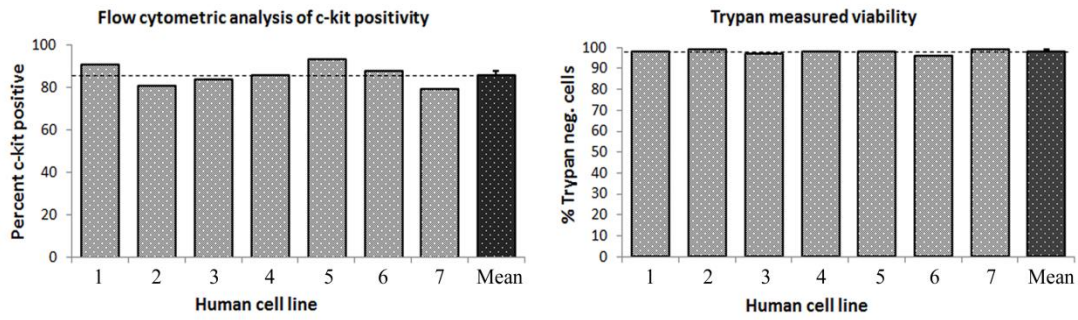


Fig. 9. Cumulative c-kit positivity by flow cytometry and Trypan blue cell product viability. The left panel shows c-kit positivity in seven cell lines utilized for the study, which averaged $85.6\% \pm 1.9\%$ (mean \pm SEM). The right panel shows viability of c-kit^{POS} hCPCs measured by cellular exclusion of Trypan blue staining prior to intracoronary infusion. Trypan negative, viable cells averaged $97.8 \pm 0.4\%$. Data are mean \pm SEM.

Cell product generation

Positively selected cells were expanded in vitro for 3-4 additional passages prior to intracoronary infusion. In vitro expanded c-kit^{POS} CPCs were trypsinized and washed with sterile PBS and resuspended in 12mL of Plasmalyte-A solution. Final cell count and viability by hemocytometer and Trypan blue were performed. Cell number was adjusted by volume to closely approximate 20 million cells in 12mL Plasmalyte-A solution. The cells were placed on wet ice and transported to the cath lab for intracoronary infusion.

Ethics Statement

This study was carried out in strict accordance with the recommendations in the Guide for the Care and Use of Laboratory Animals of the National Institutes of Health. The protocol was approved by the Institutional Animal Care and Use Committee (IACUC) of the University of Louisville (IACUC number: 12114).

Animal procedures

Female Yorkshire pigs (weight 32.4 ± 0.7 kg, age: 13.4 ± 0.3 weeks) were used for this study. All animal procedures were approved by the University of Louisville IACUC (IACUC number 12114) prior to initiation of the study. Pigs were fasted for at least 12 h prior to sedation. On the day of cell delivery, pigs received a prophylactic dose of antibiotics (Ceftiofur 3 mg/kg, IM) and a preemptive dose of analgesics (buprenorphine 0.025 mg/kg, IM). Pigs were sedated using a cocktail of ketamine (20 mg/kg, i.m.) and xylazine (2 mg/kg, i.m.). An intravenous catheter was placed in a marginal ear vein for the administration of fluids and drugs. Animal received diazepam (1 mg/kg IV) to facilitate intubation. Following adequate sedation, pigs were intubated and

mechanically ventilated. General anesthesia was maintained with isoflurane (1.5% - 2.0% 50/50 oxygen/nitrogen). Pigs received aspirin (2300 mg, IV) and heparin (300 U/kg, IV) before the catheterization procedure.

A cut-down on the right neck was performed and the right jugular was used for placement of a 7-10 F chronic cath polyurethane catheter (Access Technologies or Bard/Hickman). This catheter was implanted, secured, tunneled to the back of the neck and kept in place for the duration of the 1 month follow-up for serial blood collections; using this catheter, blood samples were obtained for serial measurement of cardiac markers at baseline (before catheterization procedure) and at 6, 12, 24 h, and 1 week, and 1 month after cell delivery (Fig. 6). The catheter dead-space was measured and filled with heparin (1000 units/mL) after each withdrawal to maintain patency. Care was taken to fill the dead-space only with no spillover into the systemic circulation after each blood collection.

At the end of the 1 month follow up, pigs were anesthetized with 22 mg/kg ketamine and 2 mg/kg xylazine IM. Pig was transported to the cath lab for final hemodynamic measurement. Animals received diazepam 1 mg/kg IV to facilitate intubation. Animals were then again intubated and ventilated. General anesthesia was maintained with isoflurane (1.5% - 2.0% 50/50 oxygen/nitrogen). Hemodynamic variables were monitored and recorded. After the final hemodynamic recording was taken, the animal was deeply anesthetized with 5% isoflurane. A bolus of 3-6 ml/kg of 3 mmol/ml potassium chloride solution was injected intravenously until the heart was completely arrested. Asystole was confirmed by cessation of cardiac electric activity

from ECG monitoring. The chest was opened via a left thoracotomy, the aorta was transected, and the pig exsanguinated. The heart was then harvested.

Cell delivery / catheterization procedure

Through a right femoral artery cut-down, a 7F fast-cath sheath was introduced. A 6 F Hockey-stick catheter (Cordis) was fluoroscopically guided to the left main coronary artery. The left main coronary ostium was engaged by the catheter and an angioplasty-type balloon catheter (Maverick 2.0 x 9 mm) and guide wire (BMW, Boston Scientific) assembly was guided into the LAD; the wire was advanced into the mid LAD and the catheter telescoped over the wire and positioned just proximal to the 1st diagonal branch. The CPC solution (20 million cells in 12 ml of sterile Plasma-Lyte A solution or vehicle, divided by 4 injections, 3 ml each, interspersed with 4'30" between each injection) or vehicle (12 ml of sterile Plasma-Lyte A solution) was injected manually at a constant rate through the central port of the angioplasty balloon catheter over the 3 min. After the procedure, the Hockey-stick catheter, and the femoral sheath were removed and the groin access site was closed in 3 layers using 3-0 PDS suture. A transdermal fentanyl patch (2.5 µg/kg/h) was placed at the end of the procedure for postoperative analgesics. The pigs were weaned from anesthesia, extubated, and moved to a post-operative area for postoperative monitoring. Ceftiofur (3 mg/kg, s.c.) was repeated on day 1 and 2 post-procedure.

Immunosuppressive Therapy

Pigs received 15 mg/kg/day of Cyclosporine A (CsA) starting 2 days before cell injection and continuing until the end of follow-up. CsA (powder from Novartis) was

mixed with a tablespoon of grape flavored Kool-Aid powder and ~60 ml of drinking water to make a suspension beverage to feed the animal orally.

Echocardiography

Echocardiograms were obtained at baseline (before CSC delivery), 24 h, 1 week, and 1 month after CSC delivery (Fig. 6) using a HP SONOS 7500 ultrasound system (Philips Medical Systems) equipped with a HP 21350A (S8) 3.0-8.0 MHz sector array ultrasound transducer. Before the echocardiographic study, pigs were anesthetized (isoflurane) and placed in the left lateral decubitus position. Temperature was monitored with a rectal temperature probe and kept between 37.0°C and 37.5°C with a heating pad. The parasternal short-axis view was used to obtain 2D and M-mode images¹⁹. Systolic and diastolic anatomic parameters were obtained from M-mode tracings at the mid-papillary level. Digital images were analyzed off-line by a single blinded observer using ComPACS Review Station (version 10.5) image analysis software (Medimatic, Las Cruces, NM 88004, USA) according to the American Society of Echocardiography standards.¹⁵⁸

Cardiac biomarkers assays: Troponin I and CK-MB

Plasma cTnI levels were measured with a pig cTnI ELISA kit according to the manufacturer's instruction (Life Diagnostics, West Chester, PA) at baseline as well as 6, 12, and 24 hrs, and one week and one month post infusion (Fig. 6). Fresh blood was collected with the heparinized tube and then centrifuged to separate plasma from the blood sample. Each assay was performed in duplicate and in a blinded fashion. The original cTnI data (i.e., the optical density absorbance values acquired from Beckman Coulter DU730 Spectrophotometer) were calibrated and converted with cTnI standard

curve. The final cTnI results were expressed as nanogram per milliliter plasma (ng/ml). All measurements were performed in duplicate.

Plasma CK-MB concentration was measured via an ELISA kit (MyBioSource) at baseline as well as 6, 12, and 24 hrs, and one week and one month post infusion (Fig. 6). Briefly, the 96-well plate was pre-coated with an antibody specific to pig CK-MB. The plasma samples were loaded onto the wells and bound by the pre-coated specific antibody. Then a biotinylated detection antibody specific for pig CK-MB and Avidin-Horseradish Peroxidase (HRP) conjugate were added to the wells. After incubation, free components were washed away. The substrate solution was added to each well. Only the wells contained CK-MB protein, biotinylated detection antibody and Avidin-HRP conjugate presented blue in color. This enzyme-substrate reaction was terminated by the addition of a sulphuric acid solution, therefore the color turned to yellow. The optical density (OD) was measured spectrophotometrically at a wavelength of 450 nm. The original CK-MB data (i.e., OD values) in the pig plasma samples were calculated and converted with pig CK-MB standard curve. Duplicate assays were performed for each sample and CK-MB concentration was expressed as nanogram per milliliter of plasma (ng/ml). All CK-MB assays and calculation were conducted in a blinded fashion relative to hCSC treated vs control group. All measurements were performed in duplicate.

Assessment of renal and hepatic function

Functions were assessed by measurement of respective biomarkers. Peripheral blood was drawn and complete metabolic panels (CMPs) were obtained in hCSC-treated and control groups at baseline and 6, 12, and 24 h, 1 week, and 1 month after intracoronary infusion (Fig. 6). All CMPs were analyzed by the veterinary lab company

Antech Diagnostics (Louisville, Ky) in a blinded fashion. Resultant biomarker values were compared with known porcine reference ranges provided by Antech Diagnostic as well as with absolute initial baseline values. Changes in blood urea nitrogen (BUN) and creatinine (Cr) were used to assess renal function. Change in AST, ALT, alkaline phosphatase (Alk Phos), and total creatine phosphokinase (CPK) were used to assess hepatic function.

DNA isolation from paraffin embedded sections and PCR

Genomic DNA was isolated from representative paraffin embedded left ventricular tissue sections using QIAamp DNA FFPE Tissue Kit (Qiagen) according to the manufacturer's instructions. Samples were analyzed for the presence of human (HLA-DMA) and pig (Pig Gapdh) genomic DNA using the following primer sets:

HLA-DMA fwd, 5'-TACAAACCTCAGCTACCTTCGTGGC-3'

HLA-DMA rev, 5'-AACCCAGCTGACTCTGGGTGG-3'

Pig Gapdh fwd, 5'-CCCCCTCAGATTTGGCCGCA-3'

Pig Gapdh rev, 5'-CACGGGGGCCACTCACCAT-3'

For PCR reaction, 100 ng of each DNA sample was amplified in a 20 µl reaction for 40 cycles (denaturation at 95 °C; annealing at 61 °C; and extension at 72 °C) using Taq 2X Master Mix (New England Biolabs). Accordingly, the limiting threshold or sensitivity of detection of human CSCs approximated 1 hCSC per 15,000 porcine cells.

Statistical Analyses

One or two-way repeated measures ANOVA statistical analysis was employed for all comparisons of echocardiographic parameters as well as cardiac, hepatic, and renal biomarkers between groups across multiple time points where applicable. All data are

represented as means \pm SEM. Datasets are illustrated in the supplemental supporting information.

Results

Intracoronary infusion of 20 million c-kit^{pos} CPCs does not impair LV function or structure

Echocardiographic measurements were performed at serial time points after intracoronary infusion of 20 million human c-kit^{pos} CPCs (n=9) or vehicle (n=5) (Fig. 10). Baseline parameters were not significantly different between the two groups. No significant change in left ventricular (LV) function or dimensions occurred as a result of the infusion. For example, LV ejection fraction (EF) did not differ between hCPC-treated and vehicle controls at any time point (baseline: 55.8 \pm 1.8% vs 60.3 \pm 2.9%, respectively; 24 h: 56.9 \pm 1.6% vs 59.2 \pm 1.6%; 1 week: 58.2 \pm 1.7% vs 58.0 \pm 1.6%; 1 month: 58.0 \pm 2.0 vs 59.0 \pm 1.1) (Fig. 10A&E); changes within groups compared with baseline were also not significantly different (P>0.05). Mean anterior wall thickening fraction was examined in the treatment group and was not observed to be significantly different before (58.4 \pm 4.9%) vs 24 h after CSC infusion (57.5 \pm 6.2%), P>0.05 (Fig. 10D). Similarly, there was no significant difference in LV end-diastolic diameter, fractional shortening, end-diastolic volume, end-systolic volume, end-systolic diameter and anterior and posterior wall thickness in both systole and diastole. These data indicate that the intracoronary infusion of hCPCs had no deleterious effect on LV function and dimensions.

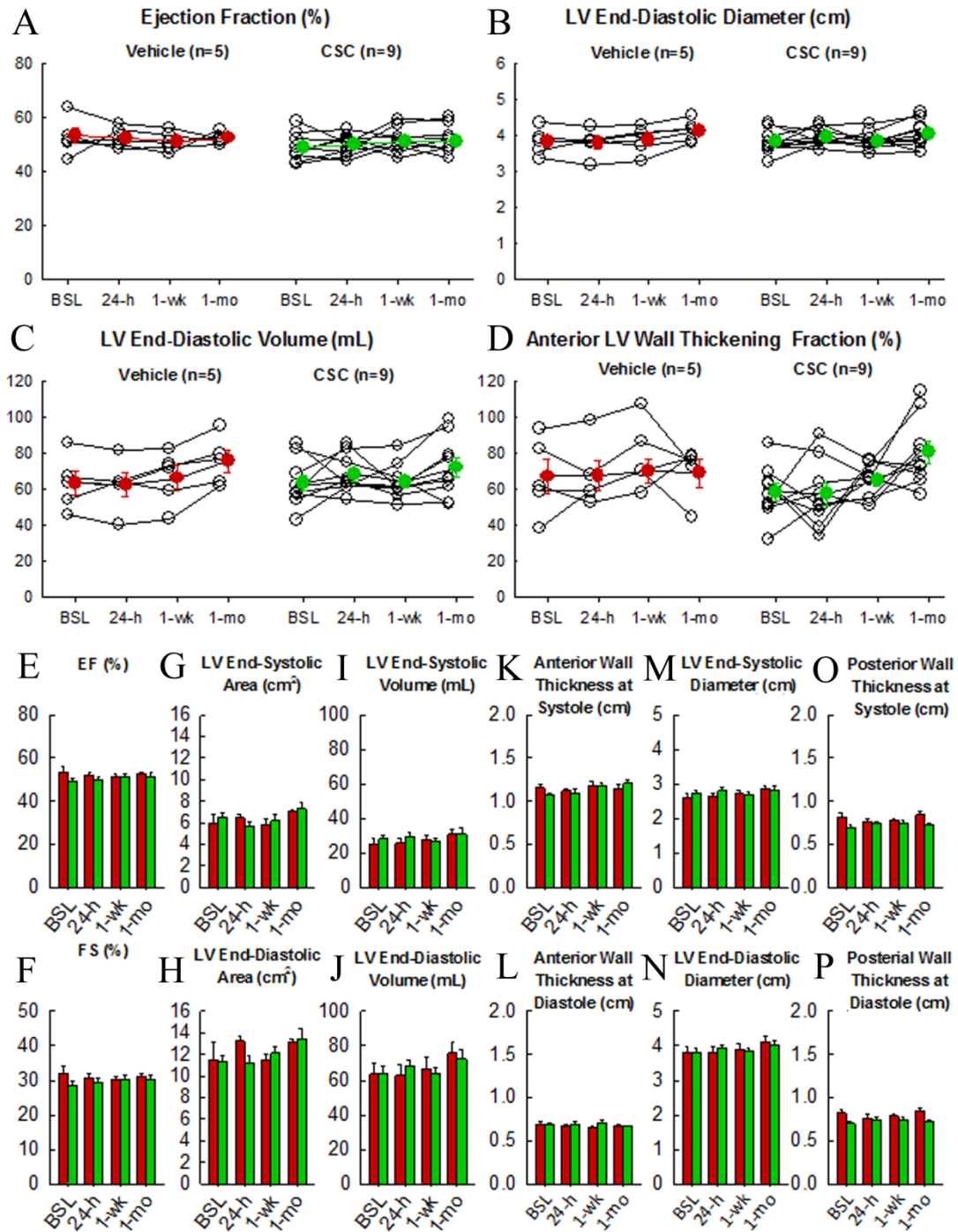


Fig. 10. Intracoronary infusion of 20 million human *c-kit*^{POS} CPCs does not impair left ventricular (LV) function or morphology. The line graphs in the top panel show individual values of each pig's progress over time (baseline, 6, 12, 24 h, 1 week, and 1 month). Individual plots are in yellow, and group means are illustrated by the red line

plots. A. ejection fraction (EF). B. LV end-diastolic diameter (EDD). C. LV end-diastolic volume (EDV), D. LV anterior wall fractional thickening. The bottom panel shows group mean \pm SEM at each time point for respective LV functional and morphologic indices. Green and red bars indicate hCSC-treated and vehicle groups respectively. E. ejection fraction, F. fractional shortening, G. LV end-systolic area, H. LV end-diastolic area, I. LV end-systolic volume, J. LV end-diastolic volume, K. LV anterior wall thickness in systole, L. LV anterior wall thickness in diastole, M. LV end-systolic diameter, N. LV end-diastolic diameter, O. LV posterior wall thickness in systole, P. LV posterior wall thickness in diastole. Data are mean \pm SEM. There were no significant differences between groups with respect to any parameter at respective time points ($P > 0.05$).

Intracoronary infusion of 20 million c-kit^{POS} CPCs does not cause ischemic myocardial injury

Myocardial injury resulting from possible micro-embolization and ischemia was assessed by serial measurements of plasma cTnI (Fig. 11) and CK-MB levels (Fig. 12). In both c-kit^{POS} CPCs-treated and vehicle controls, cTnI levels rose slightly after catheterization and intracoronary infusion, peaking at 6 h post catheterization in both groups (hCPC treated, 1.3±0.68 vs. 0.08±0.08 ng/ml at baseline; controls, 1.4±0.58 vs, 0.07±0.08 ng/ml at baseline). In both groups, cTnI returned to baseline by 12 h and remained at baseline levels at 24 h, 1 week, and 1 month after infusion. At no time-point during the study was there a significant difference in plasma cTnI levels between the two groups. In addition, total cumulative myocardial cTnI release did not differ significantly between the hCSC-treated and vehicle-treated groups. Plasma levels of CK-MB exhibited a very slight but clinically irrelevant increase from baseline in both groups, (0.068±0.01 vs 0.039±0.01 ng/ml at baseline in the treated group; 0.058±0.013 vs 0.039±0.01 ng/ml at baseline in the control group) peaking at 12 h in the treatment group and 24 h in the control group. Importantly, neither peak mean nor cumulative enzyme levels differed significantly between vehicle-treated and hCPC-treated groups, indicating that hCPC delivery was not associated with myocardial injury(P>0.05).

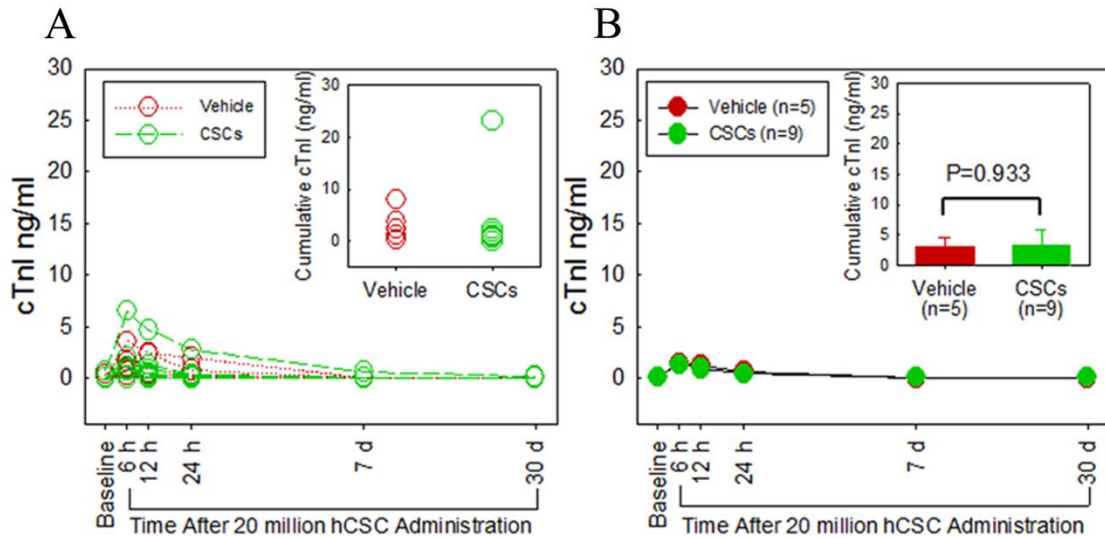


Fig. 11. Intracoronary infusion of 20 million human c-kit^{pos} CPCs does not cause myocardial damage as assessed by cardiac troponin I (cTnI) release. A. Individual plots of serum cTnI levels (ng/ml) are shown at serial time points (baseline, 6, 12, 24 h, 1 week, and 1 month). Green and red plots indicate hCPC-treated and vehicle control pigs, respectively. B. Group means at each time point are shown. The green and red plots indicate hCPC-treated and vehicle control groups, respectively. The inset in panel B shows cumulative cTnI levels. Data are mean±SEM. There were no significant differences in plasma cTnI levels over the 1 month follow up between groups ($P > 0.05$ at each time point).

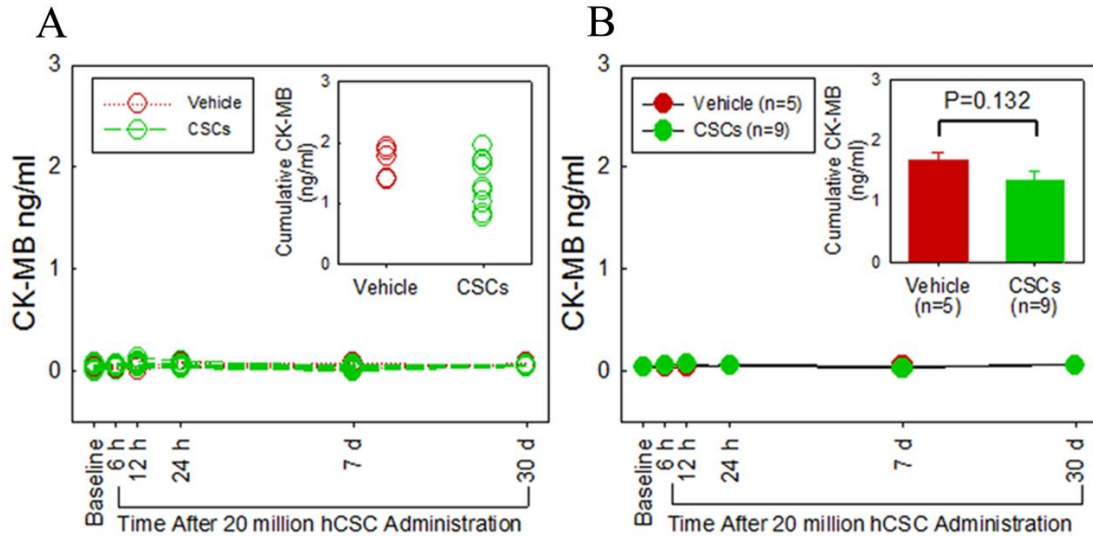


Fig. 12. Intracoronary infusion of 20 million human c-kit^{pos} CPCs does not cause myocardial damage as assessed by cardiac CK-MB release. A. Individual serum CK-MB levels (ng/ml) over serial time points (baseline, 6, 12, 24 h, 1 week, and 1 month). Green and red plots identify hCSC-treated and vehicle control pigs, respectively. B. Group means at each time point are shown. The green and red plots identify hCPC-treated and vehicle control groups, respectively. The inset in panel B shows cumulative CK-MB levels. Data are mean±SEM. There were no significant differences in plasma CK-MB levels over the 1 month follow up between groups ($P > 0.05$ at each time point).

Intracoronary infusion of 20 million c-kit^{pos} CPCs does not impair renal function

Serum creatinine and BUN levels rose approximated 25% over baseline in the first 12-24 h in both the hCPC-treated and the vehicle groups (Fig. 13). In the treated group, creatinine increased from 1.32 mg/dL to 1.68 mg/dL at 6 h after catheterization; a similar pattern was observed in the control group, in which creatinine increased from 1.54 mg/dL at baseline to 2.04 mg/dL at 6 h after catheterization. Serum creatinine levels returned to baseline values in both groups by 24 h, and no changes were observed at 1 week and 1 month (Fig. 13A). Serum BUN levels showed a similar pattern of transient increase at 6 h followed by a return to baseline levels (Fig. 13B). There was no significant difference at any time point between hCPC-treated and control pigs with respect to either creatinine or BUN serum levels, indicating that the slight increases observed at 6 h were not due to the infusion of hCPCs.

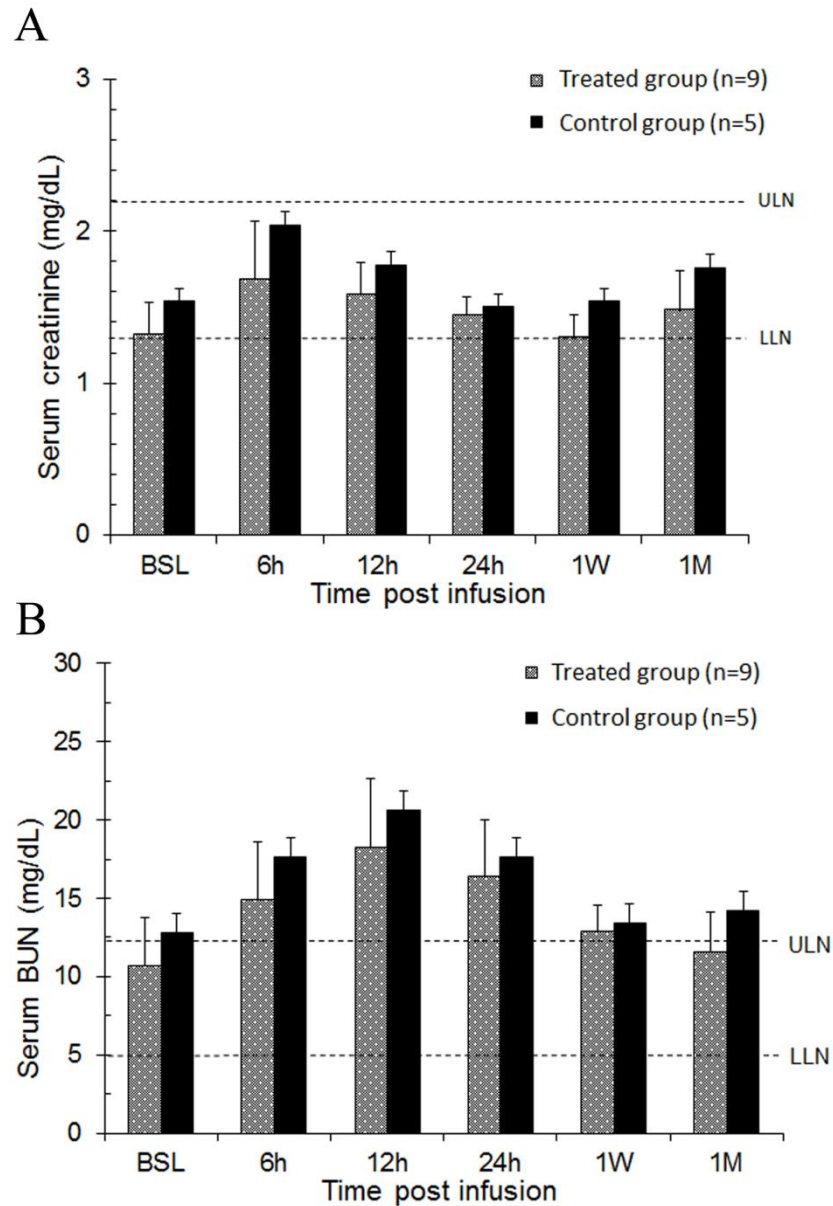


Fig. 13. Intracoronary infusion of 20 million human c c-kit^{POS} CPCs does not impair renal function. Renal function was assessed by serum creatinine and blood urea nitrogen (BUN) values over serial time-points (baseline, 6, 12, 24 h, 1 week, and 1 month). A. Bar graph of serum creatinine levels in hCPC-treated and vehicle control group . B. Bar graph of serum BUN levels in hCPC-treated and vehicle control group. Blue and purple bars identify hCPC-treated and vehicle control groups, respectively. Upper limits of

normal (ULN) and lower limits of normal (LLN) in each graph are depicted by dashed lines respectively. Data are mean \pm SEM. There were no significant differences in serum creatinine or BUN levels over the 1 month follow up between groups ($P > 0.05$ at each time point).

Intracoronary infusion of 20 million c-kit^{pos} CPCs does not impair hepatic function

Serum AST, ALT, alkaline phosphatase, and total CPK levels were significantly higher after catheterization ($P < 0.05$ vs. baseline) in both hCPC-treated and control groups (Fig. 14). Specifically, AST increased to levels four times (200-400 IU/L) the upper limit of normal (45-83 IU/L), peaking 24 h after catheterization (Fig. 14A). ALT also increased but did not surpass the upper limits of normal (52-81 IU/L) in either treatment (61.8 ± 23.6 IU/L) or control (67.6 ± 23.0 IU/L) groups (Fig. 14D). There was no significant difference between hCPC-treated and control pigs in either AST or ALT, indicating that the rise in these markers was not due to the infused cell product. All values were within normal limits 1 week and 1 month after catheterization ($P > 0.05$ vs. baseline).

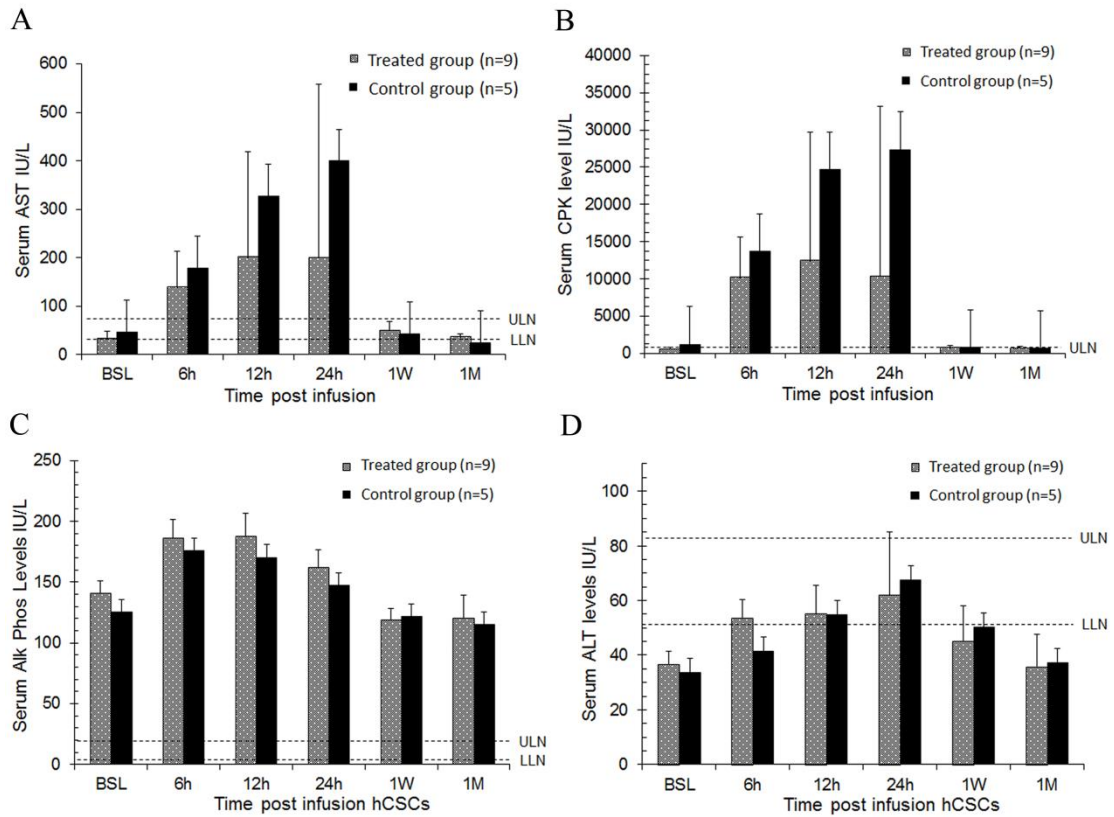


Fig. 14. Intracoronary infusion of 20 million human c-kit^{POS} CPCs does not impair liver function. Liver function was assessed by serum AST, ALT, alkaline phosphatase, and total CK levels at serial time points (baseline, 6, 12, 24 h, 1 week, and 1 month). A. Serum aspartate aminotransferase (AST), B. Serum creatine phosphokinase (CPK), C. Serum alkaline phosphatase (Alk. Phos.), D. Serum alanine aminotransferase (ALT). Upper limits of normal (ULN) and lower limits of normal (LLN) in each graph are depicted by dashed lines respectively. Data are mean±SEM. There were no significant differences in serum AST, ALT, alkaline phosphatase, or total CK levels over the 1 month follow up between groups ($P > 0.05$ at each time point).

Intracardiac retention of c-kit^{pos} CPCs in pigs 30 days post intracoronary infusion

To assess the number of hCPCs retained in the porcine heart 30 days after intracoronary infusion, genomic DNA was isolated from anterior portions of the left ventricle and analyzed by PCR for the presence of human genomic DNA (HLA-DMA) (Fig. 15). No human DNA could be detected in any control (lanes 1-5) or human CSC-treated (lanes 6-14) LV samples, indicating the retention of human CPCs was minimal and/or below the detection limit of our assay (1 hCPC per 15,000 porcine cells). Samples were also analyzed for the presence of pig genomic DNA (Gapdh) as a control for DNA quality. Porcine DNA was detected in all samples.

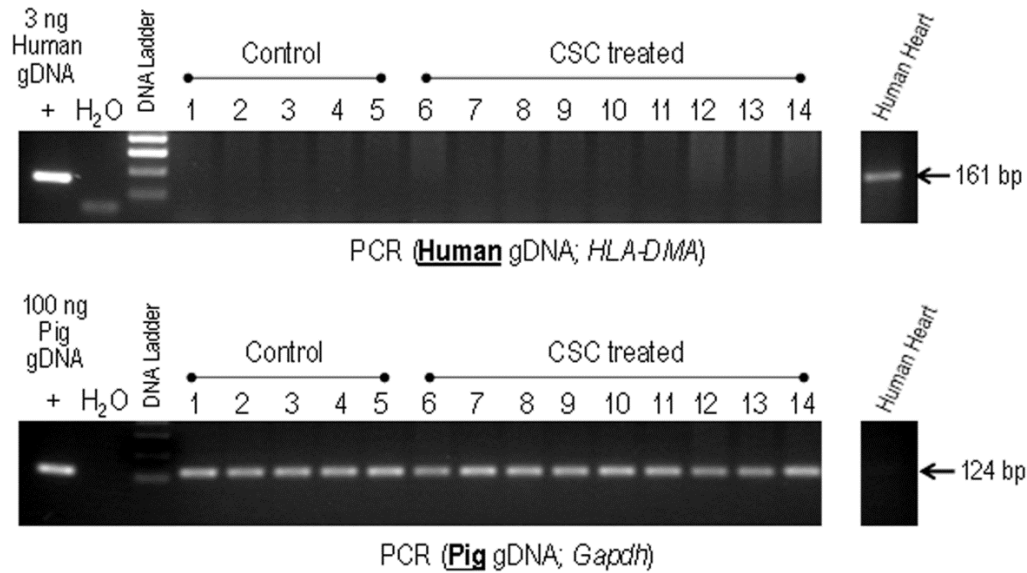


Fig. 15. Detection of human CPCs in control versus hCPC-treated pig hearts.

Genomic DNA isolated from representative LV sections from control (lanes 1-5) and human CSC-treated pigs (lanes 6-14) were analyzed by PCR for the presence of human genomic DNA (*HLA-DMA*). Samples were also analyzed for the presence of pig genomic DNA (*Gapdh*) as a control for DNA quality. Genomic DNA isolated from human heart sections was used as both positive and negative control. None of the samples, including CSC-treated ones, show detectable levels of human DNA.

Discussion

The present study was conducted to assess the safety of intracoronary infusion of 20 million c-kit^{POS} CPCs. We have previously found in a porcine model of ischemic cardiomyopathy that intracoronary delivery of 500,000 autologous c-kit^{POS} CPCs, which is roughly equivalent to 1 million CSCs in humans, does not result in apparent cardiac injury. The SCIPIO trial showed that intracoronary infusion of 1 million autologous c-kit^{POS} CPCs in humans is safe and may produce beneficial effects on cardiac function, myocardial scar size, and functional capacity. However, the dose employed in SCIPIO was relatively low (compared with other trials that have infused, for example, 25 million¹²³ or even >200 million¹⁸⁶ cells). Evidence suggests that higher doses of cells may be more efficacious.¹⁶¹ It is currently unknown whether doses of hCPCs greater than 1 million can be safely administered intracoronarily. Therefore, we conducted the present study with a dose of cells 40 times higher than that used in our previous study¹³⁹ as a preamble to future clinical trials. To our knowledge, our infused dose of 20 million human c-kit^{POS} CPCs delivered intracoronarily is the highest dose ever attempted in any clinical or preclinical model using hCSCs.

The results of the present study indicate that intracoronary infusion of 20 million c-kit^{POS} CPCs is safe. This higher dose did not result in any evidence of myocardial injury, impairment in regional or global cardiac function, deterioration of renal or hepatic function, or other adverse effects, either in the immediate post-infusion period or during the subsequent month, compared with vehicle (Figs. 10-14). Very small, transient increases in plasma troponin I were observed after catheterization in both groups (Fig. 11) but were not associated with any measurable impairment in LV function (Fig. 10).

These low-level, transient increases in plasma troponin are not dissimilar from those seen in prior studies¹³⁹; given their low magnitude and brief duration, they are likely insignificant. Importantly, since they were observed in both groups, they cannot be attributed to the hCPC product. We suspect that these early transient increases in plasma troponin I in both hCPC- and vehicle-treated animals may have been, at least in part, a result of the observed impairment in renal function caused by exposure to cyclosporine and a large intravenous contrast load. Indeed, the time-course of renal dysfunction coincided with the transient rise and resolution of plasma troponin over the first 12-24 h following catheterization. Renal dysfunction, decreased creatinine clearance, and uremia have been implicated in increased plasma levels of troponin in patients without acute myocardial injury.¹⁸⁷ In clinical studies in which elevations of plasma troponin were related to renal dysfunction, acute myocardial injury was excluded by observing a lack of parallel elevations in plasma CK-MB.¹⁸⁷ This pattern of low-level troponin increase with minimal or no concurrent increase in CK-MB during a period of renal impairment mirrors the pattern of cardiac biomarkers observed in the present study. It is possible that other factors associated with cardiac catheterization also contributed to the slight rise in plasma troponin. In any case, the fact that vehicle-treated pigs exhibited similar elevations despite receiving no hCPCs indicates the elevations in treated pigs were not caused by hCPCs but, rather, by mechanisms that affected both groups.

Our findings are consistent with previous studies documenting the safety of intracoronary infusion (without stop flow) of similar numbers of other cell types, including bone marrow derived MSCs.^{188, 189} Specifically, Suzuki et al¹⁸⁸ demonstrated the safety and efficacy of 45 million MSCs infused intracoronarily without stop-flow; the

authors observed myocyte regeneration and improved cardiac function without any evidence of myocardial necrosis related to the infusion.¹⁸⁸ The same group observed a similar safety and efficacy profile following intracoronary infusion (without stop flow) of 30 million cardiosphere-derived cells divided among each of three coronary vessels.¹⁸⁹ Again, no significant TnI elevation was observed.

As mentioned above, after the catheterization procedure renal function was transiently impaired in both treated and control groups (Fig. 13), indicating that the decline in creatinine clearance was not due to systemic distribution of hCPCs and renal microembolization. The mild degree and brief duration of renal impairment, along with the complete return of creatinine and BUN to baseline levels within 24 h after catheterization in both groups, indicates that the etiology was most likely related to the contrast administered intravenously during coronary angiography. Contrast-induced nephropathy (CIN) is commonly observed in clinical settings, with temporary decreases in creatinine clearance that usually return to normal values within 24-48 h.¹⁹⁰ Concomitant exposure of pigs to cyclosporine likely predisposed to the occurrence of CIN and decreased creatinine clearance, since both cyclosporine and intravenous contrast exposure produce vasoconstriction of renal afferent arterioles^{190, 191}, which in turn decreases the glomerular filtration rate.

A slight, transient impairment in liver function was also observed (Fig. 14). But again, this phenomenon was seen in both hCPC-treated and vehicle-treated pigs, and the duration and magnitude were not significantly different between groups, indicating that the elevated levels of AST, ALT, and alkaline phosphatase were not caused by intracoronarily delivered hCPCs. ALT, being more specific for liver injury than either

AST or alkaline phosphatase¹⁹², did not increase above the upper limits of normal (51-82 IU/L) (Fig. 14D). In fact, a hepatic source of these elevated biomarkers is highly unlikely. While leak of aminotransferases into the systemic circulation can indicate liver injury, the liver is not the only source of these biomarkers and caution should be observed in clinical interpretation.¹⁹² Increases in these biomarkers are also seen with skeletal muscle injury.^{192, 193} In our porcine model, a cut-down procedure was used to provide unrestricted access to the femoral artery for arterial sheath and catheter placement. The resultant soft tissue and skeletal muscle injury provides a non-hepatic source of elevated transaminases. This is confirmed by the concurrent increase in muscle specific creatine phosphokinase (CPK) (Fig. 14B), which mirrored the magnitude and duration of the rise in transaminase levels (Fig. 14A). All of these markers returned to baseline levels concurrently.

Despite the high dose of 20 million cells, myocardial retention of c-kit^{POS} CPCs 30 days after intracoronary infusion was observed to be minimal and below the threshold of detection as measured by PCR targeting human genomic DNA. In our experience, this finding is neither surprising nor unexpected. Previous studies^{141, 143, 170} have also found minimal retention 30-35 days after c-kit^{POS} CPCs administration in rodent models. Additionally, in the current study, human c-kit^{POS} CPCs were infused as a xenograft, and only cyclosporine was utilized to prevent acute rejection. The animal's immune reaction to these human cells is not likely to be completely suppressed by cyclosporine alone over a 35-day time period, and thus is likely to have contributed to the attrition of the human cells via immune clearance. In a recent study performed to quantify hCPC engraftment and retention in pigs after intracoronary infusion of 10 million Indium111-radiolabeled c-

kit^{POS} CPCs, we found that just 4-5% of the infused cells remained in the entire heart at 24 h.¹⁹⁴ Additionally, in this study we compared intracoronary infusion both with and without utilization of the stop-flow technique, and found no significant difference between the two methodologies with respect to hCPC retention at 24 h. This would suggest that the negligible level of hCSC cardiac retention observed in the present study was not due to the fact that we did not use the stop flow technique. However, it should be pointed out that in the current study we infused cells into normal, noninfarcted hearts (this was done in order to maximize the sensitivity of our model in detecting any myocardial damage caused by the high dose of 20 million hCPCs). This may have accelerated the disappearance of hCPCs from the myocardium by negatively impacting the homing and/or adhesion of the hCPCs to damaged tissue that occurs in the setting of ischemic cardiomyopathy.^{195, 196}

In conclusion, intracoronary infusion of 20 million human c-kit^{POS} CPCs in pigs (equivalent to ~40 million hCPCs in humans) does not cause acute myocardial injury, impaired regional or global myocardial function, adverse changes in LV dimensions, or liver and renal injury. These results have immediate translational value and lay the groundwork for using doses of CPCs >1 million in future clinical trials. Further studies are needed to determine whether doses of c-kit^{POS} CPCs >1 million result in greater efficacy in patients with ischemic cardiomyopathy.

CHAPTER IV

A NOVEL POPULATION OF HUMAN CARDIAC PROGENITOR CELLS EXPRESSING STAGE-SPECIFIC EMBRYONIC ANTIGEN-3: PHENOTYPE AND THERAPEUTIC UTILITY IN A MURINE MODEL OF ISCHEMIC CARDIOMYOPATHY

Introduction

The discovery that the human heart intrinsically possesses cells with multipotent and transdifferentiation capacities has overturned the long held dogma that the postnatal heart is a static organ. Numerous cell types have been isolated from the adult human myocardium by various methodologies and studied relative to their ability to minimize or reverse ischemic myocardial injury either by stimulation of mechanisms that initiate reverse remodeling or by induction of myocardial neovascularization and/or formation of new viable myocardium. The most widely studied include c-kit^{POS} cardiac progenitor cells (CPCs) and cardiosphere derived cells (CDCs), which have shown to impart salubrious clinical effects in patients with ischemic cardiomyopathy.^{123, 148} Epicardial derived progenitor cells (EPDCs) have also been widely characterized, but evaluation of their therapeutic potential has been limited to preclinical models. While the embryonic origin of adult EPDCs has been widely studied, originating from proepicardial progenitors during fetal cardiomyogenesis and persisting into adulthood,^{84, 197} the embryonic origins of c-kit^{POS} CPCs and cells that give rise to CDCs under in vitro conditions remain unclear.¹⁰ Evidence suggesting the possibility of an upstream c-kit

negative progenitor that may give rise to c-kit^{pos} CPCs within the heart may indirectly be proposed based on the discovery by Klarmann et al that c-kit positive hematopoietic stem cells arise from a c-kit negative, hematopoietic lineage (lin) negative precursor within the bone marrow.¹³¹ Beltrami et al allude to this hypothetical hierarchy within the heart and existence of such a progenitor population that may give rise to c-kit^{pos} CPCs.¹³⁰ Similarly, the mesenchymal phenotype and reported multipotentiality of cells generated by the cardiosphere method would indicate that the human heart harbors a yet unidentified multipotent mesenchymal stem cell population that may give rise to mature myocardial lineages.¹⁹⁸ Gaps in knowledge remain regarding intrinsic cardiac progenitor pools responsible for myocardial homeostasis and repair because discrete markers that distinguish such upstream, undifferentiated progenitor populations remain to be identified. Based on this, we began to explore markers not previously defined within the human heart that have been associated with stemness capacity in other stem cell populations, and we sought to determine whether such markers could aid in the identification of cardiac cell populations that might be utilized for therapeutic purposes.

Human embryonic stem cells (ESCs) and induced pluripotent stem cells (iPSCs), as well as some tissue specific mesenchymal stem cells (MSCs) from cord blood¹⁹⁹, adult bone marrow²⁰⁰⁻²⁰², adipose tissue^{201, 202}, and dermis²⁰²⁻²⁰⁴ have been found to express the glycosphingolipids stage-specific embryonic antigens (SSEA)-3 and SSEA-4, antigens first characterized in undifferentiated carcinomas.^{205, 206} SSEA-3 and SSEA-4 expression is observed to be lost with lineage commitment and differentiation as the core structures of glycosphingolipid expression in stem cells switches from globo- and lacto- to ganglio-series.²⁰⁷ SSEA-3 has shown to be more rapidly down regulated than SSEA-4 indicating

that the presence of SSEA-3 is associated with a more primitive state than is SSEA-4 positivity alone.²⁰⁷ The existence of myocardial cells expressing SSEA-4 has been previously described within neonatal and some adult cardiac mesenchymal cells^{202, 208} although the presence of SSEA-3 expression remained undefined. Equivalents of human SSEA-3 have been previously observed within adult rat myocardium.²⁰⁹ In the present study, we sought to ascertain whether the adult human heart harbored a yet unidentified population of cells with a stemness associated phenotype expressing SSEA-3, and whether SSEA-3 expressing myocardial cells may be utilized in therapeutic applications for myocardial repair after ischemic injury. For the first time, we report the discovery, isolation, characterization, and therapeutic potential of a novel population of cardiac progenitor cells expressing SSEA-3.

Methods

Acquisition of Human Right Atrial Appendage Specimens

Right atrial appendage specimens were obtained with IRB approval from patients undergoing open heart, on-pump, coronary artery bypass surgery from 2011 to 2015 at Jewish Hospital and Kosair Children's Hospital (IRB number 07.0062) in Louisville, KY. All research was performed in accordance with HHS Regulations (45 CFR Part 46) - Protection of Human Subjects and respective exemptions.

Tissue Processing

Right atrial appendages (~20-400 mg) were rinsed with ice-cold 1X PBS, weighed, and manually minced (fragments < 1 mm³) with sterile surgical scissors. Tissue fragments were subsequently washed twice in ice-cold Ham's F12 base media and enzymatically digested with Worthington Collagenase type II/Hams F12 solution

(1500U/mL; 10 mL per 100 mg of tissue) for 90 min at 37°C with gentle agitation. Resultant cells were harvested via centrifugation (400xg for 5 min), and washed in SSEA-3 cell growth media consisting of a combination of mTESR1 media (STEMCELL Technologies) containing 20% FBS (Seradigm) and basal growth media [Ham's F12 (Gibco) supplemented with 10% FBS (Seradigm), 10 ng/ml Recombinant Human bFGF (PeproTech), 0.2 mM L-Glutathione (Sigma), 0.005 U/mL human erythropoietin (Sigma), and 100 U/ml penicillin/streptomycin (Gibco)]. Ultimately, the mTESR1 and basal media were combined in a 60/40 ratio, respectively, to generate the initial passage (P0) SSEA-3 cell growth media. Cells were resuspended in SSEA-3 cell growth media and plated in 6-well plates for primary expansion (passage 0). Media was removed at 24 h and placed in an empty adjacent well to provide further time for adhesion of cells remaining in suspension at 24 h. These were termed secondary cultures. 2 mL of fresh SSEA-3 cell growth media was added to the primary wells. 24 h later, media was changed in secondary cultures. Additional media changes were performed every 3 days in both primary and secondary cultures. Cells were expanded until 70-80% confluence at which time they were passaged to T75 Flasks (passage 1) for additional expansion prior to immunoselection for SSEA-3 expression. Primary and secondary unsorted cultures were combined at the time of passaging to T75 flasks. Illustrations of the tissue processing and initial cell expansion are similar to what was demonstrated in Figure 7.

FACS sorting of SSEA-3^{pos} lin^{neg} cells

Passage 1 cardiac cells were trypsinized and sorted for SSEA-3 expression. Briefly, cells at 70-80% confluence were trypsinized, washed with ice-cold MACS buffer, and labeled with Ebioscience PE- or Alexa-488-conjugated Rat IgM Anti-

Human/Mouse SSEA-3 for 30 min per the manufacturer's instructions. Cells were sorted using a Beckman Coulter MoFlo cell sorter. Gates were set to isolate the highest 1-2% SSEA-3 positive events as well as the least positive (SSEA-3 negative) events.

Immunomagnetic sorting for SSEA-3^{pos} lin^{neg} cells

Passage 1 cells at 70-80% confluence were immunomagnetically sorted for SSEA-3 according to the manufacturer's specifications using Miltenyi MS columns in conjunction with pre-separation filters. Briefly, cells were trypsinized, washed twice in ice-cold MACS buffer (1% BSA), suspended in 300 μ l 1% BSA MACS buffer, and incubated with 15 μ l of primary antibody (Ebioscience PE-conjugated rat IgM anti-human/mouse SSEA-3) for 20 min. Subsequently, cells were washed with 1% BSA MACS buffer, suspended in 80 μ l 1% BSA MACS buffer, and incubated with 20 μ l Miltenyi Mouse IgG anti-PE microbead antibody for 20 min. Cells were then washed in 10 mL sterile 1% BSA MACS buffer, suspended in 500 μ l 1% BSA MACS buffer, and loaded onto a primed magnetic column with a 30 μ m pre-separation filter. Elution procedures were performed according to the manufacturer's MS column protocol. Positively selected cells were plated in T75 flasks at subconfluence for subsequent *in vitro* expansion of human SSEA-3^{pos} lin^{neg} cells. Human SSEA-3^{pos} lin^{neg} cells were used immediately or expanded exponentially over 2 additional passages to obtain approximately 3-20 x 10⁶ cells for use in both *in vitro* and *in vivo* studies. Cells were assessed by flow cytometric analysis for SSEA-3 positivity at passage 2 following immunomagnetic sorting.

Flow cytometric analysis

Cells were trypsinized from dedicated flasks at passage 2 with TrypLE (Life Technologies) and then washed 2 times with 1% BSA MACS buffer (Miltenyi). Cells were incubated with Ebioscience rat IgM anti-human SSEA-3 Alexa Fluor 488-conjugated antibody for 45 min. Isotype control Ebioscience Alexa Fluor 488-conjugated Rat IgM was used in parallel to establish gating for flow cytometric analyses. All antibodies were used at manufacturer suggested concentrations. Flow cytometric analysis was performed using a BD Accuri C6 flow cytometer or BD LSR flow cytometer. Gates were set for false positivity of <1% in respective isotype controls. Figures and illustrations of resultant flow plots were obtained by generating jpeg images directly from the instrument without the use of any additional software. A comprehensive list of antibodies utilized for flow cytometric analyses is provided in Table 1.

Table 1.

<i>Flow Cytometry</i>			
Marker	Manufacturer	Species (anti-human)	Fluorochrome(s)
SSEA-3	Ebioscience	Rat IgM	unconjugated, alexa-488, PE
SSEA-4	Ebioscience	Mouse IgG3	unconjugated, alexa-488, PE
KDR	R&D systems	Mouse IgG1	unconjugated, alexa-700
CD31	BD	Mouse IgG1	v450
CD31	Ebioscience	Mouse IgG1	PE
c-kit	Ebioscience	Mouse IgG1	PE, APC
c-kit	Sant Cruz	Rabbit IgG	unconjugated
CD34	BD	Mouse IgG1	v450
CD34	Ebioscience	Mouse IgG1	APC
CD45	BD	Mouse IgG1	v450
CD45	Ebioscience	Mouse IgG1	ACP
CD105	Ebioscience	Mouse IgG1	PE, APC, eFluor-450
CD73	Ebioscience	Mouse IgG1	PE
CD90	Ebioscience	Mouse IgG1	PE, APC
CD29	Ebioscience	Mouse IgG1	APC
CD44	Ebioscience	Rat IgG2b	efluor-450
CD166	Ebioscience	Mouse IgG1	PE
HLA-I	BD	Mouse IgG1	v450
HLA-II	BD	Mouse IgG	PE
TRA-1-60	Ebioscience	Mouse IgM	PE
TRA-1-81	Ebioscience	Rat IgG2a	APC
CD15	BD	Mouse IgM	APC, v450
<i>Isotype controls:</i>			
Species	Manufacturer	Fluorochrome(s)	
Mouse IgG1	Ebioscience	unconjugated, FITC, alexa-488, PE, APC, eFluor-450	
Mouse IgG3	Ebioscience	unconjugated, FITC, alexa-488, PE	
Rat IgM	Ebioscience	unconjugated, alexa-488, PE	
Mouse IgG1	R&D	unconjugated, alexa-700	
Rabbit IgG	Novus/Santa Cruz	unconjugated	
<i>Secondary antibodies:</i>			
goat anti-mouse IgG		Life technologies	alexa-488, PE, APC
donkey anti-mouse IgG		Life technologies	alexa-488, PE, APC
goat anti-rabbit IgG		Life technologies	alexa-488, PE, APC
goat anti-rat IgM		Life technologies	alexa-488, APC
Antibodies : used per manufacturer's recommendations and concentrations			

Immunohistochemistry

Right atrial specimens were cut longitudinally into 2-4 mm sections and fixed for 24 h with 10% neutral buffered formalin. Tissue fragments were ethanol dehydrated, xylene cleared, and paraffin embedded. Paraffin embedded specimens were sectioned (4 μm) using a microtome, deparaffinized, and rehydrated. Antigen retrieval was performed by incubating sections with DAKO citrate buffer solution for 10 min at 95°C. Slides were next blocked in 5% BSA for 1 h prior to immunostaining. Immunostaining for SSEA-3, SSEA-4, and c-kit was performed by staining overnight at 4°C with primary antibodies. Primary antibody staining for α -sarcomeric actin, myosin heavy chain, and CD45 was performed at room temperature for 1 h. After primary antibody labeling, the sections were washed 3 times in 1X PBS for 3 min. Sections were incubated at room temperature for 1 h with secondary antibodies, counterstained with DAPI, and permanently mounted using vectashield. Images were taken on a Zeiss 510 confocal microscope and analyzed with the accompanying Zeiss software with optimization of contrast and brightness applied globally to the entire image. No extrinsic software was used to process or alter images.

Immunocytochemistry

SSEA-3^{pos} lin^{neg} cells were either seeded on chamber slides or immunolabeled in suspension for immunocytochemical characterization. In both cases, primary antibody labeling for SSEA-3, SSEA-4, and other cell surface markers was performed on live cells followed by fixation in buffered 4% PFA, methanol permeabilization for additional intracellular staining, and secondary staining with fluorophore conjugated antibodies.

Briefly, cells that were seeded onto chamber slides were allowed to attach overnight. Slides were then washed with 1X PBS and stained live with anti-human SSEA-3- and SSEA-4-unconjugated antibodies (Ebioscience at 1:100 dilutions) for 1 h at room temperature in 1% BSA MACS buffer. Slides were subsequently washed with 1X PBS for 10 min, fixed with 4% PFA (Sigma) for 15 min at room temperature, and washed with 1X PBS. Cells were permeabilized with methanol for additional intracellular immunostaining in appropriate cases. Slides were incubated with secondary antibodies conjugated with fluorophores (FITC, PE, TRITC, or APC) at room temperature (all secondary antibodies were obtained from Life Technologies). After secondary labeling and nuclear counterstaining with DAPI, slides were washed with 1X PBS and images acquired.

Suspension immunostaining was performed with similar antibody concentrations, incubation periods, fixation steps, and secondary antibody labeling as previously described, but was followed with adhering cells to microscope slides via a Cytospin and mounting with Vectashield mounting medium (Vector Labs). As before, all images were taken with a Zeiss 510 confocal microscope and analyzed with the accompanying Zeiss software. Image processing was performed relative to isotype control labeling with integral instrument software only. Modifications to brightness and contrast of images were applied to the entire image fields. No accessory image software was utilized to adjust images. A list of antibodies utilized for immunohistochemistry/cytochemistry is provided in supplemental Table 2.

Table 2.

<i>Immunohistochemistry/Immunocytochemistry</i>		
Marker	Manufacturer	Species (anti-human)
hNA	Millipore	Mouse IgG1
SSEA-3	Ebioscience	Rat IgM
SSEA-4	Ebioscience	Mouse IgG3a
WT-1	Sigma	Rabbit IgG
NANOG	Abcam	Rabbit IgG
OCT4	Ebioscience	Rat IgG
c-kit	DAKO	Rabbit IgG
c-kit	Santa Cruz	Rabbit IgG
CD45	DAKO	Mouse IgG
Tryptase	DAKO	Mouse IgG
Sarcomeric actin	Sigma	Mouse IgM
a-Myosin heavy chain	Abcam	Mouse IgG
Smooth muscle actin	Sigma	Mouse IgG
alpha-tubulin	Abcam	Mouse IgG1
connexin-43	Sigma	Rabbit IgG

Doubling times

Cell population doubling times were calculated by exponential regression, where doubling time (d) can be obtained by noting the number of final cells at time t [N(t)], the initial number of cells seeded for expansion C, and the time the culture was allowed to expand in hours t within the formula $N(t)=C2^{t/d}$. Doubling times at passage 2-3 were recorded and average doubling times for SSEA-3^{pos} lin^{neg} cells at passage 3 calculated. Cell counts were performed by hemocytometer and Trypan blue in duplicate.

Clonogenicity

Freshly MACS sorted human cardiac SSEA-3^{pos} lin^{neg} cells were seeded onto Terasaki plates using the limiting dilution technique. Wells with more than one cell were marked and excluded from further analysis. In total, fifteen 72-well Terasaki plates were seeded per patient. Six patients were utilized for the assay to calculate mean clonogenicity of human SSEA-3^{pos} lin^{neg} cells. Clonogenicity was defined as a visually verified single cell proliferating to form a colony that completely covered the well. Wells that had single cells that did proliferate but spontaneously senesced and did not result in complete well coverage were deemed “negative”. The number of colonies formed was divided by the original number of visually verified single cell wells to obtain a percent for each patient’s cells. The percentages for each patient were averaged to obtain a mean clonogenicity for human cardiac SSEA-3^{pos} lin^{neg} cells.

qPCR

Total RNA was prepared from MACS/FACS sorted SSEA-3^{pos} lin^{neg} and SSEA-3^{neg} lin^{neg} cells using PureLink® RNA Mini Kit (Life Technologies). cDNA was synthesized from total RNA using the High-Capacity cDNA Reverse Transcription Kit

(Life Technologies) with random hexamers primers according to the manufacturer's instructions. Real-time PCR was performed using the Fast SYBR® Green Master Mix (Life Technologies) per the manufacturer's protocol. Reactions were performed in duplicate on a 7900 Fast Real-Time PCR System (Applied Biosystems) at 95 °C for 30 s and 40 cycles of 5 s at 95 °C, and 30 s at 60 °C. A negative control with RNA instead of cDNA was carried out, and the integrity of PCR was verified by dissociation curve analysis. Relative gene expression was quantified from fluorescence cycle threshold (Ct) values using the $\Delta\Delta C_t$ method. Primer sequences for all targets are listed in supplemental Table 3.

Table 3:

Gene name	Forward	Reverse
BRY T	GTGCTGTCCCAGGTGGCTTACA GATG	CCTTAACAGCTCAACTCTAACT ACTTG
OCT4	GATGTGGTCCGAGTGTGGTTCT	TGTGCATAGTCGCTGCTTGAT
MIXL1	GGATCCAGGTATGGTTCCAG	GGAGCACAGTGGTTGAGGAT
NANOG	GCAGAAGGCCTCAGCACCTA	AGGTTCCCAGTCGGGTTCA
TBX5	TTCTGCACTCACGTCTTTCC	TGGCAAAGGGATTATTCTCA
TBX18	CAACAGAATGGGTTTGAAG	AAGGTGGAGGAACCTGCATT
TBX20	AGCTTTGGGACAAATTCCAT	CTTGGCCTCAGGATCCAC
NKX2.5	CCCCTGGATTTTGCATTAC	CGTGCGCAAGAACAAACG
GATA4	AAGACACCAGCAGCTCCTTC	TGTGCCCGTAGTGAGATGAC
GATA6	AAAGAGGGAATTCAAACCAGGAA	GAAGTTGGAGTCATGGGAATGG ACTTGGAAGCTGTAACAGATGA GATG
KDR	GAGGAGAAGTCCCTCAGTGATGTAG	
TERT	CGTCGAGCTGCTCAGGTCTT	AGTGCTGTCTGATTCCAATGCTT
WT1	CCAGCCCCTATTTCGAA	CGAGTACTGCTGCTCACCCA
IGF-1R	TGTCCTGACATGCTGTTTGA	AGGCTCCATCTCCTCTTTGA
GAPDH	TCAGACACCATGGGGAAG	ACATGTAAACCATGTAGTTGAG
Beta2 microglobulin	AATGCGGCATCTTCAAACCT	TGACTTTGTCACAGCCCAAGATA
OCT4	GATGTGGTCCGAGTGTGGTTCT	TGTGCATAGTCGCTGCTTGAT
NANOG	GCAGAAGGCCTCAGCACCTA	AGGTTCCCAGTCGGGTTCA
NKX2.5	CCCCTGGATTTTGCATTAC	CGTGCGCAAGAACAAACG
GATA4	AACGACGGCAACAACGATAAT	GTTTTTCCCCTTTGATTTTGTATC
MEF2C	CTGGCAACAGCAACACCTACA	GCTAGTGCAAGCTCCCAACTG
GATA6	AAAGAGGGAATTCAAACCAGGAA	GAAGTTGGAGTCATGGGAATGG ACTTGGAAGCTGTAACAGATGA GATG
KDR	GAGGAGAAGTCCCTCAGTGATGTAG	

In vitro differentiation

For myogenic differentiation, cells were expanded in T75 flasks one passage after sorting to obtain approximately 3-5 million SSEA-3^{pos} lin^{neg} sorted cells. Cells were trypsinized, seeded at a density of 10⁴ cells/cm² in 6-well plates, and allowed to attach for 24 h in SSEA-3 cell growth media. Growth media was changed to myogenic differentiation media [DMEM-LG (GIBCO), 5% horse serum (Life Technologies), 10⁻⁵M dexamethasone (Sigma), 0.75% DMSO (Sigma), 20 mmol/L ascorbic acid, 0.1% ITS liquid media supplement (Sigma), 0.1% NEAA (Lonza), and 100 U/mL Pen-Strep. Media was changed every 48 h without passaging for 35 days. Cells were harvested by trypsinization at various time points for western blot analysis for myocyte and smooth muscle contractile proteins. Additionally, cells were trypsinized and reseeded on chamber slides for contractile protein immunostaining and confocal microscopy.

Endothelial differentiation was induced by changing full growth media to EGM-2MV (Lonza) media supplemented with 60 ng/mL VEGF (PeproTech). EGM-2MV media was replaced every 48 h during the 10 day duration of endothelial differentiation. Cells were trypsinized at 90% confluence and reseeded at 40% confluence when visually indicated in T75 flasks. Cells were trypsinized and submitted for flow cytometric analysis for CD31 expression at days 0, 4, and 10 for comparison.

Western blot analyses

Cells were trypsinized, washed with 1X PBS, suspended in cell lysis buffer (1% NP40, 150mM NaCl, 20mM Tris-HCl, 1% Triton X-100, 4mM PMSF, 1:100 Proteinase Inhibitor Cocktail), and briefly sonicated. Whole cell lysates were centrifuged at 14,000 x g for 20 min and resultant lysate protein concentrations determined using Bio-Rad

Protein Assay Dye Reagent (Cat#500-0006). Whole cell lysates (15-40 μ g of protein) were resolved on 10-12% SDS-PAGE gels (Reagents from Bio-Rad), transferred to PVDF membranes, and blocked in 3% milk TBST buffer at room temperature for 30 min. Membranes were subsequently incubated with primary antibody in blocking buffer (3% milk in TBST) overnight at 4°C, washed in 1X TBST, and incubated with HRP-conjugated secondary antibodies at RT for 1 h. Membranes were then rinsed with 1X TBST and proteins detected using enhanced chemiluminescence substrate (HyGOL, Denville Scientific, Cat#E2500) according to the company instructions. Western blot antibodies are listed in Table 4.

Table 4:

Marker	Manufacturer	Cat#	Species	Mw	Usage
NKX2.5	abcam	ab91196	Ms IgG1	35kDa	WB, 1:1000
NKX2.5	abcam	ab106923	Gt IgG	35kDa	WB, 1:1000
Brachyury (T)	abcam	ab20680	Rb IgG	47, 53, 75kDa	WB:higher 1:1000
sm-MHC	Sigma	M7786	Ms IgG1	200kDa	WB: 1:2000
SMA	Sigma	A5228	Ms, IgG2a	42kDa	WB: 1:10000
α -SA	Sigma	A7811	Ms IgG	42kDa	WB:higher 1:2500
α -MHC	Novas	NB300-284	Ms IgG	250kDa	WB:1:1000
MYH6	Novas	NBP2-36746 (CL2162)	Ms, IgG2b	250kDa	WB: 1:500-1000
CX43	Sigma	C6219	Rb, IgG	43KDa	WB: 1:8000
WT1	Sigma	WH0007490M1	Ms IgG2bk	56KDa	WB, 1:500
KDR	Abcam	Ab9530	Ms, IgG1	220KDa	WB, 1:500
KDR	Sigma	SAB4300657	Rb, IgG	220KDa	WB, 1:500
vWF	Abcam	Ab6994	Rb, IgG	500+ KDa	WB, 1:500
Anti- β -actin	Cell Signaling Tech	#3700	Rb, IgG	42kDa	WB :1:1000

Cytokine Array

5×10⁶ SSEA-3^{pos} lin^{neg} or dermal fibroblasts were seeded in culture flasks in identical conditions with FBS-free F-12 media for 24 h. The supernatants (conditioned media) were collected and the secretion of various cytokines was visualized by a semi-quantitative Ab array (R&D biosystems). Intensity was determined using ImageJ software (NIH) according to manufacturer's specifications.

Animal studies

This study was performed in immunodeficient NOD/SCID (NOD.CB17-Prkdcscid/J) female mice (age ~4 months), purchased from The Jackson Laboratory (Bar Harbor, ME). All mice were maintained in micro-isolator cages under specific pathogen-free conditions in a room with a temperature of 24°C, 55–65% relative humidity, and a 12-h light–dark cycle.

Murine Model of Acute Myocardial Infarction and Intramyocardial Cell Delivery

The murine model of myocardial ischemia and reperfusion has been described in detail²⁰. Briefly, mice were anesthetized with sodium pentobarbital (60 g/kg i.p.) and ventilated using carefully selected parameters. The chest was opened through a left anterolateral thoracotomy, and a nontraumatic balloon occluder was implanted around the mid-left anterior descending coronary artery using an 8–0 nylon suture. To prevent hypotension, blood from a donor mouse was given at serial times during surgery. Rectal temperature was carefully monitored and maintained between 36.7 and 37.3 °C throughout the experiment. In all groups, myocardial infarction (MI) was produced by a 45 min coronary occlusion followed by reperfusion.

The procedure for cell transplantation by intramyocardial injection was similar to that used in our previous studies¹⁴³. Briefly, 30 min after reperfusion, 2×10^5 human cardiac SSEA-3^{pos} lin^{neg}, an equivalent number of control cells (human dermal fibroblasts obtained from ATCC), or an equivalent volume of vehicle were injected intramyocardially using a 30-gauge needle. A total of four injections (10 μ l each) were made in the peri-infarct region in a circular pattern, at the border between infarcted and non-infarcted myocardium. Mice were then allowed to recover for 39 days until euthanasia and tissue collection.

Echocardiographic studies

Murine echocardiographic images were obtained with a Vevo 2100 high frequency, high resolution (30 micron) digital imaging ultrasound system (VisualSonics, Inc.) as previously described.²⁰ Serial echocardiograms were obtained at baseline (4 days prior to coronary occlusion/reperfusion and cell transplantation), 5 days after cell transplantation, and 35 days after cell transplantation (4 days prior to hemodynamic studies and euthanasia). All studies were performed under isoflurane anesthesia. Using a rectal temperature probe, body temperature was carefully maintained between 36.7 and 37.3 °C throughout the study. Digital images were analyzed off-line by blinded observers using the Vevo 2100 workstation software. At least three measurements were taken and averaged for each parameter. Standard echocardiographic parameters were derived from the two-dimensional, M-mode, and Doppler images, as in our previous studies.²⁰ Speckle-tracking echocardiographic (STE) analysis was performed with the STE software, which utilizes semi-automated border tracking (VisualSonics, Inc.), as detailed in the online Supplement.

Hemodynamic Studies

Hemodynamic studies were performed 39 days after cell or vehicle treatment, just before euthanasia, using the ARIA-1 system and Millar catheter as described.^{141, 143} Briefly, mice were anesthetized with isoflurane and rectal temperature kept between 36.7 and 37.3 °C. A 1.0 French Millar catheter was inserted into the LV via the right carotid artery. Inferior vena cava occlusion was performed with external compression to produce variably loaded beats for determination of the end-systolic PV relation (ESPVR) and other derived constructs of LV performance. As in the case of the echocardiographic studies, all hemodynamic data analyses were performed off-line by investigators blinded to treatment group.

Cardiac tissue fixation and morphometric analysis

At the conclusion of the in vivo study, the mouse heart was arrested in diastole by an intravenous injection of 0.15 ml CdCl₂ (100 mM), excised, and perfused retrogradely at 70–80 mmHg (LVEDP = 8 mmHg) with heparinized PBS followed by 10% neutral buffered formalin solution for 15 min. The heart was then sectioned into three slices from apex to base, fixed in formalin for 24 h, and subjected to tissue processing and paraffin embedding. Paraffin-embedded LV blocks were sectioned at a thickness of 4 µm for histochemistry and immunohistochemistry. Morphometric parameters, including LV cavity area, total LV area, risk region area, scar area, LV wall thickness, and infarct expansion index were measured in sections stained with Masson's Trichrome as previously described.¹⁴³ In each mouse heart, 4 – 5 slides were stained and analyzed. From apex to base, the average distance between two stained slides was 120 - 150 µm.

Images were analyzed using NIH Image J (1.42v) and measurements from the various slices per heart averaged.

Immunohistochemistry of murine cardiac specimens

Formalin-fixed, paraffin-embedded, 4 μm -thick heart sections were deparaffinized in xylene and rehydrated gradually in a series of ethanol followed by antigen retrieval procedure. After incubation with blocking solution, persistence of transplanted human stem cells was determined by human nuclear antigen (HNA) (Millipore) immunofluorescent staining and confocal microscopy. The fate of transplanted cells was assessed by staining with specific antibodies against the myocyte marker cardiac troponin I (cTnI) (Santa Cruz), endothelial cell marker isolectin IB4 (Life Technologies), and smooth muscle cell marker α -smooth muscle actin (α -SMA) (Santa Cruz). Proliferation of transplanted cells was evaluated by immunofluorescent staining of nuclei for BrdU using a rat monoclonal antibody (Santa Cruz). In all of the immunofluorescent staining procedures, secondary antibodies conjugated with the appropriate fluorochromes (Jackson ImmunoResearch) were used. The concentration of primary and secondary antibodies corresponded to that indicated by the manufacturers. Immunohistochemical signals were acquired by confocal microscopy and quantitatively analyzed by Image J (1.42q, NIH). In each heart, HNA⁺ nuclei, double positive cells (HNA⁺/cTnI⁺, HNA⁺/IB4⁺, and HNA⁺/ α -SMA⁺), triple positive cells (HNA⁺/cTnI⁺/BrdU⁺, HNA⁺/IB4⁺/BrdU⁺, and HNA⁺/ α -SMA⁺/BrdU⁺), and total nuclei were counted in 25 confocal images acquired from the infarcted area (10), two border zones (10), and noninfarcted area (5). In all cases, at least five hearts per group were examined.

Statistics

Student's t-test, one-way ANOVA, or two-way repeated measures ANOVA, as appropriate, was employed for comparisons of qPCR analyses as well as echocardiographic, hemodynamic, and immunohistochemical studies of murine hearts. All data are reported as means \pm SEM.

Results

Localization of SSEA-3^{pos} lin^{neg} cells in human right atrial tissue

Localization of human SSEA-3^{pos} lin^{neg} cardiac cells was accomplished by immunohistochemical staining of formalin fixed, paraffin embedded, human right atrial tissue samples. Immunolabeling was performed not only for localization but also for immunophenotypic characterization of the cells in situ with antibodies specific for c-kit (CD117), CD34, CD45, SSEA-3, and SSEA-4. SSEA-3^{pos} lin^{neg} cardiac cells were observed to be most highly prevalent within the subepicardium with a decreasing gradient to the compact myocardium where they were mainly visualized as single or doubly grouped cells within the interstitial space between myocytes (Fig. 16A and Fig. 17A-C). SSEA-3^{pos} lin^{neg} cells appropriately co-expressed SSEA-4 (Fig. 16B-D). In situ, SSEA-3^{pos} lin^{neg} cells were largely c-kit negative (Fig 16E-F); however, in very rare cases, overlapping expression of c-kit [i.e. SSEA-3^{pos} SSEA-4^{pos} c-kit^{pos} cells] was also observed (Fig. 17D-G). SSEA-3 expression did not overlap with mature myocytes, smooth muscle, endothelial cells, or cardiac fibroblasts.

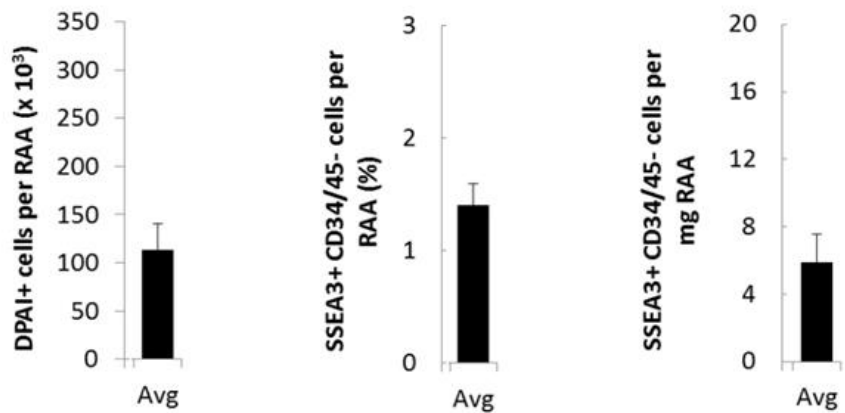
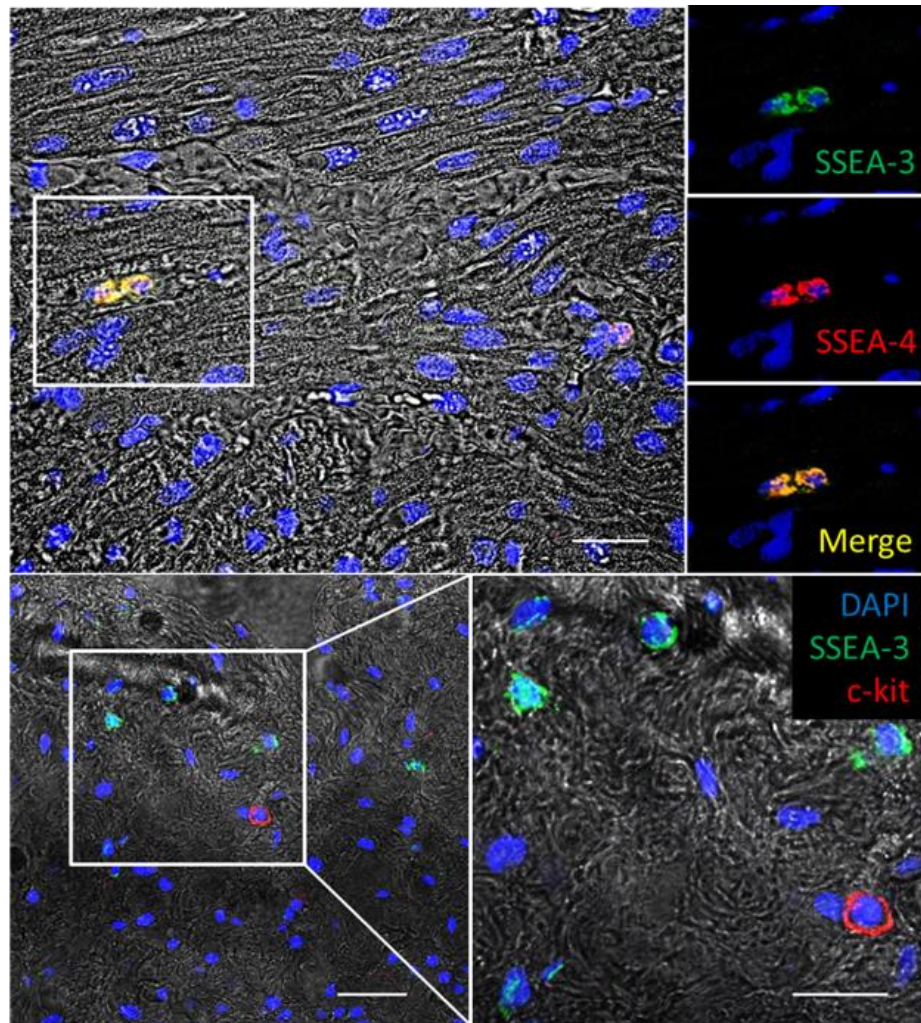


Figure 16. Cells expressing the embryonic stem cell-associate antigen SSEA-3 are present in the human heart and lack hematopoietic lineage markers (lin^{neg}). **A.** Transmission confocal microscopic image of human right atrial myocardium with

immunolabeling of SSEA-3 (green) and SSEA-4 (red). SSEA-3^{pos} cells (green) are located in the cardiac interstitium between striated myocytes. Scale bar is 50um. **B-D.** Immunolabeling of SSEA-3 (green), SSEA-4 (red), and DAPI nuclear counterstain demonstrate that SSEA-3^{pos} lin^{neg} cells appropriately co-express SSEA-4 (merged image). **E.** SSEA-3^{pos} lin^{neg} cells (green) in the white box (enlarged in panel F) lack c-kit expression. Scale bar is 50um. **F.** A c-kit^{pos} cell is shown in close proximity to the SSEA-3^{pos} lin^{neg} cells; this suggests that SSEA-3^{pos} lin^{neg} cells are distinct from previously described populations of cardiac progenitors. **G-I.** The prevalence of SSEA-3^{pos} lin^{neg} cells in human right atrial myocardium was quantified by flow cytometric analysis after total enzymatic digestion of right atrial samples and was normalized to milligrams of right atrial tissue from which the cells originated. **G.** An average of $1.13 \pm 0.27 \times 10^5$ nucleated cells were analyzed per human right atrial sample (n=12) after complete enzymatic digestion. **H.** SSEA-3^{pos} lin^{neg} cells accounted for $1.3 \pm 0.19\%$ of total nucleated cells obtained from right atrial samples. **I.** The prevalence of SSEA-3^{pos} lin^{neg} cells was 5.8 ± 1.7 cells per milligram of human right atrial tissue (n=12).

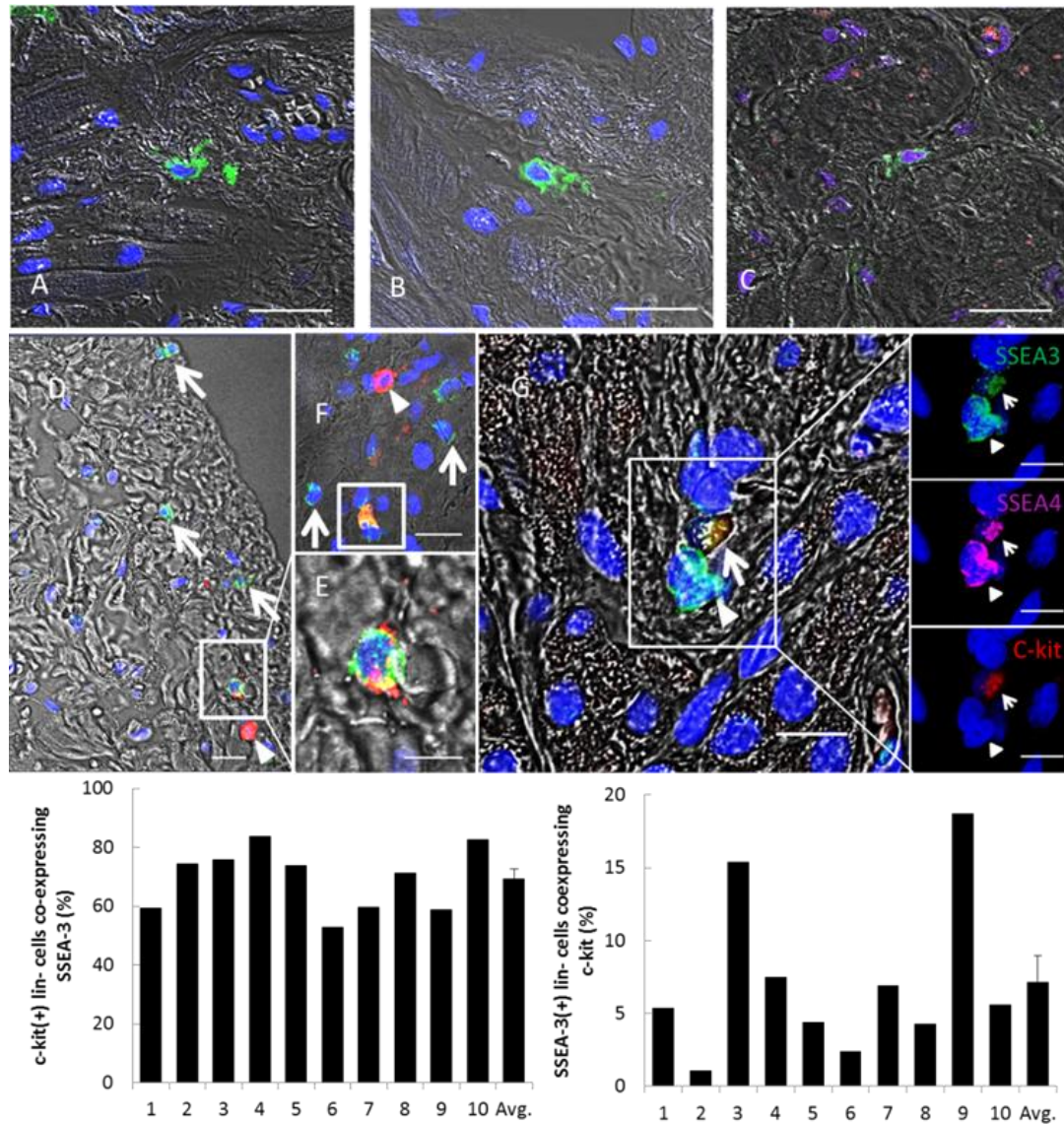


Figure 17. SSEA-3^{pos} cardiac cells are located within the subepicardium and myocardial interstitium predominantly as solitary cells, and a subpopulation of SSEA-3 positive cells express c-kit, likely representing an intermediate phenotype of cardiac progenitors. A-C. Shown (top) are three confocal microscopy images of solitary SSEA-3^{pos} cardiac cells (green) within formalin fixed adult human right atrial tissue specimens from separate patients. **D.** This confocal microscopic image demonstrates higher prevalence of SSEA-3^{pos} cells within the subepicardium. The SSEA-3^{pos} cells

within the compact myocardium were observed as single cells within the interstitium as shown in images **A-C**. SSEA-3^{pos} (green) c-kit^{neg} (red) cells are highlighted by arrows and c-kit^{pos} SSEA-3^{neg} cells by arrowheads (scale is 20um). Notably, a cell expressing both SSEA-3 and c-kit can be seen within the white box. **E**. An enlarged image of the white box in image D shows the intermediate phenotype of SSEA-3 and c-kit positivity (scale is 10um). **F**. Another example of an SSEA3^{pos} c-kit^{pos} cell within the white box. SSEA-3^{pos} c-kit^{neg} cells are indicated by arrows and a c-kit^{pos} SSEA-3^{neg} cell marked by the arrowhead (scale is 20um). **G**. A group of SSEA-3 expressing cells (arrowhead) within the myocardial interstitium between striated myofibrils is shown within the white box. These cells co-express SSEA-4 as shown on the right with fluorophore separated images expanded from the white box. One of the cells was observed to also express c-kit (arrow) in addition to SSEA-3 and SSEA-4. Scale bar is 10um. **H**. Flow cytometric based quantitation of cells obtained from freshly digested right atrial tissue samples demonstrated that cardiac SSEA-3^{pos} lin^{neg} cells displayed partial overlap with SSEA-3 expression (69.2±3.4%, n=10) validating the in vivo observation shown in images D-G. **I**. Immediately after enzymatic digestion, 7.18±1.78% of SSEA-3^{pos} lin^{neg} cells co-expressed c-kit (n=10). Data are mean±SEM.

Prevalence of SSEA-3^{pos} lin^{neg} cells in human right atrial tissue in situ

The prevalence of SSEA-3^{pos} lin^{neg} cells was quantified by immunolabeling of cardiac cells obtained after total enzymatic digestion of human right atrial tissue samples with antibodies specific to SSEA-3, CD34, and CD45. An average of $1.13 \pm 0.27 \times 10^5$ nucleated cells were analyzed per human right atrial sample (n=12). SSEA-3^{pos} lin^{neg} cells accounted for $1.3 \pm 0.19\%$ of total nucleated cells obtained from right atrial samples after robust enzymatic digestion. The prevalence of SSEA-3^{pos} lin^{neg} cells was 5.8 ± 1.7 cells per milligram of right atrial tissue (Fig. 16G-I).

Quantification of overlapping c-kit^{pos} and SSEA-3^{pos} lin^{neg} populations in situ

Quantification of c-kit^{pos} and SSEA-3^{pos} populations was performed by immunolabeling and flow cytometric analysis (excluding CD34^{pos}/45^{pos} cells) after complete enzymatic digestion of right atrial tissue samples (n=10). C-kit^{pos} lin^{neg} cardiac cells demonstrated a high degree of overlap with SSEA-3 expression ($69.2 \pm 3.41\%$). However, SSEA-3^{pos} lin^{neg} cells demonstrated much less overlap with c-kit co-expression: only $7.18 \pm 1.78\%$ of SSEA-3^{pos} lin^{neg} cells showed co-expression of c-kit (Fig. 17H-I) as assessed by flow cytometric analysis immediately after total enzymatic digestion.

SSEA-3 immunoselection confers enrichment for markers associated with stemness and early cardiac commitment

After enzymatic digestion of right atrial tissue and primary expansion of tissue culture plate adherent cardiac cells, passage 1 cells were immunolabeled with antibodies specific to SSEA-3 and c-kit. To validate the utility of SSEA-3 as a surrogate stemness associated cell surface molecular target by which cardiac precursors may be selected for

and isolated, SSEA-3^{pos} lin^{neg} cells were FACS sorted for qPCR comparison with unsorted cardiac cells to determine if selection of cells expressing SSEA-3 results in enriched expression of the pluripotency associated markers OCT4 and NANOG as well as early and late cardiac markers NKX2.5 and GATA4 and MEF2C, respectively. SSEA-3^{pos} lin^{neg} cardiac cells demonstrated higher expression of OCT4 (62.5±26.33 fold, P<0.05) and NANOG (89.7±42.6, P<0.05) as well as the early cardiac marker NKX2.5 (137.3±75.3, P<0.05) (n=5), albeit at relatively low levels compared with the internal control (GAPDH or β 2-microglobulin). There was no enrichment of GATA4 or MEF2C transcript expression in SSEA-3 expressing cells (Fig. 3) compared with unsorted cardiac cells. All SSEA-3^{pos} lin^{neg} cardiac cells at passage 1 lacked expression of the hematopoietic markers CD34 and CD45 (data not shown) and showed adherence to plastic culture plates, indicating that these cells are not hematopoietic progenitors (which are non-adherent to tissue culture plates) and are not immediately from the bone marrow.

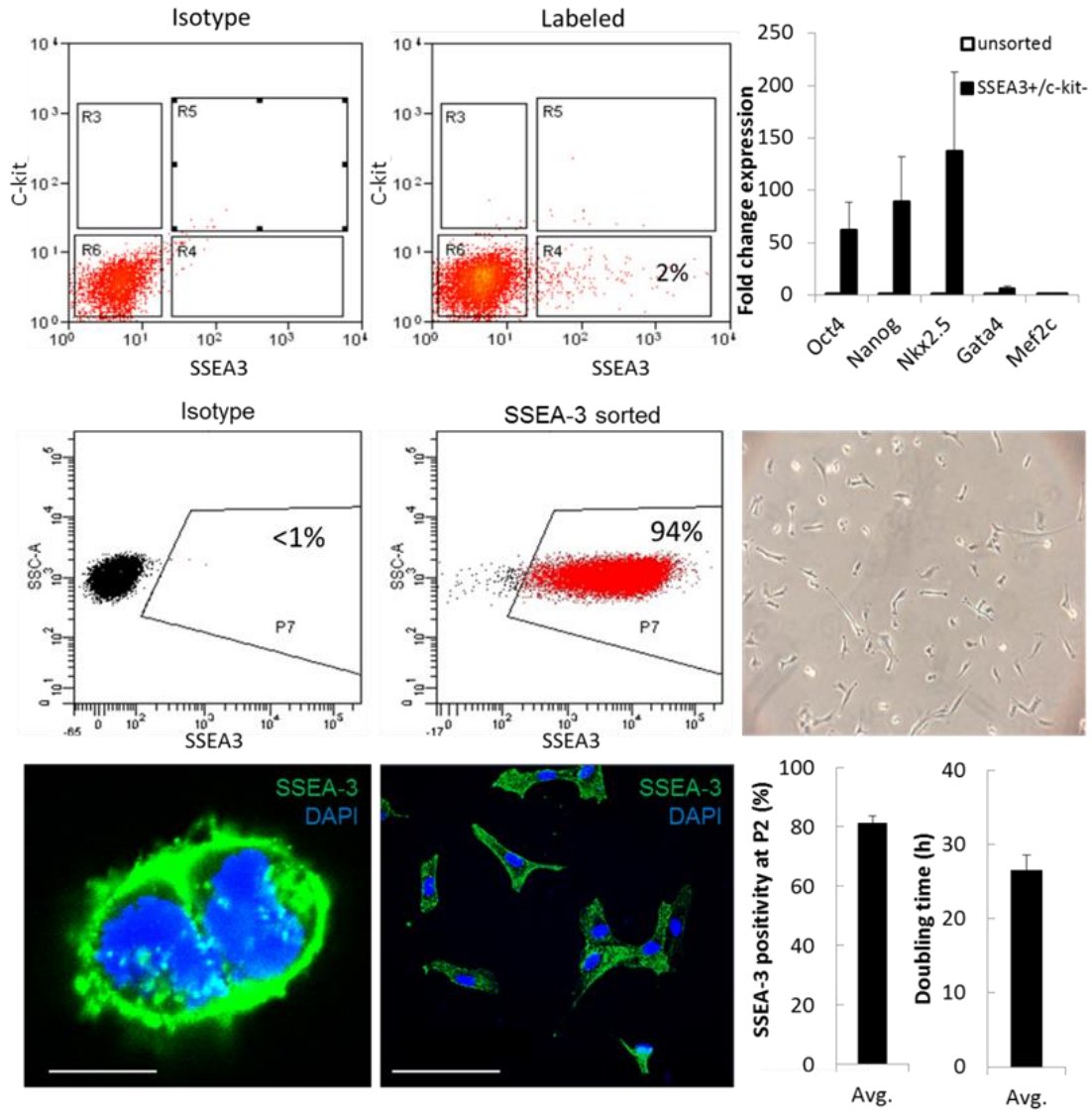


Figure 18. SSEA-3 immunoselection: Enrichment of pluripotency associated markers, cardiac mesodermal markers, isolation and expansion. A. A representative FACS sorting plot of SSEA-3^{pos} lin^{neg} cardiac cells at passage 2 is shown with sorting gate R4 (center panel) established with respect to isotype control (left panel) for false positivity <1%. In this patient, SSEA-3^{pos} lin^{neg} cells were 2% of the total *in vitro* expanded cell population that were FACS sorted for qPCR-based comparison. Comparison of SSEA-3^{pos} lin^{neg} FACS sorted cells to the unsorted population by qPCR demonstrated enriched relative expression of *OCT-4* (62.5±26.33 fold, P<0.05), *NANOG*

(89.7 ± 42.6 , $P < 0.05$), and *NKX2.5* (137.3 ± 75.3 , $P < 0.05$), $n=5$. **B.** Flow cytometric analysis of resultant magnetically sorted SSEA-3^{pos} lin^{neg} cardiac cells is shown with gates established by isotype control <1% false positivity in P7 (left panel). Immunomagnetically sorted SSEA-3^{pos} cells were 94% positive for SSEA-3 after MACS sorting in this particular patient. A representative light microscopic image of SSEA-3^{pos} lin^{neg} cardiac cells is shown in the right panel (10x magnification). **C.** Confocal images of SSEA-3^{pos} lin^{neg} cells (green) are shown in the left (10 μ m scale) and center (100 μ m scale). SSEA-3^{pos} lin^{neg} cells at passage 2-3 demonstrated an average doubling time of 26.5 ± 2.11 h ($n=9$ patients). **D.** Immunomagnetically selected SSEA-3^{pos} lin^{neg} cardiac cells were assessed by flow cytometric analysis at the end of passage 2 for SSEA-3 positivity. A mean SSEA-3 positivity of $81.4 \pm 2.34\%$ was achieved demonstrating reproducibility of isolation and *in vitro* expansion ($n=32$). **E.** Doubling times of immunomagnetically selected SSEA-3^{pos} lin^{neg} cells calculated during passage 2-3 averaged 26.5 ± 2.1 h.

Validation of clinically relevant methods of SSEA-3^{pos} lin^{neg} cell isolation and expansion

SSEA-3^{pos} lin^{neg} cells could be sorted and enriched with high efficiency. A representative flow cytometric plot of MACS enriched SSEA-3^{pos} lin^{neg} cells as well as phase contrast and confocal microscopic immunocytochemical images of freshly MACS sorted SSEA-3^{pos} lin^{neg} cardiac cells prior to passage 2 *in vitro* expansion are shown (Fig. 18). *In vitro* expansion of SSEA-3^{pos} lin^{neg} cells yielded approximately 3-5 x 10⁶ cells at the end of passage 2 (demonstrating an average SSEA-3 positivity of 81.4±2.34%, n=32) which were able to be expanded exponentially to 30-50 x 10⁶ cells by the end of passage 3 for potential therapeutic utilization. The doubling time of SSEA-3^{pos} lin^{neg} cells at passage 2-3 averaged 26.5±2.11 h (n=9) (Fig. 18).

To validate the MACS based sorting methodology, a similar comparison of immuno-magnetically (MACS) selected SSEA-3^{pos} lin^{neg} cardiac cells with the negatively sorted fraction was performed via qPCR (Fig. 4). MACS selection of cells expressing SSEA-3 demonstrated consistent enrichment of cells expressing higher levels of NANOG (30.7±5.63 fold), OCT4 (8.48±2.01), MIXL1 (45.4±6.6), NKX2.5 (14.8±3.73), and TERT (48.2±13.3), P<0.05 (Fig 4A). NANOG was detected by immunostaining with nuclear localization in some SSEA-3^{pos} cells (Fig. 4D). KDR and GATA6 exhibited a trend toward enrichment; however this was not statistically significant. Although there was no significant difference in the expression of TBX5, TBX18, TBX20, or GATA4 transcripts between SSEA-3^{pos} and SSEA^{neg} cells, qPCR cycle times revealed relatively high expression of TBX18, TBX20, and GATA4 in both populations (data not shown).

TBX5 was detectable by qPCR, but lowly expressed in both SSEA3^{pos} and SSEA3^{neg} sorted cells (data not shown). Transcripts for ISL-1 and MESP1 were not detected.

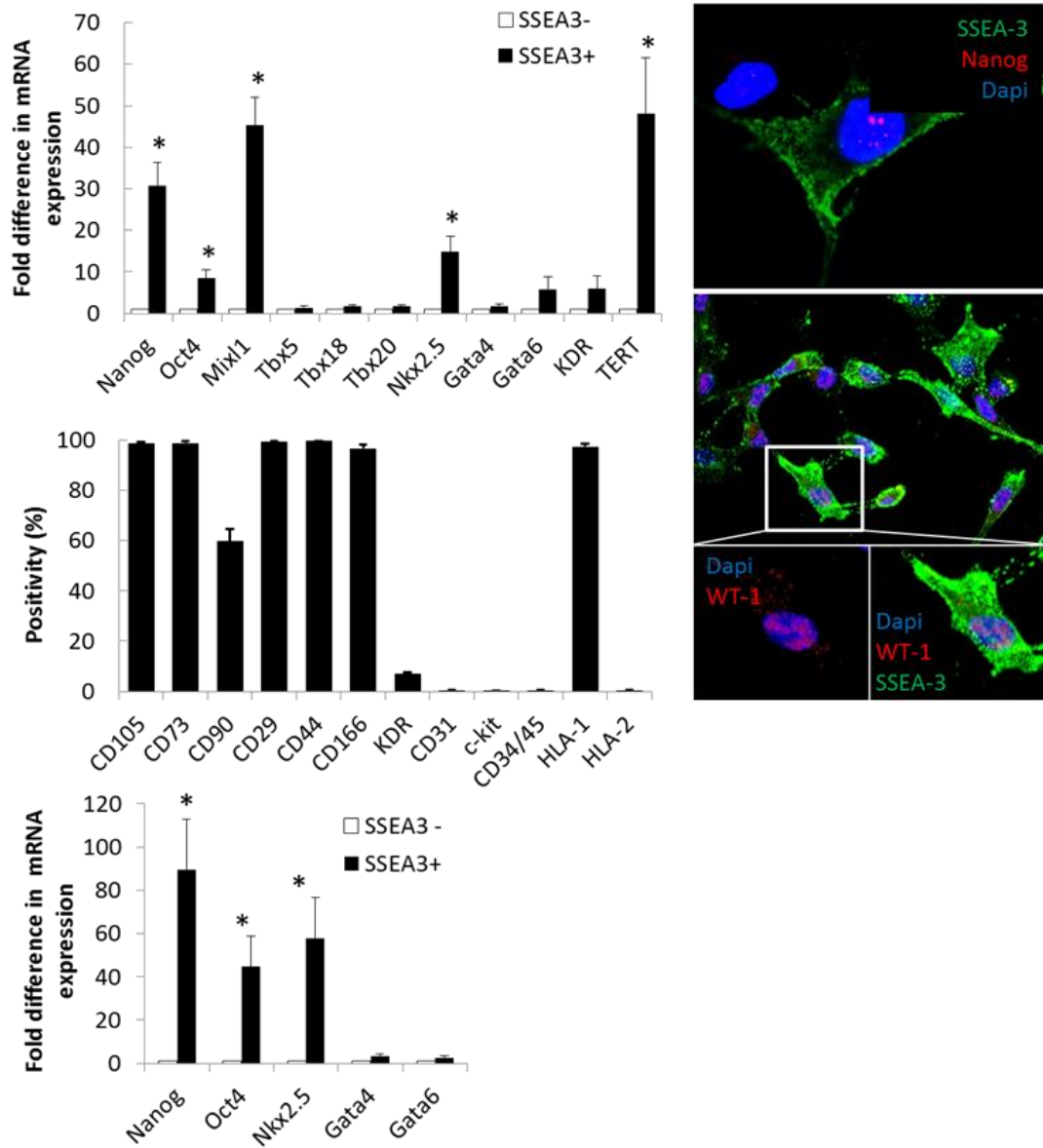


Figure 19. Characterization of in vitro expanded SSEA-3^{pos} lin^{neg}. **A.** qPCR of immunomagnetically selected SSEA-3^{pos} cardiac cells demonstrated similar patterns of enrichment for pluripotency associated markers *NANOG* (30.6±5.63) and *OCT4* (8.48±2.01), early cardiac mesodermal markers *MIXL1* (45.4±6.60) and *NKX2.5* (14.8±3.73), and telomerase reverse transcriptase, *TERT* (48.15±13.3), P<0.05. **B.** Flow cytometric analyses of in vitro expanded SSEA-3^{pos} lin^{neg} cells isolated from 6 human

right atrial tissue samples consistently demonstrated a mesenchymal phenotype with near complete positivity for CD105 (98.8±0.43%), CD73 (98.8±0.74%), CD29 (99.5±0.11%), CD44 (99.5±0.31%), CD166 (96.7±3.90%), and HLA class 1 (97.4±1.18%) and heterogeneity of CD90 (59.6±4.77%) expression. SSEA-3^{pos} lin^{neg} cells lacked expression of hematopoietic markers CD34 and CD45 (0.53±0.09%), c-kit (0.28±0.06%), CD31 (0.48±0.13%) and HLA class 2 (0.35±0.11%). Heterogeneity of KDR expression was observed (7.0±0.56%). C. As SSEA-3 expression was observed to decrease over time and with passaging, qPCR performed after SSEA-3 re-enrichment by immunoselection of cells retaining SSEA-3 expression at advanced passage (passage 9) showed continued enrichment of pluripotency associated markers *NANOG* (89.6±23.3) and *OCT4* (44.6±14.0) as well the early cardiac marker *NKX2.5* (57.6±19.0) compared with that of the SSEA-3 negative fraction. *GATA4* and *GATA6* expression was not observed to differ significantly. Asterisks mark statistical significance with P<0.05 in all graphs.

Immunophenotypic analyses of SSEA-3^{pos} lin^{neg} cells

SSEA-3^{pos} lin^{neg} cardiac cells at passage 2 were analyzed by flow cytometry for co-expression of mesenchymal, endothelial, and hematopoietic lineage markers (Fig. 20). SSEA-3^{pos} lin^{neg} cells demonstrated a predominantly mesenchymal phenotype, with near complete positivity for CD105 (98.8±0.43%), CD73 (98.8±0.74%), CD29 (99.5±0.11%), CD44 (99.5±0.31%), CD166 (96.7±3.90%), and human leukocyte antigen (HLA) class 1 (97.4±1.18%) and heterogeneity for CD90 (59.6±4.77%) and KDR (7.0±0.56%) expression (Fig. 20). SSEA-3^{pos} lin^{neg} cells lacked the endothelial marker CD31 (0.48±0.13%), hematopoietic lineage markers CD34 and CD45 (0.53±0.09%), and HLA class 2 (0.35±0.11%). Despite showing positivity for SSEA-3 and SSEA-4, *in vitro* expanded cells did not express the tumor related antigen (TRA)-1-60 or TRA-1-81 that are commonly observed, in addition to SSEAs, in iPSCs and ESCs.²⁰⁷ Although overlapping c-kit expression was observed *in situ* (vide supra) (~ 8% of SSEA-3^{pos} lin^{neg} cardiac cells immediately after total enzymatic digestion, n=10) (Fig. 17), analyses at passage 2 after *in vitro* expansion did not demonstrate any appreciable c-kit expression (0.28±0.06%), indicating that c-kit expression is transient, that SSEA-3^{pos} c-kit^{pos} cells do not expand in the present culture conditions, or that SSEA-3^{pos} c-kit^{pos} cells proliferate at a much slower rate than SSEA-3^{pos} c-kit^{neg} cells, if they are in fact separate populations.

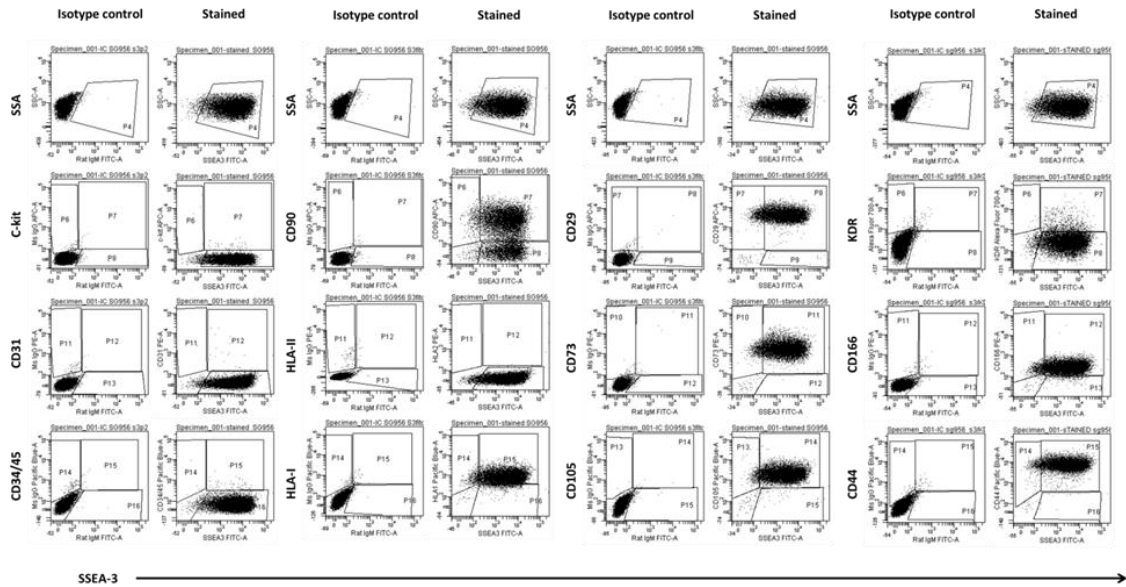


Figure 20. Immunophenotype of *in vitro* expanded SSEA-3^{pos} lin^{neg} CPCs. Flow cytometric detection of progenitor (SSEA3, C-KIT), endothelial (CD31, KDR), mesenchymal (CD29, CD44, CD73, CD90, CD105, CD166), human leukocyte (HLA-1, HLA-II), and hematopoietic (CD34/45) cell surface antigens in SSEA-3^{pos} lin^{neg} CPCs.

TBX18 has been observed to be expressed in proepicardial progenitors¹¹⁰, although recent evidence suggests that it is not completely confined to this compartment within the fetal or mature heart.¹¹¹ Therefore, our observation of TBX18 mRNA expression within SSEA-3^{pos} lin^{neg} cells (vide supra) cannot conclusively link these cells to a particular cardiac progenitor lineage from fetal development. In contrast, Wilms tumor gene 1 (WT-1), a marker with significant overlapping expression with TBX18, has been utilized to exclusively define and track distinct proepicardial lineage derivatives, epicardial derived cells (EPDCs), and epicardial epithelial to mesenchymal transition (EMT) during cardiac development.^{84, 104, 105} WT-1 has also been demonstrated to be expressed in response to myocardial injury within epicardial cells, essentially reactivating a fetal gene program for cardiac repair after infarction.^{197, 210, 211} We observed WT-1 expression within *in vitro* expanded SSEA-3^{pos} lin^{neg} cells. Immunostaining showed primarily nuclear with some cytoplasmic localization of WT-1 (Fig. 19E). PCR analysis of SSEA-3^{pos} lin^{neg} cells confirmed transcript expression of WT-1 (Fig. 21). Observation of WT-1 expression may suggest SSEA-3^{pos} lin^{neg} cells are originally of proepicardial origin. Incidentally, SSEA-3^{pos} lin^{neg} cells also demonstrated robust expression of IGF-1R by PCR (Fig. 21) similar to other described cardiac derived cell populations.²¹²

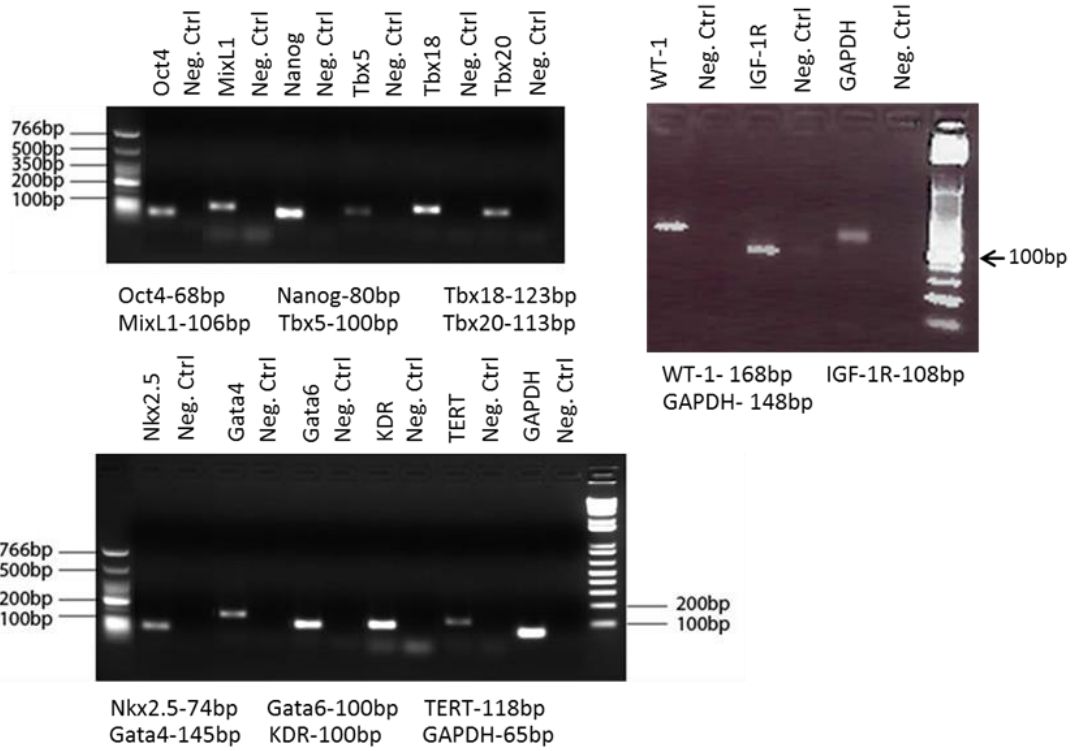


Figure 21. Validation of PCR products. Shown are representative gels validating target sizes of PCR products ensuring specificity and appropriate target size with negative controls.

SSEA-3^{pos} lin^{neg} cells are clonogenic and display multipotent differentiation potential toward myocytes, smooth muscle, and endothelial cells

Freshly sorted human cardiac SSEA-3^{pos} lin^{neg} cells were plated at low density in suspension culture for assessment of their ability to expand and form spheres spontaneously, which would indirectly imply clonogenic ability. SSEA-3^{pos} lin^{neg} cells formed spheres in suspension culture resembling previously described cardiospheres (Fig. 22A).²¹³ Spheres were allowed to expand; replating of spheres on normal tissue culture plates resulted in expansion of cells contained within the spheres, confirming that the spheres consisted of viable cells. The cell surface immunophenotype of SSEA-3^{pos} lin^{neg} cells that were expanded in suspension and allowed to form spheres did not differ, after replating and in vitro expansion, from those expanded in adherent monolayer conditions. The immunophenotype of SSEA-3^{pos} lin^{neg} cells was similar to that of cardiosphere-derived cells^{214, 215} as well as c-kit sorted cardiac cells¹⁴⁰ with respect to cell surface CD marker expression (Fig. 20).

Terasaki plates were seeded by limiting dilution with one cell per well to evaluate clonogenicity. Singly seeded SSEA-3^{pos} lin^{neg} cells formed colonies at an average frequency of 21.16±3.8%, n=8. Representative single cell cloning progression is shown in Figure 22B.

SSEA-3^{pos} lin^{neg} cells at passage 2 were placed in directed differentiation conditions to induce myocyte, smooth muscle, and endothelial differentiation. Immunocytochemistry of cells placed in myogenic differentiation conditions demonstrated upregulation of the sarcomeric proteins alpha-myosin heavy chain (α -MHC) and α -sarcomeric actin after 35 days (Fig. 22C). Connexin 43 expression was

visualized at sites of cell-cell contact, indicating functional gap junction formation between adjacent cells (Fig. 22B). However, the staining pattern of sarcomeric proteins did not yield mature, striated sarcomeric structures, indicating incomplete differentiation. Robust smooth muscle differentiation was observed, with marked upregulation of smooth muscle actin and upregulation of smooth muscle myosin heavy chain (Fig. 22E). After differentiation, cell morphology was consistent with mature appearing smooth muscle cells. Endothelial differentiation conditions resulted in marked upregulation of CD31 (PECAM) by immunostaining and confocal microscopy (Fig. 22F) and flow cytometric analysis (Fig. 22G), with changes in morphology resembling typical endothelial cells. Flow cytometric analysis of SSEA-3^{pos} lin^{neg} cells during endothelial differentiation demonstrated upregulation of CD31 at day 4 and appropriate down regulation of SSEA-3. By day 10, >75% of cells had become CD31 positive with complete loss of SSEA-3 expression. Endothelial differentiated cells formed tubes when seeded in matrigel, demonstrating phenomena typical of functional endothelial cells (Fig. 22H).

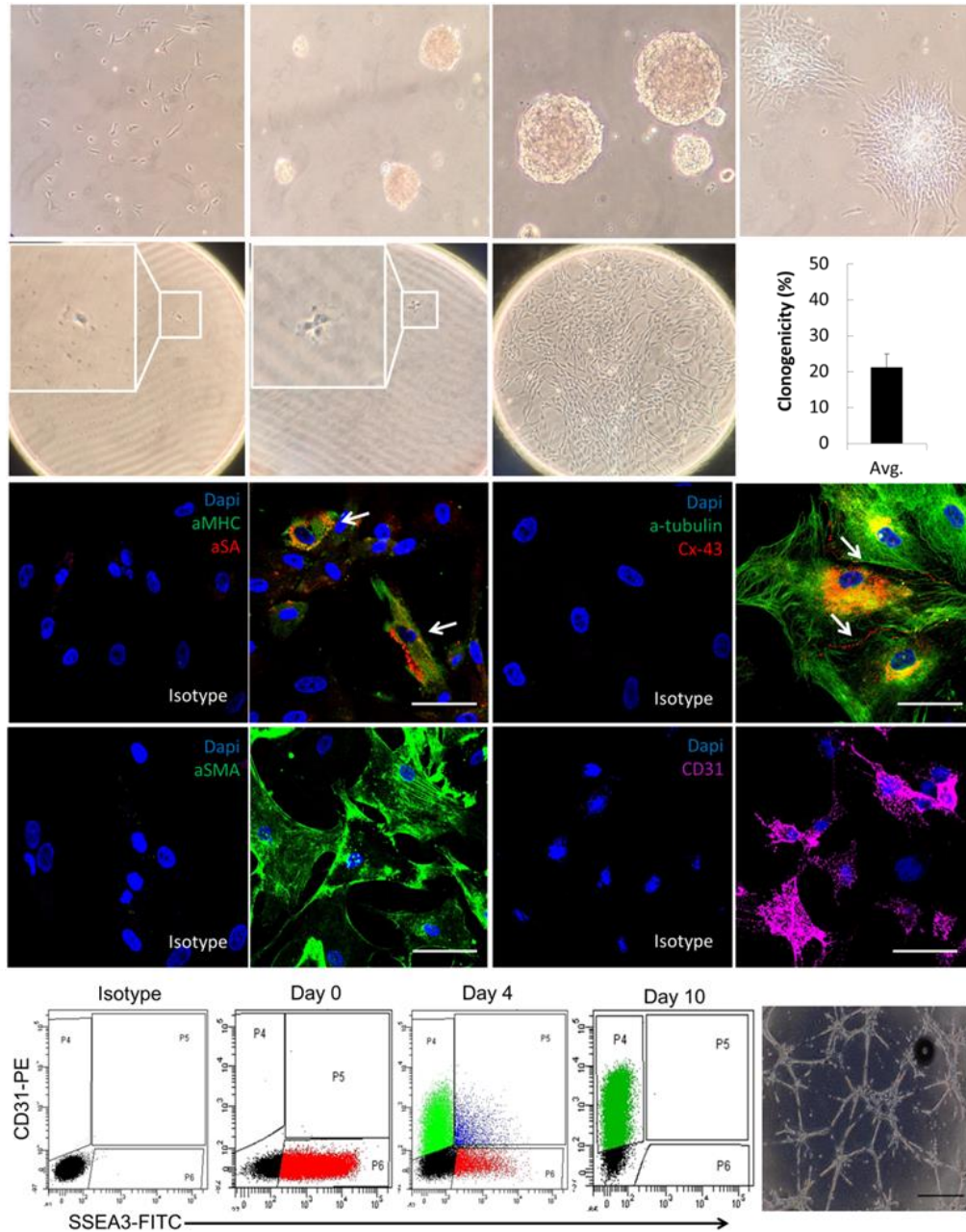


Figure 22. SSEA-3^{pos} lin^{neg} cells display clonogenic and multipotent differentiation capacities expressing mature cardiac markers of myocytes, smooth muscle, and endothelial cells under directed *in vitro* differentiation conditions. A. SSEA-3^{pos} lin^{neg} cardiac cells demonstrated the ability to form expanded spheres in suspension when seeded at very low density, indicative of clonogenic ability. Attached SSEA-3^{pos} lin^{neg}

cells are shown after immunoselection (top left panel). Multicellular spheres formed and expanded after low density seeding in suspension culture (center panels). These multicellular spheres contained viable cells as evidenced by the attachment and expansion of cells when seeded into normal tissue culture plates (right image). **B.** True clonogenic ability was evaluated by singly seeded SSEA-3^{pos} lin^{neg} cardiac cells in Terasaki plates shown (left) with enlarged image expanded in the box. Clonogenic expansion is seen in the center panel with four cells having originated from a single SSEA-3^{pos} lin^{neg}, ultimately giving rise to a colony (right panel). Singly seeded SSEA-3^{pos} lin^{neg} cells from different human patients formed clonal colonies in Terasaki plates at an average frequency of $21.16 \pm 3.8\%$ as shown in the bar graph on the right (n=8). Values in graphs are represented as mean \pm SEM. **C.** Immunocytochemistry showing expression of alpha-myosin heavy chain (green) and alpha-sarcomeric actin (red) after directed myogenic differentiation. Nuclei were counterstained with DAPI (blue). **D.** Differentiated SSEA-3^{pos} lin^{neg} cells formed gap junctions with adjacent cells highlighted by connexin 43 (red) expression (arrow) and alpha-tubulin (green). **E.** SSEA-3^{pos} lin^{neg} cells robustly formed smooth muscle like cells illustrated by smooth muscle actin (green) expression. **F.** Expression of CD31 (magenta) is shown resulting from 10 days of endothelial directed differentiation conditions. **G.** The time course of endothelial differentiation is illustrated over 10 days for SSEA-3 positive cells [81% SSEA-3^{pos}/ $<1\%$ CD31^{pos}] at day 0 with respect to isotype control. CD31 was upregulated at day 4 and robustly at day 10 [78% CD31^{pos}] with loss of SSEA-3 during differentiation ($<1\%$ at day 10). Functional capacity with endothelial tube formation of CD31^{pos} differentiated SSEA-3^{pos} lin^{neg} CPCs is shown in the right panel. Scale bars are 50um.

SSEA-3^{pos} lin^{neg} cells induce cardiac repair and functional recovery after ischemia/reperfusion injury

The effect of SSEA-3^{pos} lin^{neg} cardiac cell administration on LV remodeling after myocardial infarction was investigated by morphometric analysis of Masson's trichrome stained sections (Fig. 23A). Although the LV risk region was similar across all groups (Fig. 23B), mice that received SSEA-3^{pos} lin^{neg} cells exhibited a statistically significant increase in viable myocardium relative to vehicle (Fig. 23A&B). Further, as there were no significant differences in mean anterior wall (infarcted wall) thickness across groups, LV expansion indices were markedly reduced in SSEA-3^{pos} lin^{neg} cell-treated animals relative to vehicle (Fig. 23C).

The effect of SSEA-3^{pos} lin^{neg} cardiac cell therapy on ventricular volume and function after myocardial infarction was investigated by echocardiographic analyses and Millar methodology. Significantly reduced left ventricular end-diastolic (Fig. 24A) and end-systolic (Fig. 24B) volumes were observed in the SSEA-3^{pos} lin^{neg} cell treatment group compared to vehicle treated controls. Accordingly, measurements of left ventricular ejection fraction were significantly higher in the SSEA-3^{pos} lin^{neg} cell treatment group compared to controls by both single plane B-mode (44.4±2.8% vs. 29.8±2.8%) and Simpson's biplane (44.8±2.5% vs. 31.3±1.8%) methods of assessment. In the setting of comparable body weights and heart rates between the treatment and control group (data not shown), high ejection fraction in the cell treatment group translated to increased stroke work and total cardiac output in SSEA-3^{pos} lin^{neg} cell treated hearts.

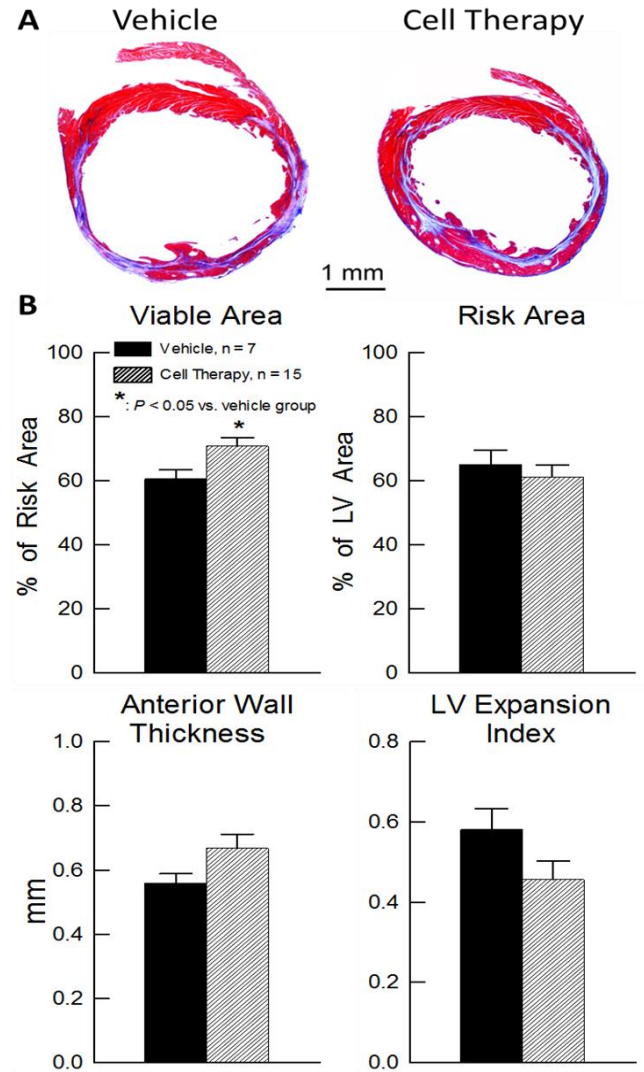


Figure 23. Left ventricular morphometric analyses. Vehicle (*black*), cell control (*white*), and SSEA-3^{pos} lin^{neg} cells (*grey*) groups. Serial echocardiographic studies were performed under isoflurane anesthesia at baseline (4 days prior to surgery) and 5 and 35 days after myocardial infarction. Data are mean \pm SEM. A. Mason's trichome staining shows increased viable myocardium and decreased scar size in a representative cross-section of the left ventricle from a cell treated heart vs. that of control. B. Viable tissue was significantly larger with similar size of risk region in the cell treated hearts over those of controls.

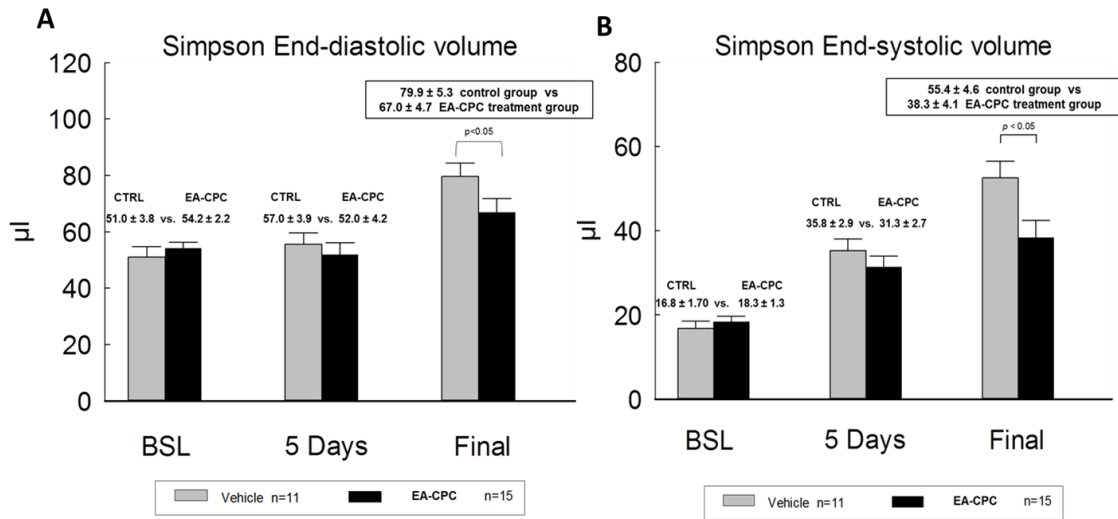


Figure 24. Left ventricular volumetric comparison. Left ventricular end diastolic and end systolic volumes were assessed by Simpson’s method echocardiography comparing SSEA-3^{pos} lin^{neg} cells (EA-CPC) treatment and vehicle control groups at baseline, 5 days and 35 days after I/R injury. **A.** The average left ventricular end diastolic volume was significantly smaller in the SSEA-3^{pos} lin^{neg} cells treatment group (67.0ul) vs that of the control (79.9ul) indicating less adverse LV remodeling and less decompensatory LV dilatation in the SSEA-3^{pos} lin^{neg} cells treatment group. **B.** Similarly, end systolic volumes were significantly smaller in the SSEA-3^{pos} lin^{neg} cells treatment group than control group. Human SSEA-3^{pos} lin^{neg} cells abrogate LV dilatation and adverse remodeling after ischemia/reperfusion injury that is known to lead to heart failure as well as promote restoration of systolic function after ischemic injury. There was no difference between groups at baseline or at 5 days ($p > 0.05$) indicating similar starting cohorts of female SCID mice and similar initial ischemic cardiac injury.

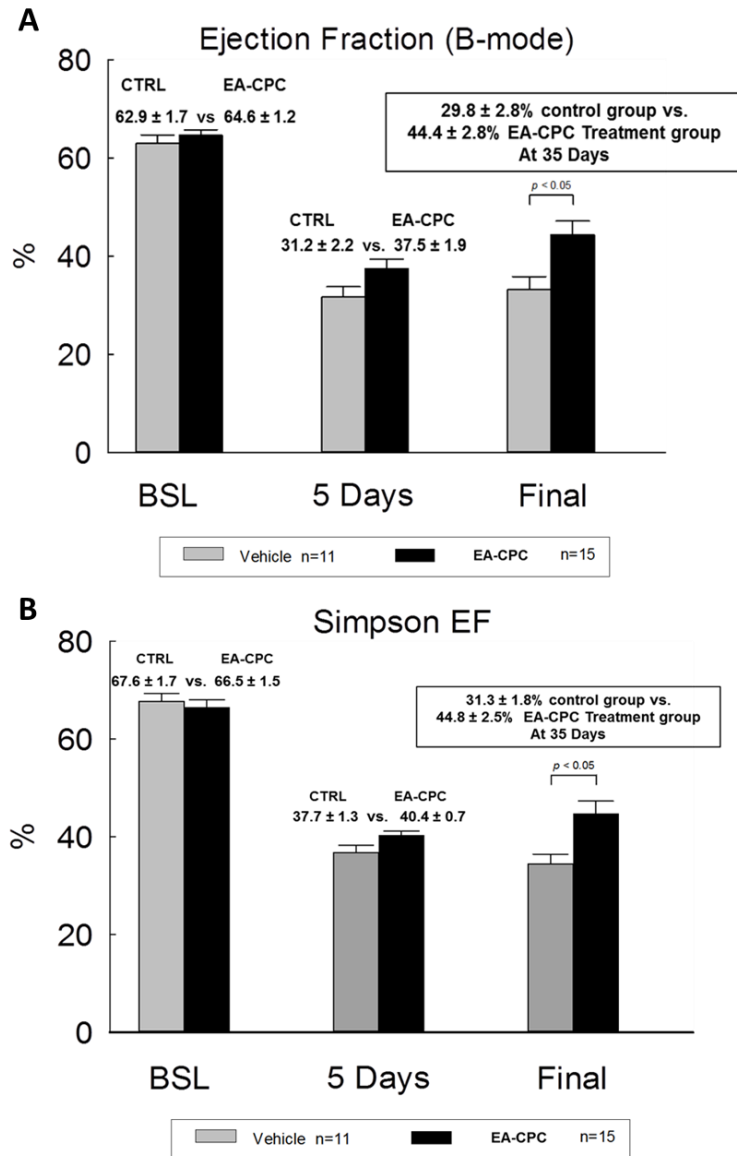


Figure 25. Ejection Fraction. Echocardiography (echo) was performed for left ventricular functional assessment in an immunocompromised murine model (SCID mice) of ischemia/reperfusion (I/R) injury and subsequent human SSEA-3^{pos} lin^{neg} cell intramyocardial administration. Echo was performed at baseline prior to injury as well as 5 days and 35 days post I/R with subsequent cell therapy by intramyocardial injection of 200K human SSEA-3^{pos} lin^{neg} cells or normal saline control in the border zones of the infarction area. **A.** Significant improvement in cardiac function was seen over 35 days in

the SSEA-3^{pos} lin^{neg} cells treatment group (EA-CPCs) vs that of the control group (CTRL). The control group had an average ejection fraction (EF) of 29.8% while the human SSEA-3^{pos} lin^{neg} cell treated group saw significant functional improvement to 44.4% (p<0.05) as measured in B Mode echocardiography. **B.** Ejection fraction assessed by Simpson's method echocardiography showed similar a pattern of improvement in the SSEA-3^{pos} lin^{neg} cell (EA-CPC) treatment with 44.8% EF vs. 31.3% EF in the control group. There was no significant difference between groups at baseline or at 5 days by either measurement methodology indicating no difference in starting populations/cohorts of SCID mice and no difference in the extent of induced myocardial injury. Improvements observed at 35 days are solely due to the treatment with SSEA-3^{pos} lin^{neg} cells (EA-CPCs).

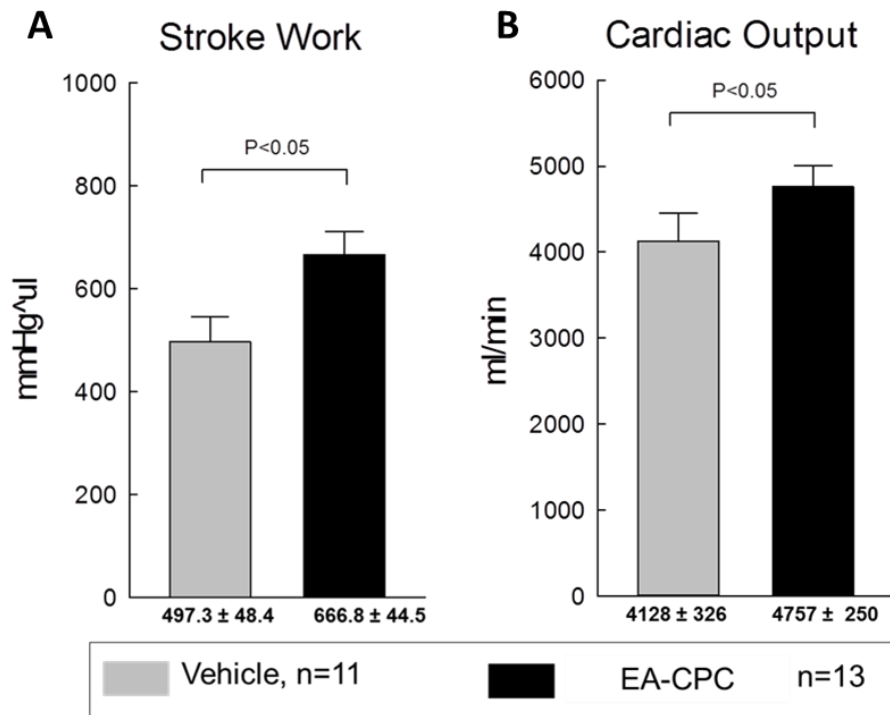


Figure 26. Stroke work and cardiac output. A. Stroke work and B. cardiac output were measured by standard Millar methodology. These functional parameters were observed to be significantly increased/improved as a result of human SSEA-3^{pos} lin^{neg} cells administration vs vehicle control in SCID mice that had undergone ischemic injury as previously outlined.

Discussion

In summary, we have provided for the first time direct evidence of the existence of multipotent SSEA-3^{pos} lin^{neg} cardiac progenitor cells, which are not a culture derived phenotype but exist in the native human neonatal and adult myocardium. We have shown for the first time that these SSEA-3^{pos} lin^{neg} cardiac progenitor cells can be isolated and expanded *in vitro* for the ultimate purpose of use in inducing repair of damaged and/or poorly functioning myocardium. To confirm that these cells truly have a phenotype expected of progenitor cells, we have performed the most extensive characterization ever attempted in any adult progenitor cell population. We validated not only the expression of markers such as pluripotent stem cell associated markers of oct4 and nanog but also telomerase, which allows these cells to preserve their progenitor phenotype and avoid excessive shortening of their telomeres with repetitive cell proliferation *in vitro*. Thusly, these cells retain a large proliferative reserve allowing sufficient numbers of cells for a therapeutic cell product of SSEA-3^{pos} lin^{neg} cells to be generated. We have shown these cells possess a cardiac predisposition as they have heterogeneous baseline expression of transcription factors showing early commitment to mature cardiac lineages of endothelial, smooth muscle, and cardiomyocytes. Furthermore, SSEA-3^{pos} lin^{neg} cardiac progenitor cells up-regulate mature sarcomeric proteins of smooth muscle and myocytes as well as surface markers and functional characteristic of endothelial cells in *in vitro* myogenic and endothelial differentiation conditions respectively. In other words, SSEA-3^{pos} lin^{neg} cardiac progenitor cells have cardiac multilineage potential. This pattern of gene expression and organ specific predisposition is unique to progenitor cells isolated from the human heart and in contrast

to any ability of other non-embryonic or neonatal non-cardiac stem cell populations (i.e. MSCs from various tissues other than heart, HSCs, non-cardiac local tissue progenitors) whose native function is not to contribute directly to lineages of the heart or directly to its homeostasis. We have shown that our methods of isolation and expansion are reproducible, and that SSEA-3^{pos} lin^{neg} cardiac progenitor cells populations from different patients have very similar progenitor gene expression patterns. We have utilized clinically relevant methodologies that show exactly the characteristics and capabilities of SSEA-3^{pos} lin^{neg} cardiac progenitor cells that would be used in a clinically relevant therapeutic application. With these methodologies we have verified within a model of ischemically damaged myocardium that administration of SSEA-3^{pos} lin^{neg} cardiac progenitor cells can induce cardiac repair and abrogate adverse myocardial remodeling that leads to functional decompensation. Again, to our knowledge, a comprehensive report of the discovery, isolation, characterization, and evidence of therapeutic utility of this kind, related to adult progenitor cells, has never been put forth. The clinically applicable methodology demonstrated above enables rapid bench to bedside applications.

Future directions

Presently, analyses of the SSEA-3^{pos} lin^{neg} cardiac progenitor cell treated hearts are underway to evaluate whether donor cells engrafted into recipient hearts. Moreover, did donor cells differentiate into mature cardiac phenotypes representing true regeneration? If this is not observed, it would indicate primarily a paracrine action of these cells on the recipient myocardium by which preservation and recovery of LV function was observed compared to controls, similar to other cell types utilized for cardiac cell based therapies to date. Regardless of whether the SSEA-3^{pos} lin^{neg} cardiac

cells work by engrafting and differentiating into mature myocytes or via paracrine mechanisms, the discovery of this heretofore unknown cell population is an important advance in the field of cell therapy and may have significant therapeutic applications.

REFERENCES

1. Go AS, Mozaffarian D, Roger VL, Benjamin EJ, Berry JD, Borden WB, Bravata DM, Dai S, Ford ES, Fox CS, Franco S, Fullerton HJ, Gillespie C, Hailpern SM, Heit JA, Howard VJ, Huffman MD, Kissela BM, Kittner SJ, Lackland DT, Lichtman JH, Lisabeth LD, Magid D, Marcus GM, Marelli A, Matchar DB, McGuire DK, Mohler ER, Moy CS, Mussolino ME, Nichol G, Paynter NP, Schreiner PJ, Sorlie PD, Stein J, Turan TN, Virani SS, Wong ND, Woo D, Turner MB, American Heart Association Statistics C, Stroke Statistics S. Heart disease and stroke statistics--2013 update: A report from the american heart association. *Circulation*. 2013;127:e6-e245
2. Roger VL, Go AS, Lloyd-Jones DM, Benjamin EJ, Berry JD, Borden WB, Bravata DM, Dai S, Ford ES, Fox CS, Fullerton HJ, Gillespie C, Hailpern SM, Heit JA, Howard VJ, Kissela BM, Kittner SJ, Lackland DT, Lichtman JH, Lisabeth LD, Makuc DM, Marcus GM, Marelli A, Matchar DB, Moy CS, Mozaffarian D, Mussolino ME, Nichol G, Paynter NP, Soliman EZ, Sorlie PD, Sotoodehnia N, Turan TN, Virani SS, Wong ND, Woo D, Turner MB, American Heart Association Statistics C, Stroke Statistics S. Executive summary: Heart disease and stroke statistics--2012 update: A report from the american heart association. *Circulation*. 2012;125:188-197
3. Heidenreich PA, Albert NM, Allen LA, Bluemke DA, Butler J, Fonarow GC, Ikonomidis JS, Khavjou O, Konstam MA, Maddox TM, Nichol G, Pham M, Pina IL, Trogdon JG, American Heart Association Advocacy Coordinating C, Council on Arteriosclerosis T, Vascular B, Council on Cardiovascular R, Intervention, Council on Clinical C, Council on E, Prevention, Stroke C. Forecasting the impact of heart failure in the united states: A

- policy statement from the american heart association. *Circulation. Heart failure*. 2013;6:606-619
4. McMurray JJ, Pfeffer MA. Heart failure. *Lancet*. 2005;365:1877-1889
 5. Pfeffer MA, Braunwald E. Ventricular remodeling after myocardial infarction. Experimental observations and clinical implications. *Circulation*. 1990;81:1161-1172
 6. Sylvester KG, Longaker MT. Stem cells: Review and update. *Archives of surgery*. 2004;139:93-99
 7. Loughran JH, Chugh AR, Ismail I, Bolli R. Stem cell therapy: Promising treatment in heart failure? *Current heart failure reports*. 2013;10:73-80
 8. Sanganalmath SK, Bolli R. Cell therapy for heart failure: A comprehensive overview of experimental and clinical studies, current challenges, and future directions. *Circulation research*. 2013;113:810-834
 9. Oskouei BN, Lamirault G, Joseph C, Treuer AV, Landa S, Da Silva J, Hatzistergos K, Dauer M, Balkan W, McNiece I, Hare JM. Increased potency of cardiac stem cells compared with bone marrow mesenchymal stem cells in cardiac repair. *Stem cells translational medicine*. 2012;1:116-124
 10. Keith MC, Bolli R. "String theory" of c-kit(pos) cardiac cells: A new paradigm regarding the nature of these cells that may reconcile apparently discrepant results. *Circulation research*. 2015;116:1216-1230
 11. Buckingham M, Montarras D. Skeletal muscle stem cells. *Current opinion in genetics & development*. 2008;18:330-336
 12. Mauro A. Satellite cell of skeletal muscle fibers. *The Journal of biophysical and biochemical cytology*. 1961;9:493-495

13. Chachques JC, Acar C, Herreros J, Trainini JC, Prosper F, D'Attellis N, Fabiani JN, Carpentier AF. Cellular cardiomyoplasty: Clinical application. *The Annals of thoracic surgery*. 2004;77:1121-1130
14. Chachques JC, Herreros J, Trainini J, Juffe A, Rendal E, Prosper F, Genovese J. Autologous human serum for cell culture avoids the implantation of cardioverter-defibrillators in cellular cardiomyoplasty. *International journal of cardiology*. 2004;95 Suppl 1:S29-33
15. Taylor DA, Atkins BZ, Hungspreugs P, Jones TR, Reedy MC, Hutcheson KA, Glower DD, Kraus WE. Regenerating functional myocardium: Improved performance after skeletal myoblast transplantation. *Nature medicine*. 1998;4:929-933
16. Menasche P, Hagege AA, Scorsin M, Pouzet B, Desnos M, Duboc D, Schwartz K, Vilquin JT, Marolleau JP. Myoblast transplantation for heart failure. *Lancet*. 2001;357:279-280
17. Siminiak T, Fiszer D, Jerzykowska O, Grygielska B, Rozwadowska N, Kalmucki P, Kurpisz M. Percutaneous trans-coronary-venous transplantation of autologous skeletal myoblasts in the treatment of post-infarction myocardial contractility impairment: The poznan trial. *European heart journal*. 2005;26:1188-1195
18. Dib N, McCarthy P, Campbell A, Yeager M, Pagani FD, Wright S, MacLellan WR, Fonarow G, Eisen HJ, Michler RE, Binkley P, Buchele D, Korn R, Ghazoul M, Dinsmore J, Opie SR, Diethrich E. Feasibility and safety of autologous myoblast transplantation in patients with ischemic cardiomyopathy. *Cell transplantation*. 2005;14:11-19
19. Dib N, Michler RE, Pagani FD, Wright S, Kereiakes DJ, Lengerich R, Binkley P, Buchele D, Anand I, Swingen C, Di Carli MF, Thomas JD, Jaber WA, Opie SR, Campbell A, McCarthy P, Yeager M, Dilsizian V, Griffith BP, Korn R, Kreuger SK, Ghazoul M, MacLellan WR, Fonarow G, Eisen HJ, Dinsmore J, Diethrich E. Safety and

- feasibility of autologous myoblast transplantation in patients with ischemic cardiomyopathy: Four-year follow-up. *Circulation*. 2005;112:1748-1755
20. Durrani S, Konoplyannikov M, Ashraf M, Haider KH. Skeletal myoblasts for cardiac repair. *Regenerative medicine*. 2010;5:919-932
 21. Menasche P, Alfieri O, Janssens S, McKenna W, Reichenspurner H, Trinquart L, Vilquin JT, Marolleau JP, Seymour B, Larghero J, Lake S, Chatellier G, Solomon S, Desnos M, Hagege AA. The myoblast autologous grafting in ischemic cardiomyopathy (magic) trial: First randomized placebo-controlled study of myoblast transplantation. *Circulation*. 2008;117:1189-1200
 22. Reinecke H, MacDonald GH, Hauschka SD, Murry CE. Electromechanical coupling between skeletal and cardiac muscle. Implications for infarct repair. *The Journal of cell biology*. 2000;149:731-740
 23. Dawn B, Abdel-Latif A, Sanganalmath SK, Flaherty MP, Zuba-Surma EK. Cardiac repair with adult bone marrow-derived cells: The clinical evidence. *Antioxidants & redox signaling*. 2009;11:1865-1882
 24. Afzal MR, Samanta A, Shah ZI, Jeevanantham V, Abdel-Latif A, Zuba-Surma EK, Dawn B. Adult bone marrow cell therapy for ischemic heart disease: Evidence and insights from randomized controlled trials. *Circulation research*. 2015;117:558-575
 25. Pompilio G, Nigro P, Bassetti B, Capogrossi MC. Bone marrow cell therapy for ischemic heart disease: The never ending story. *Circulation research*. 2015;117:490-493
 26. Perin EC, Dohmann HF, Borojevic R, Silva SA, Sousa AL, Mesquita CT, Rossi MI, Carvalho AC, Dutra HS, Dohmann HJ, Silva GV, Belem L, Vivacqua R, Rangel FO, Esporcatte R, Geng YJ, Vaughn WK, Assad JA, Mesquita ET, Willerson JT. Transendocardial, autologous bone marrow cell transplantation for severe, chronic ischemic heart failure. *Circulation*. 2003;107:2294-2302

27. Perin EC, Dohmann HF, Borojevic R, Silva SA, Sousa AL, Silva GV, Mesquita CT, Belem L, Vaughn WK, Rangel FO, Assad JA, Carvalho AC, Branco RV, Rossi MI, Dohmann HJ, Willerson JT. Improved exercise capacity and ischemia 6 and 12 months after transendocardial injection of autologous bone marrow mononuclear cells for ischemic cardiomyopathy. *Circulation*. 2004;110:II213-218
28. Willerson JT, Taylor D, Perin EC. Till truth makes all things plain: Human hearts and stem cells. *Circulation research*. 2014;115:908-910
29. Blatt A, Cotter G, Leitman M, Krakover R, Kaluski E, Milo-Cotter O, Resnick IB, Samuel S, Gozal D, Vered Z, Slavin S, Shapira MY. Intracoronary administration of autologous bone marrow mononuclear cells after induction of short ischemia is safe and may improve hibernation and ischemia in patients with ischemic cardiomyopathy. *American heart journal*. 2005;150:986
30. Galinanes M, Loubani M, Davies J, Chin D, Pasi J, Bell PR. Autotransplantation of unmanipulated bone marrow into scarred myocardium is safe and enhances cardiac function in humans. *Cell transplantation*. 2004;13:7-13
31. Assmus B, Honold J, Schachinger V, Britten MB, Fischer-Rasokat U, Lehmann R, Teupe C, Pistorius K, Martin H, Abolmaali ND, Tonn T, Dimmeler S, Zeiher AM. Transcoronary transplantation of progenitor cells after myocardial infarction. *The New England journal of medicine*. 2006;355:1222-1232
32. Hendrikx M, Hensen K, Clijsters C, Jongen H, Koninckx R, Bijnens E, Ingels M, Jacobs A, Geukens R, Dendale P, Vijgen J, Dilling D, Steels P, Mees U, Rummens JL. Recovery of regional but not global contractile function by the direct intramyocardial autologous bone marrow transplantation: Results from a randomized controlled clinical trial. *Circulation*. 2006;114:II101-107
33. Hare JM, Fishman JE, Gerstenblith G, DiFede Velazquez DL, Zambrano JP, Suncion VY, Tracy M, Ghersin E, Johnston PV, Brinker JA, Breton E, Davis-Sproul J, Schulman

- IH, Byrnes J, Mendizabal AM, Lowery MH, Rouy D, Altman P, Wong Po Foo C, Ruiz P, Amador A, Da Silva J, McNiece IK, Heldman AW, George R, Lardo A. Comparison of allogeneic vs autologous bone marrow-derived mesenchymal stem cells delivered by transendocardial injection in patients with ischemic cardiomyopathy: The poseidon randomized trial. *Jama*. 2012;308:2369-2379
34. Boyle AJ, McNiece IK, Hare JM. Mesenchymal stem cell therapy for cardiac repair. *Methods in molecular biology*. 2010;660:65-84
35. Thakker R, Yang P. Mesenchymal stem cell therapy for cardiac repair. *Current treatment options in cardiovascular medicine*. 2014;16:323
36. Pittenger MF, Mackay AM, Beck SC, Jaiswal RK, Douglas R, Mosca JD, Moorman MA, Simonetti DW, Craig S, Marshak DR. Multilineage potential of adult human mesenchymal stem cells. *Science*. 1999;284:143-147
37. Toma C, Pittenger MF, Cahill KS, Byrne BJ, Kessler PD. Human mesenchymal stem cells differentiate to a cardiomyocyte phenotype in the adult murine heart. *Circulation*. 2002;105:93-98
38. Reyes M, Dudek A, Jahagirdar B, Koodie L, Marker PH, Verfaillie CM. Origin of endothelial progenitors in human postnatal bone marrow. *The Journal of clinical investigation*. 2002;109:337-346
39. Reinecke H, Minami E, Zhu WZ, Laflamme MA. Cardiogenic differentiation and transdifferentiation of progenitor cells. *Circulation research*. 2008;103:1058-1071
40. Shadrin IY, Yoon W, Li L, Shepherd N, Bursac N. Rapid fusion between mesenchymal stem cells and cardiomyocytes yields electrically active, non-contractile hybrid cells. *Scientific reports*. 2015;5:12043
41. Barry FP, Murphy JM. Mesenchymal stem cells: Clinical applications and biological characterization. *The international journal of biochemistry & cell biology*. 2004;36:568-584

42. Schuleri KH, Feigenbaum GS, Centola M, Weiss ES, Zimmet JM, Turney J, Kellner J, Zviman MM, Hatzistergos KE, Detrick B, Conte JV, McNiece I, Steenbergen C, Lardo AC, Hare JM. Autologous mesenchymal stem cells produce reverse remodelling in chronic ischaemic cardiomyopathy. *European heart journal*. 2009;30:2722-2732
43. Jo J, Nagaya N, Miyahara Y, Kataoka M, Harada-Shiba M, Kangawa K, Tabata Y. Transplantation of genetically engineered mesenchymal stem cells improves cardiac function in rats with myocardial infarction: Benefit of a novel nonviral vector, cationized dextran. *Tissue engineering*. 2007;13:313-322
44. Nagaya N, Kangawa K, Itoh T, Iwase T, Murakami S, Miyahara Y, Fujii T, Uematsu M, Ohgushi H, Yamagishi M, Tokudome T, Mori H, Miyatake K, Kitamura S. Transplantation of mesenchymal stem cells improves cardiac function in a rat model of dilated cardiomyopathy. *Circulation*. 2005;112:1128-1135
45. Yokokawa M, Ohnishi S, Ishibashi-Ueda H, Obata H, Otani K, Miyahara Y, Tanaka K, Shimizu W, Nakazawa K, Kangawa K, Kamakura S, Kitamura S, Nagaya N. Transplantation of mesenchymal stem cells improves atrioventricular conduction in a rat model of complete atrioventricular block. *Cell transplantation*. 2008;17:1145-1155
46. Liu JF, Wang BW, Hung HF, Chang H, Shyu KG. Human mesenchymal stem cells improve myocardial performance in a splenectomized rat model of chronic myocardial infarction. *Journal of the Formosan Medical Association = Taiwan yi zhi*. 2008;107:165-174
47. Karantalis V, DiFede DL, Gerstenblith G, Pham S, Symes J, Zambrano JP, Fishman J, Pattany P, McNiece I, Conte J, Schulman S, Wu K, Shah A, Breton E, Davis-Sproul J, Schwarz R, Feigenbaum G, Mushtaq M, Suncion VY, Lardo AC, Borrello I, Mendizabal A, Karas TZ, Byrnes J, Lowery M, Heldman AW, Hare JM. Autologous mesenchymal stem cells produce concordant improvements in regional function, tissue perfusion, and fibrotic burden when administered to patients undergoing coronary artery bypass

- grafting: The prospective randomized study of mesenchymal stem cell therapy in patients undergoing cardiac surgery (prometheus) trial. *Circulation research*. 2014;114:1302-1310
48. Kalka C, Masuda H, Takahashi T, Kalka-Moll WM, Silver M, Kearney M, Li T, Isner JM, Asahara T. Transplantation of ex vivo expanded endothelial progenitor cells for therapeutic neovascularization. *Proceedings of the National Academy of Sciences of the United States of America*. 2000;97:3422-3427
49. Rehman J, Li J, Orschell CM, March KL. Peripheral blood "endothelial progenitor cells" are derived from monocyte/macrophages and secrete angiogenic growth factors. *Circulation*. 2003;107:1164-1169
50. Krause DS, Fackler MJ, Civin CI, May WS. Cd34: Structure, biology, and clinical utility. *Blood*. 1996;87:1-13
51. Patel AN, Geffner L, Vina RF, Saslavsky J, Urschel HC, Jr., Kormos R, Benetti F. Surgical treatment for congestive heart failure with autologous adult stem cell transplantation: A prospective randomized study. *The Journal of thoracic and cardiovascular surgery*. 2005;130:1631-1638
52. Vrtovec B, Poglajen G, Lezaic L, Sever M, Socan A, Domanovic D, Cernelc P, Torre-Amione G, Haddad F, Wu JC. Comparison of transendocardial and intracoronary cd34⁺ cell transplantation in patients with nonischemic dilated cardiomyopathy. *Circulation*. 2013;128:S42-49
53. Vrtovec B, Poglajen G, Sever M, Lezaic L, Domanovic D, Cernelc P, Haddad F, Torre-Amione G. Effects of intracoronary stem cell transplantation in patients with dilated cardiomyopathy. *Journal of cardiac failure*. 2011;17:272-281
54. van der Bogt KE, Schrepfer S, Yu J, Sheikh AY, Hoyt G, Govaert JA, Velotta JB, Contag CH, Robbins RC, Wu JC. Comparison of transplantation of adipose tissue- and bone

- marrow-derived mesenchymal stem cells in the infarcted heart. *Transplantation*. 2009;87:642-652
55. Miyahara Y, Nagaya N, Kataoka M, Yanagawa B, Tanaka K, Hao H, Ishino K, Ishida H, Shimizu T, Kangawa K, Sano S, Okano T, Kitamura S, Mori H. Monolayered mesenchymal stem cells repair scarred myocardium after myocardial infarction. *Nature medicine*. 2006;12:459-465
 56. Mazo M, Planat-Benard V, Abizanda G, Pelacho B, Leobon B, Gavira JJ, Penuelas I, Cemborain A, Penicaud L, Laharrague P, Joffre C, Boisson M, Ecay M, Collantes M, Barba J, Casteilla L, Prosper F. Transplantation of adipose derived stromal cells is associated with functional improvement in a rat model of chronic myocardial infarction. *European journal of heart failure*. 2008;10:454-462
 57. Li L, Zhang S, Zhang Y, Yu B, Xu Y, Guan Z. Paracrine action mediate the antifibrotic effect of transplanted mesenchymal stem cells in a rat model of global heart failure. *Molecular biology reports*. 2009;36:725-731
 58. Chen L, Qin F, Ge M, Shu Q, Xu J. Application of adipose-derived stem cells in heart disease. *Journal of cardiovascular translational research*. 2014;7:651-663
 59. Bilic J, Izpisua Belmonte JC. Concise review: Induced pluripotent stem cells versus embryonic stem cells: Close enough or yet too far apart? *Stem cells*. 2012;30:33-41
 60. Puri MC, Nagy A. Concise review: Embryonic stem cells versus induced pluripotent stem cells: The game is on. *Stem cells*. 2012;30:10-14
 61. Arbel G, Caspi O, Huber I, Gepstein A, Weiler-Sagie M, Gepstein L. Methods for human embryonic stem cells derived cardiomyocytes cultivation, genetic manipulation, and transplantation. *Methods in molecular biology*. 2010;660:85-95
 62. Kehat I, Gepstein L. Human embryonic stem cells for myocardial regeneration. *Heart failure reviews*. 2003;8:229-236

63. Kehat I, Kenyagin-Karsenti D, Snir M, Segev H, Amit M, Gepstein A, Livne E, Binah O, Itskovitz-Eldor J, Gepstein L. Human embryonic stem cells can differentiate into myocytes with structural and functional properties of cardiomyocytes. *The Journal of clinical investigation*. 2001;108:407-414
64. Kehat I, Khimovich L, Caspi O, Gepstein A, Shofti R, Arbel G, Huber I, Satin J, Itskovitz-Eldor J, Gepstein L. Electromechanical integration of cardiomyocytes derived from human embryonic stem cells. *Nature biotechnology*. 2004;22:1282-1289
65. Menard C, Hagege AA, Agbulut O, Barro M, Morichetti MC, Brasselet C, Bel A, Messas E, Bissery A, Bruneval P, Desnos M, Puceat M, Menasche P. Transplantation of cardiac-committed mouse embryonic stem cells to infarcted sheep myocardium: A preclinical study. *Lancet*. 2005;366:1005-1012
66. Caspi O, Huber I, Kehat I, Habib M, Arbel G, Gepstein A, Yankelson L, Aronson D, Beyar R, Gepstein L. Transplantation of human embryonic stem cell-derived cardiomyocytes improves myocardial performance in infarcted rat hearts. *Journal of the American College of Cardiology*. 2007;50:1884-1893
67. Cai J, Yi FF, Yang XC, Lin GS, Jiang H, Wang T, Xia Z. Transplantation of embryonic stem cell-derived cardiomyocytes improves cardiac function in infarcted rat hearts. *Cytotherapy*. 2007;9:283-291
68. Chong JJ, Yang X, Don CW, Minami E, Liu YW, Weyers JJ, Mahoney WM, Van Biber B, Cook SM, Palpant NJ, Gantz JA, Fugate JA, Muskheli V, Gough GM, Vogel KW, Astley CA, Hotchkiss CE, Baldessari A, Pabon L, Reinecke H, Gill EA, Nelson V, Kiem HP, Laflamme MA, Murry CE. Human embryonic-stem-cell-derived cardiomyocytes regenerate non-human primate hearts. *Nature*. 2014;510:273-277
69. Shiba Y, Fernandes S, Zhu WZ, Filice D, Muskheli V, Kim J, Palpant NJ, Gantz J, Moyes KW, Reinecke H, Van Biber B, Dardas T, Mignone JL, Izawa A, Hanna R, Viswanathan M, Gold JD, Kotlikoff MI, Sarvazyan N, Kay MW, Murry CE, Laflamme

- MA. Human es-cell-derived cardiomyocytes electrically couple and suppress arrhythmias in injured hearts. *Nature*. 2012;489:322-325
70. Anderson ME, Goldhaber J, Houser SR, Puceat M, Sussman MA. Embryonic stem cell-derived cardiac myocytes are not ready for human trials. *Circulation research*. 2014;115:335-338
71. Murry CE, Chong JJ, Laflamme MA. Letter by murry et al regarding article, "embryonic stem cell-derived cardiac myocytes are not ready for human trials". *Circulation research*. 2014;115:e28-29
72. Nussbaum J, Minami E, Laflamme MA, Virag JA, Ware CB, Masino A, Muskheli V, Pabon L, Reinecke H, Murry CE. Transplantation of undifferentiated murine embryonic stem cells in the heart: Teratoma formation and immune response. *FASEB journal : official publication of the Federation of American Societies for Experimental Biology*. 2007;21:1345-1357
73. Thomson JA, Itskovitz-Eldor J, Shapiro SS, Waknitz MA, Swiergiel JJ, Marshall VS, Jones JM. Embryonic stem cell lines derived from human blastocysts. *Science*. 1998;282:1145-1147
74. Takahashi K, Yamanaka S. Induction of pluripotent stem cells from mouse embryonic and adult fibroblast cultures by defined factors. *Cell*. 2006;126:663-676
75. Yamanaka S, Takahashi K. [induction of pluripotent stem cells from mouse fibroblast cultures]. *Tanpakushitsu kakusan koso. Protein, nucleic acid, enzyme*. 2006;51:2346-2351
76. Pfannkuche K, Liang H, Hannes T, Xi J, Fatima A, Nguemo F, Matzkies M, Wernig M, Jaenisch R, Pillekamp F, Halbach M, Schunkert H, Saric T, Hescheler J, Reppel M. Cardiac myocytes derived from murine reprogrammed fibroblasts: Intact hormonal regulation, cardiac ion channel expression and development of contractility. *Cellular*

physiology and biochemistry : international journal of experimental cellular physiology, biochemistry, and pharmacology. 2009;24:73-86

77. Gu M, Nguyen PK, Lee AS, Xu D, Hu S, Plews JR, Han L, Huber BC, Lee WH, Gong Y, de Almeida PE, Lyons J, Ikeno F, Pacharinsak C, Connolly AJ, Gambhir SS, Robbins RC, Longaker MT, Wu JC. Microfluidic single-cell analysis shows that porcine induced pluripotent stem cell-derived endothelial cells improve myocardial function by paracrine activation. *Circulation research.* 2012;111:882-893
78. Miao Q, Shim W, Tee N, Lim SY, Chung YY, Ja KP, Ooi TH, Tan G, Kong G, Wei H, Lim CH, Sin YK, Wong P. Ipsc-derived human mesenchymal stem cells improve myocardial strain of infarcted myocardium. *Journal of cellular and molecular medicine.* 2014;18:1644-1654
79. Xiong Q, Ye L, Zhang P, Lepley M, Swingen C, Zhang L, Kaufman DS, Zhang J. Bioenergetic and functional consequences of cellular therapy: Activation of endogenous cardiovascular progenitor cells. *Circulation research.* 2012;111:455-468
80. Xiong Q, Ye L, Zhang P, Lepley M, Tian J, Li J, Zhang L, Swingen C, Vaughan JT, Kaufman DS, Zhang J. Functional consequences of human induced pluripotent stem cell therapy: Myocardial atp turnover rate in the in vivo swine heart with postinfarction remodeling. *Circulation.* 2013;127:997-1008
81. Ye L, Chang YH, Xiong Q, Zhang P, Zhang L, Somasundaram P, Lepley M, Swingen C, Su L, Wendel JS, Guo J, Jang A, Rosenbush D, Greder L, Dutton JR, Zhang J, Kamp TJ, Kaufman DS, Ge Y, Zhang J. Cardiac repair in a porcine model of acute myocardial infarction with human induced pluripotent stem cell-derived cardiovascular cells. *Cell stem cell.* 2014;15:750-761
82. Kaji K, Norrby K, Paca A, Mileikovsky M, Mohseni P, Woltjen K. Virus-free induction of pluripotency and subsequent excision of reprogramming factors. *Nature.* 2009;458:771-775

83. Ma T, Xie M, Laurent T, Ding S. Progress in the reprogramming of somatic cells. *Circulation research*. 2013;112:562-574
84. Brade T, Pane LS, Moretti A, Chien KR, Laugwitz KL. Embryonic heart progenitors and cardiogenesis. *Cold Spring Harbor perspectives in medicine*. 2013;3:a013847
85. Sturzu AC, Wu SM. Developmental and regenerative biology of multipotent cardiovascular progenitor cells. *Circulation research*. 2011;108:353-364
86. Xin M, Olson EN, Bassel-Duby R. Mending broken hearts: Cardiac development as a basis for adult heart regeneration and repair. *Nature reviews. Molecular cell biology*. 2013;14:529-541
87. Kattman SJ, Huber TL, Keller GM. Multipotent flk-1⁺ cardiovascular progenitor cells give rise to the cardiomyocyte, endothelial, and vascular smooth muscle lineages. *Developmental cell*. 2006;11:723-732
88. Kimelman D. Mesoderm induction: From caps to chips. *Nature reviews. Genetics*. 2006;7:360-372
89. Nosedá M, Peterkin T, Simoes FC, Patient R, Schneider MD. Cardiopoietic factors: Extracellular signals for cardiac lineage commitment. *Circulation research*. 2011;108:129-152
90. Bondue A, Blanpain C. Mesp1: A key regulator of cardiovascular lineage commitment. *Circulation research*. 2010;107:1414-1427
91. Bondue A, Tannler S, Chiapparo G, Chabab S, Ramialison M, Paulissen C, Beck B, Harvey R, Blanpain C. Defining the earliest step of cardiovascular progenitor specification during embryonic stem cell differentiation. *The Journal of cell biology*. 2011;192:751-765
92. Wu SM. Mesp1 at the heart of mesoderm lineage specification. *Cell stem cell*. 2008;3:1-2
93. Abu-Issa R. Heart fields: Spatial polarity and temporal dynamics. *Anatomical record*. 2014;297:175-182

94. Abu-Issa R, Waldo K, Kirby ML. Heart fields: One, two or more? *Developmental biology*. 2004;272:281-285
95. Gittenberger-de Groot AC, Blom NM, Aoyama N, Sucov H, Wenink AC, Poelmann RE. The role of neural crest and epicardium-derived cells in conduction system formation. *Novartis Foundation symposium*. 2003;250:125-134; discussion 134-141, 276-129
96. Bu L, Jiang X, Martin-Puig S, Caron L, Zhu S, Shao Y, Roberts DJ, Huang PL, Domian IJ, Chien KR. Human isl1 heart progenitors generate diverse multipotent cardiovascular cell lineages. *Nature*. 2009;460:113-117
97. Wessels A, Perez-Pomares JM. The epicardium and epicardially derived cells (epdcs) as cardiac stem cells. *The anatomical record. Part A, Discoveries in molecular, cellular, and evolutionary biology*. 2004;276:43-57
98. Arstall MA, Sawyer DB, Fukazawa R, Kelly RA. Cytokine-mediated apoptosis in cardiac myocytes: The role of inducible nitric oxide synthase induction and peroxynitrite generation. *Circulation research*. 1999;85:829-840
99. Laugwitz KL, Moretti A, Lam J, Gruber P, Chen Y, Woodard S, Lin LZ, Cai CL, Lu MM, Reth M, Platoshyn O, Yuan JX, Evans S, Chien KR. Postnatal isl1⁺ cardioblasts enter fully differentiated cardiomyocyte lineages. *Nature*. 2005;433:647-653
100. Sun Y, Liang X, Najafi N, Cass M, Lin L, Cai CL, Chen J, Evans SM. Islet 1 is expressed in distinct cardiovascular lineages, including pacemaker and coronary vascular cells. *Developmental biology*. 2007;304:286-296
101. Harris IS, Black BL. Development of the endocardium. *Pediatric cardiology*. 2010;31:391-399
102. Kraus F, Haenig B, Kispert A. Cloning and expression analysis of the mouse t-box gene *tbx18*. *Mechanisms of development*. 2001;100:83-86

103. Katz TC, Singh MK, Degenhardt K, Rivera-Feliciano J, Johnson RL, Epstein JA, Tabin CJ. Distinct compartments of the proepicardial organ give rise to coronary vascular endothelial cells. *Developmental cell*. 2012;22:639-650
104. von Gise A, Pu WT. Endocardial and epicardial epithelial to mesenchymal transitions in heart development and disease. *Circulation research*. 2012;110:1628-1645
105. von Gise A, Zhou B, Honor LB, Ma Q, Petryk A, Pu WT. Wt1 regulates epicardial epithelial to mesenchymal transition through beta-catenin and retinoic acid signaling pathways. *Developmental biology*. 2011;356:421-431
106. Poelmann RE, Lie-Venema H, Gittenberger-de Groot AC. The role of the epicardium and neural crest as extracardiac contributors to coronary vascular development. *Texas Heart Institute journal / from the Texas Heart Institute of St. Luke's Episcopal Hospital, Texas Children's Hospital*. 2002;29:255-261
107. van Tuyn J, Atsma DE, Winter EM, van der Velde-van Dijke I, Pijnappels DA, Bax NA, Knaan-Shanzer S, Gittenberger-de Groot AC, Poelmann RE, van der Laarse A, van der Wall EE, Schaliij MJ, de Vries AA. Epicardial cells of human adults can undergo an epithelial-to-mesenchymal transition and obtain characteristics of smooth muscle cells in vitro. *Stem cells*. 2007;25:271-278
108. Wada AM, Smith TK, Osler ME, Reese DE, Bader DM. Epicardial/mesothelial cell line retains vasculogenic potential of embryonic epicardium. *Circulation research*. 2003;92:525-531
109. Zhou B, Ma Q, Rajagopal S, Wu SM, Domian I, Rivera-Feliciano J, Jiang D, von Gise A, Ikeda S, Chien KR, Pu WT. Epicardial progenitors contribute to the cardiomyocyte lineage in the developing heart. *Nature*. 2008;454:109-113
110. Cai CL, Martin JC, Sun Y, Cui L, Wang L, Ouyang K, Yang L, Bu L, Liang X, Zhang X, Stallcup WB, Denton CP, McCulloch A, Chen J, Evans SM. A myocardial lineage derives from tbx18 epicardial cells. *Nature*. 2008;454:104-108

111. Christoffels VM, Grieskamp T, Norden J, Mommersteeg MT, Rudat C, Kispert A. Tbx18 and the fate of epicardial progenitors. *Nature*. 2009;458:E8-9; discussion E9-10
112. Zhou B, Honor LB, He H, Ma Q, Oh JH, Butterfield C, Lin RZ, Melero-Martin JM, Dolmatova E, Duffy HS, Gise A, Zhou P, Hu YW, Wang G, Zhang B, Wang L, Hall JL, Moses MA, McGowan FX, Pu WT. Adult mouse epicardium modulates myocardial injury by secreting paracrine factors. *The Journal of clinical investigation*. 2011;121:1894-1904
113. Acharya A, Baek ST, Banfi S, Eskiocak B, Tallquist MD. Efficient inducible cre-mediated recombination in tcf21 cell lineages in the heart and kidney. *Genesis*. 2011;49:870-877
114. Kikuchi K, Gupta V, Wang J, Holdway JE, Wills AA, Fang Y, Poss KD. Tcf21⁺ epicardial cells adopt non-myocardial fates during zebrafish heart development and regeneration. *Development*. 2011;138:2895-2902
115. Porrello ER, Olson EN. A neonatal blueprint for cardiac regeneration. *Stem cell research*. 2014;13:556-570
116. Rinkevich Y, Mori T, Sahoo D, Xu PX, Bermingham JR, Jr., Weissman IL. Identification and prospective isolation of a mesothelial precursor lineage giving rise to smooth muscle cells and fibroblasts for mammalian internal organs, and their vasculature. *Nature cell biology*. 2012;14:1251-1260
117. Misfeldt AM, Boyle SC, Tompkins KL, Bautch VL, Labosky PA, Baldwin HS. Endocardial cells are a distinct endothelial lineage derived from flk1⁺ multipotent cardiovascular progenitors. *Developmental biology*. 2009;333:78-89
118. de la Pompa JL, Timmerman LA, Takimoto H, Yoshida H, Elia AJ, Samper E, Potter J, Wakeham A, Marengere L, Langille BL, Crabtree GR, Mak TW. Role of the nf-atc transcription factor in morphogenesis of cardiac valves and septum. *Nature*. 1998;392:182-186

119. Puri MC, Partanen J, Rossant J, Bernstein A. Interaction of the tek and tie receptor tyrosine kinases during cardiovascular development. *Development*. 1999;126:4569-4580
120. Messina E, De Angelis L, Frati G, Morrone S, Chimenti S, Fiordaliso F, Salio M, Battaglia M, Latronico MV, Coletta M, Vivarelli E, Frati L, Cossu G, Giacomello A. Isolation and expansion of adult cardiac stem cells from human and murine heart. *Circulation research*. 2004;95:911-921
121. Smith RR, Barile L, Cho HC, Leppo MK, Hare JM, Messina E, Giacomello A, Abraham MR, Marban E. Regenerative potential of cardiosphere-derived cells expanded from percutaneous endomyocardial biopsy specimens. *Circulation*. 2007;115:896-908
122. Johnson TV, Bull ND, Martin KR. Identification of barriers to retinal engraftment of transplanted stem cells. *Investigative ophthalmology & visual science*. 2010;51:960-970
123. Makkar RR, Smith RR, Cheng K, Malliaras K, Thomson LE, Berman D, Czer LS, Marban L, Mendizabal A, Johnston PV, Russell SD, Schuleri KH, Lardo AC, Gerstenblith G, Marban E. Intracoronary cardiosphere-derived cells for heart regeneration after myocardial infarction (caduceus): A prospective, randomised phase 1 trial. *Lancet*. 2012;379:895-904
124. Bayes-Genis A, Salido M, Sole Ristol F, Puig M, Brossa V, Camprecios M, Corominas JM, Marinosa ML, Baro T, Vela MC, Serrano S, Padro JM, Bayes de Luna A, Cinca J. Host cell-derived cardiomyocytes in sex-mismatch cardiac allografts. *Cardiovascular research*. 2002;56:404-410
125. Mirotsov M, Jayawardena TM, Schmeckpeper J, Gneccchi M, Dzau VJ. Paracrine mechanisms of stem cell reparative and regenerative actions in the heart. *Journal of molecular and cellular cardiology*. 2011;50:280-289
126. Nygren JM, Jovinge S, Breitbach M, Sawen P, Roll W, Hescheler J, Taneera J, Fleischmann BK, Jacobsen SE. Bone marrow-derived hematopoietic cells generate

cardiomyocytes at a low frequency through cell fusion, but not transdifferentiation.

Nature medicine. 2004;10:494-501

127. Acquistapace A, Bru T, Lesault PF, Figeac F, Coudert AE, le Coz O, Christov C, Baudin X, Auber F, Yiou R, Dubois-Rande JL, Rodriguez AM. Human mesenchymal stem cells reprogram adult cardiomyocytes toward a progenitor-like state through partial cell fusion and mitochondria transfer. *Stem cells*. 2011;29:812-824
128. Bergmann O, Bhardwaj RD, Bernard S, Zdunek S, Barnabe-Heider F, Walsh S, Zupicich J, Alkass K, Buchholz BA, Druid H, Jovinge S, Frisen J. Evidence for cardiomyocyte renewal in humans. *Science*. 2009;324:98-102
129. Goldman BI, Wurzel J. Evidence that human cardiac myocytes divide after myocardial infarction. *The New England journal of medicine*. 2001;345:1131
130. Beltrami AP, Barlucchi L, Torella D, Baker M, Limana F, Chimenti S, Kasahara H, Rota M, Musso E, Urbanek K, Leri A, Kajstura J, Nadal-Ginard B, Anversa P. Adult cardiac stem cells are multipotent and support myocardial regeneration. *Cell*. 2003;114:763-776
131. Klarmann K, Ortiz M, Davies M, Keller JR. Identification of in vitro growth conditions for c-kit-negative hematopoietic stem cells. *Blood*. 2003;102:3120-3128
132. Dawn B, Stein AB, Urbanek K, Rota M, Whang B, Rastaldo R, Torella D, Tang XL, Rezazadeh A, Kajstura J, Leri A, Hunt G, Varma J, Prabhu SD, Anversa P, Bolli R. Cardiac stem cells delivered intravascularly traverse the vessel barrier, regenerate infarcted myocardium, and improve cardiac function. *Proceedings of the National Academy of Sciences of the United States of America*. 2005;102:3766-3771
133. Guan K, Hasenfuss G. Cardiac resident progenitor cells: Evidence and functional significance. *European heart journal*. 2013;34:2784-2787
134. D'Amario D, Fiorini C, Campbell PM, Goichberg P, Sanada F, Zheng H, Hosoda T, Rota M, Connell JM, Gallegos RP, Welt FG, Givertz MM, Mitchell RN, Leri A, Kajstura J, Pfeffer MA, Anversa P. Functionally competent cardiac stem cells can be isolated from

- endomyocardial biopsies of patients with advanced cardiomyopathies. *Circulation research*. 2011;108:857-861
135. Itzhaki-Alfia A, Leor J, Raanani E, Sternik L, Spiegelstein D, Netser S, Holbova R, Pevsner-Fischer M, Lavee J, Barbash IM. Patient characteristics and cell source determine the number of isolated human cardiac progenitor cells. *Circulation*. 2009;120:2559-2566
136. Wu SM, Fujiwara Y, Cibulsky SM, Clapham DE, Lien CL, Schultheiss TM, Orkin SH. Developmental origin of a bipotential myocardial and smooth muscle cell precursor in the mammalian heart. *Cell*. 2006;127:1137-1150
137. Ferreira-Martins J, Ogorek B, Cappetta D, Matsuda A, Signore S, D'Amario D, Kostyla J, Steadman E, Ide-Iwata N, Sanada F, Iaffaldano G, Ottolenghi S, Hosoda T, Leri A, Kajstura J, Anversa P, Rota M. Cardiomyogenesis in the developing heart is regulated by c-kit-positive cardiac stem cells. *Circulation research*. 2012;110:701-715
138. Rota M, Padin-Iruegas ME, Misao Y, De Angelis A, Maestroni S, Ferreira-Martins J, Fiumana E, Rastaldo R, Arcarese ML, Mitchell TS, Boni A, Bolli R, Urbanek K, Hosoda T, Anversa P, Leri A, Kajstura J. Local activation or implantation of cardiac progenitor cells rescues scarred infarcted myocardium improving cardiac function. *Circulation research*. 2008;103:107-116
139. Bolli R, Tang XL, Sanganalmath SK, Rimoldi O, Mosna F, Abdel-Latif A, Jneid H, Rota M, Leri A, Kajstura J. Intracoronary delivery of autologous cardiac stem cells improves cardiac function in a porcine model of chronic ischemic cardiomyopathy. *Circulation*. 2013;128:122-131
140. Gambini E, Pompilio G, Biondi A, Alamanni F, Capogrossi MC, Agrifoglio M, Pesce M. C-kit⁺ cardiac progenitors exhibit mesenchymal markers and preferential cardiovascular commitment. *Cardiovascular research*. 2011;89:362-373

141. Hong KU, Guo Y, Li QH, Cao P, Al-Maqtari T, Vajravelu BN, Du J, Book MJ, Zhu X, Nong Y, Bhatnagar A, Bolli R. C-kit⁺ cardiac stem cells alleviate post-myocardial infarction left ventricular dysfunction despite poor engraftment and negligible retention in the recipient heart. *PLoS one*. 2014;9:e96725
142. Jesty SA, Steffey MA, Lee FK, Breitbach M, Hesse M, Reining S, Lee JC, Doran RM, Nikitin AY, Fleischmann BK, Kotlikoff MI. C-kit⁺ precursors support postinfarction myogenesis in the neonatal, but not adult, heart. *Proceedings of the National Academy of Sciences of the United States of America*. 2012;109:13380-13385
143. Li Q, Guo Y, Ou Q, Chen N, Wu WJ, Yuan F, O'Brien E, Wang T, Luo L, Hunt GN, Zhu X, Bolli R. Intracoronary administration of cardiac stem cells in mice: A new, improved technique for cell therapy in murine models. *Basic research in cardiology*. 2011;106:849-864
144. Matuszczak S, Czaplak J, Jarosz-Biej M, Wisniewska E, Cichon T, Smolarczyk R, Kobusinska M, Gajda K, Wilczek P, Sliwka J, Zembala M, Zembala M, Szala S. Characteristic of c-kit progenitor cells in explanted human hearts. *Clinical research in cardiology : official journal of the German Cardiac Society*. 2014
145. Tang XL, Rokosh G, Sanganalmath SK, Yuan F, Sato H, Mu J, Dai S, Li C, Chen N, Peng Y, Dawn B, Hunt G, Leri A, Kajstura J, Tiwari S, Shirk G, Anversa P, Bolli R. Intracoronary administration of cardiac progenitor cells alleviates left ventricular dysfunction in rats with a 30-day-old infarction. *Circulation*. 2010;121:293-305
146. Tang XL, Rokosh G, Sanganalmath SK, Tokita Y, Keith MC, Shirk G, Stowers H, Hunt GN, Wu W, Dawn B, Bolli R. Effects of intracoronary infusion of escalating doses of cardiac stem cells in rats with acute myocardial infarction. *Circulation. Heart failure*. 2015;8:757-765
147. Linke A, Muller P, Nurzynska D, Casarsa C, Torella D, Nascimbene A, Castaldo C, Cascapera S, Bohm M, Quaini F, Urbanek K, Leri A, Hintze TH, Kajstura J, Anversa P.

- Stem cells in the dog heart are self-renewing, clonogenic, and multipotent and regenerate infarcted myocardium, improving cardiac function. *Proceedings of the National Academy of Sciences of the United States of America*. 2005;102:8966-8971
148. Bolli R, Chugh AR, D'Amario D, Loughran JH, Stoddard MF, Ikram S, Beache GM, Wagner SG, Leri A, Hosoda T, Sanada F, Elmore JB, Goichberg P, Cappetta D, Solankhi NK, Fahsah I, Rokosh DG, Slaughter MS, Kajstura J, Anversa P. Cardiac stem cells in patients with ischaemic cardiomyopathy (scipio): Initial results of a randomised phase 1 trial. *Lancet*. 2011;378:1847-1857
149. Delewi R, Andriessen A, Tijssen JG, Zijlstra F, Piek JJ, Hirsch A. Impact of intracoronary cell therapy on left ventricular function in the setting of acute myocardial infarction: A meta-analysis of randomised controlled clinical trials. *Heart*. 2013;99:225-232
150. Lipinski MJ, Biondi-Zoccai GG, Abbate A, Khianey R, Sheiban I, Bartunek J, Vanderheyden M, Kim HS, Kang HJ, Strauer BE, Vetrovec GW. Impact of intracoronary cell therapy on left ventricular function in the setting of acute myocardial infarction: A collaborative systematic review and meta-analysis of controlled clinical trials. *Journal of the American College of Cardiology*. 2007;50:1761-1767
151. Martin-Rendon E, Brunskill SJ, Hyde CJ, Stanworth SJ, Mathur A, Watt SM. Autologous bone marrow stem cells to treat acute myocardial infarction: A systematic review. *European heart journal*. 2008;29:1807-1818
152. Levine GN, Bates ER, Blankenship JC, Bailey SR, Bittl JA, Cercek B, Chambers CE, Ellis SG, Guyton RA, Hollenberg SM, Khot UN, Lange RA, Mauri L, Mehran R, Moussa ID, Mukherjee D, Nallamothu BK, Ting HH. 2011 accf/aha/scai guideline for percutaneous coronary intervention: Executive summary: A report of the american college of cardiology foundation/american heart association task force on practice

- guidelines and the society for cardiovascular angiography and interventions. *Circulation*. 2011;124:2574-2609
153. Levine GN, Bates ER, Blankenship JC, Bailey SR, Bittl JA, Cercek B, Chambers CE, Ellis SG, Guyton RA, Hollenberg SM, Khot UN, Lange RA, Mauri L, Mehran R, Moussa ID, Mukherjee D, Nallamothu BK, Ting HH, Accf, Aha, Scai. 2011 accf/aha/scai guideline for percutaneous coronary intervention: Executive summary: A report of the american college of cardiology foundation/american heart association task force on practice guidelines and the society for cardiovascular angiography and interventions. *Catheterization and cardiovascular interventions : official journal of the Society for Cardiac Angiography & Interventions*. 2012;79:453-495
154. Heusch G. Cardioprotection: Chances and challenges of its translation to the clinic. *Lancet*. 2013;381:166-175
155. Heusch G, Kleinbongard P, Bose D, Levkau B, Haude M, Schulz R, Erbel R. Coronary microembolization: From bedside to bench and back to bedside. *Circulation*. 2009;120:1822-1836
156. Keith MC, Tang XL, Tokita Y, Li QH, Ghafghazi S, Moore Iv J, Hong KU, Elmore B, Amraotkar A, Ganzel BL, Grubb KJ, Flaherty MP, Hunt G, Vajravelu B, Wysoczynski M, Bolli R. Safety of intracoronary infusion of 20 million c-kit positive human cardiac stem cells in pigs. *PLoS One*. 2015;10:e0124227
157. Nowak B, Weber C, Schober A, Zeiffer U, Liehn EA, von Hundelshausen P, Reinartz P, Schaefer WM, Buell U. Indium-111 oxine labelling affects the cellular integrity of haematopoietic progenitor cells. *European journal of nuclear medicine and molecular imaging*. 2007;34:715-721
158. Schiller NB, Shah PM, Crawford M, DeMaria A, Devereux R, Feigenbaum H, Gutgesell H, Reichek N, Sahn D, Schnittger I, et al. Recommendations for quantitation of the left ventricle by two-dimensional echocardiography. American society of echocardiography

- committee on standards, subcommittee on quantitation of two-dimensional echocardiograms. *Journal of the American Society of Echocardiography : official publication of the American Society of Echocardiography*. 1989;2:358-367
159. Doyle B, Kemp BJ, Chareonthaitawee P, Reed C, Schmeckpeper J, Sorajja P, Russell S, Araoz P, Riederer SJ, Caplice NM. Dynamic tracking during intracoronary injection of 18f-fdg-labeled progenitor cell therapy for acute myocardial infarction. *Journal of nuclear medicine : official publication, Society of Nuclear Medicine*. 2007;48:1708-1714
160. Leiker M, Suzuki G, Iyer VS, Canty JM, Jr., Lee T. Assessment of a nuclear affinity labeling method for tracking implanted mesenchymal stem cells. *Cell transplantation*. 2008;17:911-922
161. Meluzin J, Vlasin M, Groch L, Mayer J, Kren L, Rauser P, Tichy B, Hornacek I, Sitar J, Palsa S, Klabusay M, Koristek Z, Doubek M, Pospisilova S, Lexmaulova L, Dusek L. Intracoronary delivery of bone marrow cells to the acutely infarcted myocardium. Optimization of the delivery technique. *Cardiology*. 2009;112:98-106
162. Musialek P, Tekieli L, Kostkiewicz M, Majka M, Szot W, Walter Z, Zebzda A, Pieniazek P, Kadzielski A, Banys RP, Olszowska M, Pasowicz M, Zmudka K, Tracz W. Randomized transc coronary delivery of cd34(+) cells with perfusion versus stop-flow method in patients with recent myocardial infarction: Early cardiac retention of (9)(9)(m)tc-labeled cells activity. *Journal of nuclear cardiology : official publication of the American Society of Nuclear Cardiology*. 2011;18:104-116
163. Perin EC, Willerson JT, Pepine CJ, Henry TD, Ellis SG, Zhao DX, Silva GV, Lai D, Thomas JD, Kronenberg MW, Martin AD, Anderson RD, Traverse JH, Penn MS, Anwaruddin S, Hatzopoulos AK, Gee AP, Taylor DA, Cogle CR, Smith D, Westbrook L, Chen J, Handberg E, Olson RE, Geither C, Bowman S, Francescon J, Baraniuk S, Piller LB, Simpson LM, Loghin C, Aguilar D, Richman S, Zierold C, Bettencourt J, Sayre SL, Vojvodic RW, Skarlatos SI, Gordon DJ, Ebert RF, Kwak M, Moye LA, Simari RD,

- Cardiovascular Cell Therapy Research N. Effect of transendocardial delivery of autologous bone marrow mononuclear cells on functional capacity, left ventricular function, and perfusion in chronic heart failure: The focus-cctrn trial. *Jama*. 2012;307:1717-1726
164. Tossios P, Krausgrill B, Schmidt M, Fischer T, Halbach M, Fries JW, Fahnenstich S, Frommolt P, Heppelmann I, Schmidt A, Schomacker K, Fischer JH, Bloch W, Mehlhorn U, Schwinger RH, Muller-Ehmsen J. Role of balloon occlusion for mononuclear bone marrow cell deposition after intracoronary injection in pigs with reperfused myocardial infarction. *European heart journal*. 2008;29:1911-1921
165. Vrtovec B, Poglajen G, Lezaic L, Sever M, Domanovic D, Cernelc P, Socan A, Schrepfer S, Torre-Amione G, Haddad F, Wu JC. Effects of intracoronary cd34⁺ stem cell transplantation in nonischemic dilated cardiomyopathy patients: 5-year follow-up. *Circulation research*. 2013;112:165-173
166. Malliaras K, Smith RR, Kanazawa H, Yee K, Seinfeld J, Tseliou E, Dawkins JF, Kreke M, Cheng K, Luthringer D, Ho CS, Blusztajn A, Valle I, Chowdhury S, Makkar RR, Dharmakumar R, Li D, Marban L, Marban E. Validation of contrast-enhanced magnetic resonance imaging to monitor regenerative efficacy after cell therapy in a porcine model of convalescent myocardial infarction. *Circulation*. 2013;128:2764-2775
167. Vulliet PR, Greeley M, Halloran SM, MacDonald KA, Kittleson MD. Intra-coronary arterial injection of mesenchymal stromal cells and microinfarction in dogs. *Lancet*. 2004;363:783-784
168. Gomez FA, Ballesteros LE. Morphologic expression of the left coronary artery in pigs. An approach in relation to human heart. *Revista brasileira de cirurgia cardiovascular : orgao oficial da Sociedade Brasileira de Cirurgia Cardiovascular*. 2014;29:214-220
169. Sahni D, Kaur GD, Jit H, Jit I. Anatomy & distribution of coronary arteries in pig in comparison with man. *The Indian journal of medical research*. 2008;127:564-570

170. Hong KU, Li QH, Guo Y, Patton NS, Moktar A, Bhatnagar A, Bolli R. A highly sensitive and accurate method to quantify absolute numbers of c-kit⁺ cardiac stem cells following transplantation in mice. *Basic research in cardiology*. 2013;108:346
171. Suzuki K, Murtuza B, Suzuki N, Smolenski RT, Yacoub MH. Intracoronary infusion of skeletal myoblasts improves cardiac function in doxorubicin-induced heart failure. *Circulation*. 2001;104:I213-217
172. Meluzin J, Mayer J, Groch L, Janousek S, Hornacek I, Hlinomaz O, Kala P, Panovsky R, Prasek J, Kaminek M, Stanicek J, Klabusay M, Koristek Z, Navratil M, Dusek L, Vinklarkova J. Autologous transplantation of mononuclear bone marrow cells in patients with acute myocardial infarction: The effect of the dose of transplanted cells on myocardial function. *American heart journal*. 2006;152:975 e979-915
173. Chen S, Liu Z, Tian N, Zhang J, Yei F, Duan B, Zhu Z, Lin S, Kwan TW. Intracoronary transplantation of autologous bone marrow mesenchymal stem cells for ischemic cardiomyopathy due to isolated chronic occluded left anterior descending artery. *The Journal of invasive cardiology*. 2006;18:552-556
174. Gao LR, Pei XT, Ding QA, Chen Y, Zhang NK, Chen HY, Wang ZG, Wang YF, Zhu ZM, Li TC, Liu HL, Tong ZC, Yang Y, Nan X, Guo F, Shen JL, Shen YH, Zhang JJ, Fei YX, Xu HT, Wang LH, Tian HT, Liu da Q, Yang Y. A critical challenge: Dosage-related efficacy and acute complication intracoronary injection of autologous bone marrow mesenchymal stem cells in acute myocardial infarction. *International journal of cardiology*. 2013;168:3191-3199
175. Katritsis DG, Sotiropoulou PA, Karvouni E, Karabinos I, Korovesis S, Perez SA, Voridis EM, Papamichail M. Transcoronary transplantation of autologous mesenchymal stem cells and endothelial progenitors into infarcted human myocardium. *Catheterization and cardiovascular interventions : official journal of the Society for Cardiac Angiography & Interventions*. 2005;65:321-329

176. Lakota J, Dubrovcakova M, Bohovic R, Goncalvesova E. Intracoronary mesenchymal stem cell transplantation in patients with ischemic cardiomyopathy. *International journal of cardiology*. 2014;176:547-549
177. Lee JW, Lee SH, Youn YJ, Ahn MS, Kim JY, Yoo BS, Yoon J, Kwon W, Hong IS, Lee K, Kwan J, Park KS, Choi D, Jang YS, Hong MK. A randomized, open-label, multicenter trial for the safety and efficacy of adult mesenchymal stem cells after acute myocardial infarction. *Journal of Korean medical science*. 2014;29:23-31
178. Chen SL, Fang WW, Ye F, Liu YH, Qian J, Shan SJ, Zhang JJ, Chunhua RZ, Liao LM, Lin S, Sun JP. Effect on left ventricular function of intracoronary transplantation of autologous bone marrow mesenchymal stem cell in patients with acute myocardial infarction. *The American journal of cardiology*. 2004;94:92-95
179. Freyman T, Polin G, Osman H, Crary J, Lu M, Cheng L, Palasis M, Wilensky RL. A quantitative, randomized study evaluating three methods of mesenchymal stem cell delivery following myocardial infarction. *European heart journal*. 2006;27:1114-1122
180. Grieve SM, Bhindi R, Seow J, Doyle A, Turner AJ, Tomka J, Lay W, Gill A, Hunyor SN, Figtree GA. Microvascular obstruction by intracoronary delivery of mesenchymal stem cells and quantification of resulting myocardial infarction by cardiac magnetic resonance. *Circulation. Heart failure*. 2010;3:e5-6
181. Johnston PV, Sasano T, Mills K, Evers R, Lee ST, Smith RR, Lardo AC, Lai S, Steenbergen C, Gerstenblith G, Lange R, Marban E. Engraftment, differentiation, and functional benefits of autologous cardiosphere-derived cells in porcine ischemic cardiomyopathy. *Circulation*. 2009;120:1075-1083, 1077 p following 1083
182. Kassab GS, Fung YC. Topology and dimensions of pig coronary capillary network. *The American journal of physiology*. 1994;267:H319-325
183. Jeevanantham V, Butler M, Saad A, Abdel-Latif A, Zuba-Surma EK, Dawn B. Adult bone marrow cell therapy improves survival and induces long-term improvement in

cardiac parameters: A systematic review and meta-analysis. *Circulation*. 2012;126:551-568

184. Traverse JH, Henry TD, Ellis SG, Pepine CJ, Willerson JT, Zhao DX, Forder JR, Byrne BJ, Hatzopoulos AK, Penn MS, Perin EC, Baran KW, Chambers J, Lambert C, Raveendran G, Simon DI, Vaughan DE, Simpson LM, Gee AP, Taylor DA, Cogle CR, Thomas JD, Silva GV, Jorgenson BC, Olson RE, Bowman S, Francescon J, Geither C, Handberg E, Smith DX, Baraniuk S, Piller LB, Loghin C, Aguilar D, Richman S, Zierold C, Bettencourt J, Sayre SL, Vojvodic RW, Skarlatos SI, Gordon DJ, Ebert RF, Kwak M, Moye LA, Simari RD, Cardiovascular Cell Therapy R. Effect of intracoronary delivery of autologous bone marrow mononuclear cells 2 to 3 weeks following acute myocardial infarction on left ventricular function: The late-time randomized trial. *Jama*. 2011;306:2110-2119
185. Traverse JH, Henry TD, Pepine CJ, Willerson JT, Zhao DX, Ellis SG, Forder JR, Anderson RD, Hatzopoulos AK, Penn MS, Perin EC, Chambers J, Baran KW, Raveendran G, Lambert C, Lerman A, Simon DI, Vaughan DE, Lai D, Gee AP, Taylor DA, Cogle CR, Thomas JD, Olson RE, Bowman S, Francescon J, Geither C, Handberg E, Kappenman C, Westbrook L, Piller LB, Simpson LM, Baraniuk S, Loghin C, Aguilar D, Richman S, Zierold C, Spoon DB, Bettencourt J, Sayre SL, Vojvodic RW, Skarlatos SI, Gordon DJ, Ebert RF, Kwak M, Moye LA, Simari RD, Cardiovascular Cell Therapy Research N. Effect of the use and timing of bone marrow mononuclear cell delivery on left ventricular function after acute myocardial infarction: The time randomized trial. *Jama*. 2012;308:2380-2389
186. Schachinger V, Erbs S, Elsasser A, Haberbosch W, Hambrecht R, Holschermann H, Yu J, Corti R, Mathey DG, Hamm CW, Suselbeck T, Assmus B, Tonn T, Dimmeler S, Zeiher AM, Investigators R-A. Intracoronary bone marrow-derived progenitor cells in acute myocardial infarction. *The New England journal of medicine*. 2006;355:1210-1221

187. Diris JH, Hackeng CM, Kooman JP, Pinto YM, Hermens WT, van Dieijen-Visser MP. Impaired renal clearance explains elevated troponin t fragments in hemodialysis patients. *Circulation*. 2004;109:23-25
188. Suzuki G, Iyer V, Lee TC, Cauty JM, Jr. Autologous mesenchymal stem cells mobilize ckit⁺ and cd133⁺ bone marrow progenitor cells and improve regional function in hibernating myocardium. *Circulation research*. 2011;109:1044-1054
189. Suzuki G, Weil BR, Leiker MM, Ribbeck AE, Young RF, Cimato TR, Cauty JM, Jr. Global intracoronary infusion of allogeneic cardiosphere-derived cells improves ventricular function and stimulates endogenous myocyte regeneration throughout the heart in swine with hibernating myocardium. *PloS one*. 2014;9:e113009
190. Gleeson TG, Bulugahapitiya S. Contrast-induced nephropathy. *AJR. American journal of roentgenology*. 2004;183:1673-1689
191. English J, Evan A, Houghton DC, Bennett WM. Cyclosporine-induced acute renal dysfunction in the rat. Evidence of arteriolar vasoconstriction with preservation of tubular function. *Transplantation*. 1987;44:135-141
192. Weibrecht K, Dayno M, Darling C, Bird SB. Liver aminotransferases are elevated with rhabdomyolysis in the absence of significant liver injury. *Journal of medical toxicology : official journal of the American College of Medical Toxicology*. 2010;6:294-300
193. Nathwani RA, Pais S, Reynolds TB, Kaplowitz N. Serum alanine aminotransferase in skeletal muscle diseases. *Hepatology*. 2005;41:380-382
194. Keith MC, Elmore JB, Tang X-L, Tokita Y, Amraotkar A, Ghafghazi S, Hong KU, Vajravelu BN, Wysoczynski M, Moore JB, Hunt G, Bolli R. Abstract 15763: Does the stop-flow technique improve cardiac retention of intracoronarily delivered cells? A study of cardiac retention of c-kit positive human cardiac stem cells (hcses) after intracoronary infusion in a porcine model of chronic ischemic cardiomyopathy. *Circulation*. 2014;130:A15763

195. Askari AT, Unzek S, Popovic ZB, Goldman CK, Forudi F, Kiedrowski M, Rovner A, Ellis SG, Thomas JD, DiCorleto PE, Topol EJ, Penn MS. Effect of stromal-cell-derived factor 1 on stem-cell homing and tissue regeneration in ischaemic cardiomyopathy. *The Lancet*. 2003;362:697-703
196. Taghavi S, George JC. Homing of stem cells to ischemic myocardium. *American journal of translational research*. 2013;5:404-411
197. Limana F, Capogrossi MC, Germani A. The epicardium in cardiac repair: From the stem cell view. *Pharmacology & therapeutics*. 2011;129:82-96
198. White AJ, Smith RR, Matsushita S, Chakravarty T, Czer LS, Burton K, Schwarz ER, Davis DR, Wang Q, Reinsmoen NL, Forrester JS, Marban E, Makkar R. Intrinsic cardiac origin of human cardiosphere-derived cells. *European heart journal*. 2013;34:68-75
199. Suila H, Pitkanen V, Hirvonen T, Heiskanen A, Anderson H, Laitinen A, Natunen S, Miller-Podraza H, Satomaa T, Natunen J, Laitinen S, Valmu L. Are globoseries glycosphingolipids ssea-3 and -4 markers for stem cells derived from human umbilical cord blood? *Journal of molecular cell biology*. 2011;3:99-107
200. Gang EJ, Bosnakovski D, Figueiredo CA, Visser JW, Perlingeiro RC. Ssea-4 identifies mesenchymal stem cells from bone marrow. *Blood*. 2007;109:1743-1751
201. Kuroda Y, Wakao S, Kitada M, Murakami T, Nojima M, Dezawa M. Isolation, culture and evaluation of multilineage-differentiating stress-enduring (muse) cells. *Nature protocols*. 2013;8:1391-1415
202. Riekstina U, Cakstina I, Parfejevs V, Hoogduijn M, Jankovskis G, Muiznieks I, Muceniece R, Ancans J. Embryonic stem cell marker expression pattern in human mesenchymal stem cells derived from bone marrow, adipose tissue, heart and dermis. *Stem cell reviews*. 2009;5:378-386
203. Byrne JA, Nguyen HN, Reijo Pera RA. Enhanced generation of induced pluripotent stem cells from a subpopulation of human fibroblasts. *PloS one*. 2009;4:e7118

204. Vega Crespo A, Awe JP, Reijo Pera R, Byrne JA. Human skin cells that express stage-specific embryonic antigen 3 associate with dermal tissue regeneration. *BioResearch open access*. 2012;1:25-33
205. Andrews PW, Fenderson B, Hakomori S. Human embryonal carcinoma cells and their differentiation in culture. *International journal of andrology*. 1987;10:95-104
206. Przyborski SA. Isolation of human embryonal carcinoma stem cells by immunomagnetic sorting. *Stem cells*. 2001;19:500-504
207. Liang YJ, Kuo HH, Lin CH, Chen YY, Yang BC, Cheng YY, Yu AL, Khoo KH, Yu J. Switching of the core structures of glycosphingolipids from globo- and lacto- to ganglio-series upon human embryonic stem cell differentiation. *Proceedings of the National Academy of Sciences of the United States of America*. 2010;107:22564-22569
208. Amir G, Ma X, Reddy VM, Hanley FL, Reinhartz O, Ramamoorthy C, Riemer RK. Dynamics of human myocardial progenitor cell populations in the neonatal period. *The Annals of thoracic surgery*. 2008;86:1311-1319
209. Ott HC, Matthiesen TS, Brechtken J, Grindle S, Goh SK, Nelson W, Taylor DA. The adult human heart as a source for stem cells: Repair strategies with embryonic-like progenitor cells. *Nature clinical practice. Cardiovascular medicine*. 2007;4 Suppl 1:S27-39
210. Braitsch CM, Kanisicak O, van Berlo JH, Molkentin JD, Yutzey KE. Differential expression of embryonic epicardial progenitor markers and localization of cardiac fibrosis in adult ischemic injury and hypertensive heart disease. *Journal of molecular and cellular cardiology*. 2013;65:108-119
211. Limana F, Bertolami C, Mangoni A, Di Carlo A, Avitabile D, Mocini D, Iannelli P, De Mori R, Marchetti C, Pozzoli O, Gentili C, Zacheo A, Germani A, Capogrossi MC. Myocardial infarction induces embryonic reprogramming of epicardial c-kit(+) cells:

- Role of the pericardial fluid. *Journal of molecular and cellular cardiology*. 2010;48:609-618
212. D'Amario D, Cabral-Da-Silva MC, Zheng H, Fiorini C, Goichberg P, Steadman E, Ferreira-Martins J, Sanada F, Piccoli M, Cappetta D, D'Alessandro DA, Michler RE, Hosoda T, Anastasia L, Rota M, Leri A, Anversa P, Kajstura J. Insulin-like growth factor-1 receptor identifies a pool of human cardiac stem cells with superior therapeutic potential for myocardial regeneration. *Circulation research*. 2011;108:1467-1481
213. Davis DR, Zhang Y, Smith RR, Cheng K, Terrovitis J, Malliaras K, Li TS, White A, Makkar R, Marban E. Validation of the cardiosphere method to culture cardiac progenitor cells from myocardial tissue. *PloS one*. 2009;4:e7195
214. Li TS, Cheng K, Malliaras K, Smith RR, Zhang Y, Sun B, Matsushita N, Blusztajn A, Terrovitis J, Kusuoka H, Marban L, Marban E. Direct comparison of different stem cell types and subpopulations reveals superior paracrine potency and myocardial repair efficacy with cardiosphere-derived cells. *Journal of the American College of Cardiology*. 2012;59:942-953
215. Malliaras K, Li TS, Luthringer D, Terrovitis J, Cheng K, Chakravarty T, Galang G, Zhang Y, Schoenhoff F, Van Eyk J, Marban L, Marban E. Safety and efficacy of allogeneic cell therapy in infarcted rats transplanted with mismatched cardiosphere-derived cells. *Circulation*. 2012;125:100-112

CURRICULUM VITAE

Matthew C.L. Keith, MD

PERSONAL INFORMATION:

Legal Name: Matthew Cody Lee Keith
Date of Birth: October 1, 1981
Citizenship: USA
Originally from: Bossier City, Louisiana

Current Home Address:
15108 Abington Ridge Place
Louisville, Kentucky 40245
Phone: 318.393.2575
Email: matthew.keith.1@louisville.edu

Work Mailing Address:
Department of Cardiovascular Medicine
University of Louisville
530 South Jackson Street
Ambulatory Care Building, 3rd Floor
Louisville, Kentucky 40202

Contact:
c: (318) 393-2575
f: (502) 749-4120
Matthew.Keith.1@louisville.edu

EDUCATION & TRAINING:

Aug. 2001 – May 2005
B.S., *Oklahoma State University*, Stillwater, Oklahoma
Major: Physiology
Summa cum Laude Graduate
GPA: 4.0
NCAA Division I Big 12 Conference Baseball Oklahoma State University, (2001-2003)

Aug. 2005 – May 2009
M.D., *Louisiana State University Health Sciences Center*, Shreveport, Louisiana.
USMLE Step 1: 250/99
USMLE Step 2: 251/99
USMLE Step 3: 218/93

Jul. 2009 – May 2012
Internal Medicine Residency Program (3 years, Categorical) – *University of Louisville*,
Louisville, Kentucky.

Apr. 2010 – Present
PhD Program University of Louisville, Dept. of Physiology and Biophysics
Mentor: Dr. Roberto Bolli
Defense of Thesis: February 2016
GPA: 4.0
Topic: Repair and Regeneration of Ischemically Damaged Myocardium
via Embryonic Antigen Expressing Adult Cardiac Progenitor Cells (EA-CPCs).

Jul. 2012 – Present
Cardiovascular Medicine Fellowship Program (3 years pre-clinical research with
completion of PhD, 2 years clinical fellowship) – *University of Louisville*, Louisville,
Kentucky, PGY-7 currently.

BOARD CERTIFICATIONS & LICENSURES

Oct. 2011 – Present
State of Kentucky, Board of Medical Licensure approved Medical License.(KY#44841).
(In good standing)

Oct. 2011 – Present
National Provider Identifier (NPI), HIPPA compliant (NPI# 1215179908)

Oct. 2013 – Present
ABIM Board Certified Physician of Internal Medicine. (August 13, 2013, In good
standing with ABIM-MOC requirements) (ABIM ID. 326335).

Oct. 2012 – Present
Drug Enforcement Agency (DEA) controlled substances prescriber license. (In good
standing)

Jun. 2008 – Present
ACLS Certified Provider, Louisville, Kentucky (Recertification completed
2014)

AWARDS & HONORS

2014 – 2015	Research Fellow of the Year Award, Department of Cardiology, University of Louisville, Award bestowed by Dr. Roberto Bolli.
2014 – 2015	University of Louisville Graduate/Professional Student of the Year Award, Nominated by Dr. Roberto Bolli.
2013 – 2014	Fellow of the Year Award, Department of Cardiology, University of Louisville, Award bestowed by Dr. Roberto Bolli.
2013 – 2014	Research Fellow of the Year Award, Department of Cardiology, University of Louisville, Award bestowed by Dr. Roberto Bolli.
2012 – 2016	University of Louisville, School of Interdisciplinary Graduate Studies (SIGS) Tuition Scholarship Awards, yearly bestowed.
2005 – 2007	<i>LSUHSC</i> Bernstein Scholarship Award
2004 – Present	Phi Kappa Phi Honor Society
2002 – Present	National Honor Society of Collegiate Scholars
2002 – Present	Alpha Epsilon Delta Medical Honor Society

2002 – 2005	Academic Excellence Scholar Award
2002 – 2005	Lew Wentz Foundation Scholarship Award
2001 – 2005	Oklahoma State University Valedictorian Scholarship Award
2001 – 2005	Louisiana TOPS Full Tuition Scholarship Award

PROFESSIONAL SOCIETIES

American Medical Association
 American Medical Student Association
 American College of Physicians, Internal Medicine Member
 American Heart Association
 American College of Cardiology

PUBLICATIONS:

Aravind Sekhar, Brad S Sutton, Prafull Raheja, Amr Mohsen, Emily Angelis, Chris N Angelis, Matthew C Keith, Buddhadeb Dawn, Michael Flaherty. Femoral arterial closure using Proglide is more efficacious and cost-effective when ambulating early following cardiac catheterization. *Int. J. Cardiol.* 2016. (In press).

Shahab Ghafghazi, Marcin Wysoczynski, Matthew Cody Lee Keith, Joseph B. Moore IV, Roberto Bolli. “Ventricular Remodeling. The appropriate surrogate endpoint for cell based therapy?” *Dialogues in Cardiovascular Medicine.* 2015 Oct; 20 . No. 2.

Vajravelu BN, Hong KU, Al-Maqtari T, Cao P, Keith MC, Wysoczynski M, Zhao J, Moore IV JB, Bolli R. C-Kit Promotes Growth and Migration of Human Cardiac Progenitor Cells via the PI3K-AKT and MEK-ERK Pathways. *PLoS One.* 2015 Oct 16;10(10):e0140798. doi: 10.1371/journal.pone.0140798.

Amraotkar AR, Hargis CW, Cambon AC, Rai SN, Keith MC, Ghafghazi S, Bolli R, DeFilippis AP. Comparison of coliform contamination in non-municipal waters consumed by the Mennonite versus the non-Mennonite rural populations. *Environ Health Prev Med.* 2015 Jun 12. doi 10.1007/s12199-015-0472-4.

Xian-Liang Tang, D. Gregg Rokosh, Santosh K. Sanganalmath, Yukichi Tokita, Matthew Keith, Gregg Shirk, Heather Stowers, Gregory Hunt, Wenjian Wu, Buddhadeb Dawn, Roberto Bolli. “Effects of Intracoronary Infusion of Escalating Doses of Cardiac Stem Cells in Rats With Acute Myocardial Infarction”. *Circulation Heart Failure.* 5/2015. DOI: 10.1161/CIRCHEARTFAILURE.115.002210.

Matthew C. L. Keith, Yukichi Tokita, Xian-Liang Tang, Shahab Ghafghazi, Joseph Moore IV, Kyung U. Hong, Brandon Elmore, Alok Amraotkar, Haixun Guo, Brian L. Ganzel, Kendra J. Grubb, Michael P. Flaherty, Gregory Hunt, Bathri Vajravelu, Marcin Wysoczynski, Roberto Bolli. Effect of the Stop-Flow Technique on Cardiac Retention of c-kit Positive Human Cardiac Stem Cells After Intracoronary Infusion in a Porcine Model of Chronic Ischemic Cardiomyopathy. *Basic Research in Cardiology.* *Basic Res Cardiol.* 2015 Sep;110(5):503. doi:10.1007/s00395-015-0503-8. Epub 2015 Jul 7.

Matthew C. L. Keith, Roberto Bolli. “String Theory” of c-kit^{POS} Cardiac Cells: A New Paradigm Regarding the Nature of These Cells That May Reconcile Apparently Discrepant Results”. *Circulation Research.* 2015; 116:1216-1230. DOI: 10.1161/CIRCRESAHA.116.305557.

Keith MC, Tang XL, Tokita Y, Li QH, Ghafghazi S, Moore IV J, Hong KU, Elmore B, Amraotkar A, Ganzel BL, Grubb KJ, Flaherty MP, Hunt G, Vajravelu B, Wysoczynski M, Bolli R. Safety of intracoronary infusion of 20 million C-kit positive human cardiac stem cells in pigs. *PLoS One*. 2015 Apr 23;10(4):e0124227. DOI: 10.1371/journal.pone.0124227.

Bolli Roberto, Birks Emma, Flaherty Michael P, Keith Matthew, Ghafghazi Shahab. Response to letter regarding article, "Cell therapy for heart failure: a comprehensive overview of experimental and clinical studies, current challenges, and future directions". *Circulation Research*. 2014 Nov 7;115(11):e33-4. DOI: 10.1161/CIRCRESAHA.114.305263.

ABSTRACTS

Matthew C. L. Keith; Brandon Elmore; Xian-Liang Tang; Yukichi Tokita; Alok Amraotkar; Shahab Ghafghazi; Kyung U. Hong; Bathri Vajravelu; Marcin Wysoczynski; Joseph Moore; Gregory Hunt; Roberto Bolli. Abstract 15763: "Does the stop-flow technique improve cardiac retention of intracoronarily delivered cells? A study of cardiac retention of c-kit positive human cardiac stem cells (hCSCs) after intracoronary infusion in a porcine model of chronic ischemic cardiomyopathy." *Circulation*, 2014 Nov 25; 130(A15763).

Martin A. Espinosa Ginic, Ziad Alnabki, Matthew C. Keith, Haree Vongooru, Brenda Underwood, Timothy Wiemken, Stephen Wagner, Kelly C. McCants, Emma Birks, Sumanth D. Prabhu. "Myocardial Recovery with Optimization of Medical Management in Patients with Advanced Systolic Heart Failure". *Journal of Cardiac Failure* 2013 Aug; 19(8):s47. DOI: 10.1016/j.cardfail.2013.06.155

Justin R Kingery, Allison L Keskey, Heather B Clair, Robert K Lewis, Kenneth R Brittan, Mohamed A. Ismahil, Kehak Goel, Shang Z Guo, Matthew Keith, Tariq Hamid, Sumanth Prabhu, Macrophages and Dendritic Cells Modulate the Inflammatory Milieu and Hypertrophic Stimuli in the Normal Heart. (abstract) 2010, *AHA Scientific Sessions*, Chicago. APS.512.02a- 15692

Oral presentation / Posters:

Matthew C. L. Keith; Brandon Elmore; Xian-Liang Tang; Yukichi Tokita; Alok Amraotkar; Shahab Ghafghazi; Kyung U. Hong; Bathri Vajravelu; Marcin Wysoczynski; Joseph Moore; Gregory Hunt; Roberto Bolli. "Does the stop-flow technique improve cardiac retention of intracoronarily delivered cells? A study of cardiac retention of c-kit positive human cardiac stem cells (hCSCs) after intracoronary infusion in a porcine model of chronic ischemic cardiomyopathy." – *American Heart Association Scientific Sessions, Chicago, Nov 2014*.

Matthew C. L. Keith; Xian-Liang Tang; Yukichi Tokita; Qian-hong Li; Brandon Elmore; Shahab Ghafghazi; Alok Amraotkar; Kyung U. Hong; Bathri Vajravelu; Marcin Wysoczynski; Joseph Moore; Gregory Hunt; Roberto Bolli. "Are higher doses of c-kit positive hCSCs delivered intracoronarily safe? A safety study in pigs using 20 million c-kit positive hCSCs." - *American College of Cardiology-Kentucky Chapter, Sept 2014*.

Espinosa Ginic, M., Keith, M., Lewis, R., Underwood, B., Prabhu, S. "Myocardial Recovery with Optimization of Intensive Medical Management in Patients with Advanced Heart Failure. *American College of Cardiology-Kentucky Chapter, 2012*.

Justin R Kingery, Allison L Keskey, Heather B Clair, Robert K Lewis, Kenneth R Brittan, Mohamed A. Ismahil, Kehak Goel, Shang Z Guo, Matthew Keith, Tariq Hamid, Sumanth Prabhu, University of Louisville and VAMC Louisville, Kentucky. "Macrophages and Dendritic Cells Modulate the Inflammatory Milieu and Hypertrophic Stimuli in the Normal Heart." - *American Heart Association Scientific Sessions, Nov 2010*.

Kingery JR, Lewis RL, Keith M, Keskey A, Clair HB, Brittian K, Hamid T, Ishamil MA, Prabhu SD. "Inflammatory Cell-Derived iNOS Exacerbates Post-infarction LV Remodeling." - *Keystone National MD-PhD Conference, 2010.*

PRECLINICAL RESEARCH & CLINICAL TRIALS

2014 – present	C-kit Positive Cardiac Stem Cells in Congenital Hypoplastic Left Heart Syndrome, a phase I/II clinical trial.
2013 – present	PIM-1 Kinase Over Expressing C-kit positive CSCs, A Phase I/II clinical Trial.
2013 – present	CCTR N SENECA Trial: Allogeneic hCSCs in Patients with Anthracycline Induce Cardiomyopathy, a Phase I/II clinical trial.
2013 – present	CCTR N CONCERT trial: c-kit ^{pos} cardiac stem cells and bone marrow mesenchymal stem cells in patients with ischemic cardiomyopathy, a Phase I/II clinical trial.
2012 – present	Human Cardiac Stem Cell laboratory University of Louisville, Louisville, Kentucky, USA.

PATENTS

1. United States of America Provisional Patent Application Serial No. 61/909,729, filed November 27, 2013.
2. United States of America Finalized Patent Application - PCT 1577-36, filed November 27, 2014. University of Louisville, Office of Technology Transfer, Technology #13079. (<http://louisville.flintbox.com/public/project/26530/>)

AD HOC REVIEWER

2013 – present	<i>Circulation Research</i>
2014 – present	<i>PLoS One</i>
2015 – present	<i>Circulation</i>

VOLUNTEER ACTIVITIES:

2010 – present	University of Louisville SOM Physio-simulator Instructor
2007 – 2009	Northwest Louisiana Food Bank
2008 – Present	Guest Speaker Apollo Elementary – “Future in Medicine”
2008 – Present	River Bend Rotary in partnership with Life Share Blood Center

REFERENCES

Available on request.